Optical Biosensors for Glucose

Alexander H. Bjørndal

Master Thesis in Chemistry
Chemistry Department

UNIVERSITY OF OSLO

May 2014

There is no doubt that methods based on catalysis by enzymes will increase in number and practicability as advances are made in the study of these substances and as more enzymes of known activity and purity become commercially available

Thomas S. Lee in 1954

Acknowledgements

This master thesis was carried out at the University of Oslo and Oslo University College between August 2012 and May 2014.

I want to thank some people for making it possible to complete the master thesis:

Silje Anderdal Bakken
Magne Kringberg
Jaan Roots
Peyman Mirtaheri
Sissel Jørgensen
Per Ola Rønning
Eddy Walter Hansen
Mathias Grønvoll
Massoud Kaboli
Gunnar Isaksen
Bendik Grøthe
Simen Snellingen
Martin Hennum
Marita Clausen
Aud Bouzga
Øyvind Mathias Fjell

List of abbreviations

Abbreviations	Complete name
DGS	Diglycerylsilane
EtOH	Ethanol
FAD/$FADH_2$	Flavin adenine dinucleotide (oxidized and reduced form)
FRET	Förster resonance energy transfer
GLS	Gluconamidylsilane
GOx	Glucose Oxidase
IR	Infrared spectrometry
LED	Light emitting diode
MeOH	Methanol
MS	Mass spectrometry
NMR	Nuclear magnetic resonance
PBS	Phosphate buffered saline
PGS	Poly(glyceryl silicate)
SS	Sodium Silicate
ssNMR	Solid state nuclear magnetic resonance
TEOS	Tetraethyl orthosilicate
TMOS	Tetramethyl orthosilicate

Abstract

GOx was, to the authors knowledge, for the first time successfully immobilized in DGS. The intrinsic fluorescence of GOx was measured in both solution and a sol-gel derived matrix in both the presence and absence of glucose. A setup to measure the fluorescence intensity in a plate array was developed.

Table of Contents

List of Figures

List of Tables

1 Introduction and background

1.1 Diabetes and the importance of glucose sensors

The number of people with diabetes mellitus worldwide was in 2009 estimated to be 285,000,000 in 2010 and calculated to become 439,000,000 by 2030 [1]. In another paper from 2011 [2] the number was estimated to be as high as 347,000,000 already in 2008. It is clear that the number of people in need of glucose sensors is high and increasing. This can be indicated by searching for "Glucose sensor" on the Internet. When searching for "Glucose sensor" 19,735 hits were found by SciFinder (search done 25.04.2014). To prove that the interest is increasing a second search some weeks later (15.05.2014) gave 19,826 hits, which is an increase of almost 100 papers in three weeks.

Since the body of diabetic patients does not automatically regulate the concentration of insulin proportional to the glucose concentration in the blood, this has to be regulated manually [3]. Analysis of blood sugar levels, the glucose concentration in their blood, has to be done many times a day [4]. This is normally done by drawing blood, which is analyzed by hand-held glucose sensors to give the patient the blood sugar level. While the hand-held machines have been an important progress [5], this method is not ideal, as it is invasive, forcing the diabetic to draw blood. Usually this is done from a finger, and multiple pricks in a single finger can over time lead to numbness. Other disadvantages are that these sensors needs a reference signal, a person has to be awake to use the sensors, and dangerous states of hyper-/hypoglycemia can also occur when the diabetic is asleep [5, 6].

Optical biosensors utilize light and the selective nature of biological components for responding to specific analytes [7]. Immense research is done on optical biosensors [8], and great progress has been made [9] since the first optical biosensor by Lübbers and Opitz [10]. The use of optical sensor can help avoid many of the problems caused by electrochemical sensors [6, 11]. Unlike many other analytical methods, like electrochemical methods, the light used is mostly not harmful to the body or system it is used in, and in theory the excitation and measuring can be done noninvasively from outside of the body [5]. Using fluorescence can be extremely sensitive [8, 12], and the

signal can travel great distances making it possible to measure glucose concentrations in hard to reach places [11]. The equipment used is fairly cheap, easy to use and is not disturbed by electrical or magnetic fields [11]. Another advantage is that there are different methods, which can be applied within the field of fluorescence; using a steady-state approximation by measurement of the intensity differences, time-resolved fluorescence, Förster resonance energy transfer (FRET) and other techniques that can provide information about micro-environment and structure of the molecules [5, 7, 8].

The first glucose biosensor was proposed in 1962 by Clark and Lyons [13] using Glucose Oxidase (GOx) entrapped over an oxygen electrode with a dialysis membrane. In 1975 the first available commercial glucose sensor was launched by Yellow Spring Instruments Inc. [14]. A demonstration of *in vivo* glucose monitoring was shown in 1982 by Shichiri *et al.* [15], and a wearable and noninvasive glucose sensor was produced by Cygnus Inc. in 2000 [16].

In December 2011 Microsoft Research revealed that they were working on making noninvasive glucose sensing contact lenses [17], on which an article was published [18]. Three years later Google started working on a similar project [19]. The fact that two multi-billion companies like Microsoft and Google invests time and money into noninvasive glucose sensors is proof of how important this field of research is, and that noninvasive sensors are the future.

The fact that a company can profit from putting up a commercial for a glucose sensor in the middle of Oslo, as seen in Figure 1, is yet another proof of the importance of glucose sensors.

Figure 1: A commercial seen in a central part of Oslo for a glucose sensor (11.09.2012). It reads: "FreeStyle Lite – The glow-in-the-dark blood sugar meter".

1.2 Fluorescence; history and applications

Fluorescence is a phenomenon first observed by Sir John Fredrich William Herschel in 1845 [20]. Further observations were done by Gabriel George Stokes in 1852 [21]. They both observed fluorescence from a quinine solution. Stokes saw that light was emitted from the solution when shone upon by the sun through a church window. The church

window was blue and acted as a excitation filter that transmitted light with wavelengths under 400 nm. He then saw that the light from the quinine solution was also visible through a yellow glass of wine which was his primitive emission filter that transmitted light with wavelengths above 400 nm. Stokes understood that the light had changed some characteristics, although which were not known at the time [8]. The first to describe what occurred was Professor Alexander Jablonski, who is regarded as the father of fluorescence spectroscopy [8]. In 1933 he presented the first Jablonski diagram seen in Figure 2 in a short paper [22], which was further elaborated on in a paper from 1935 [23].

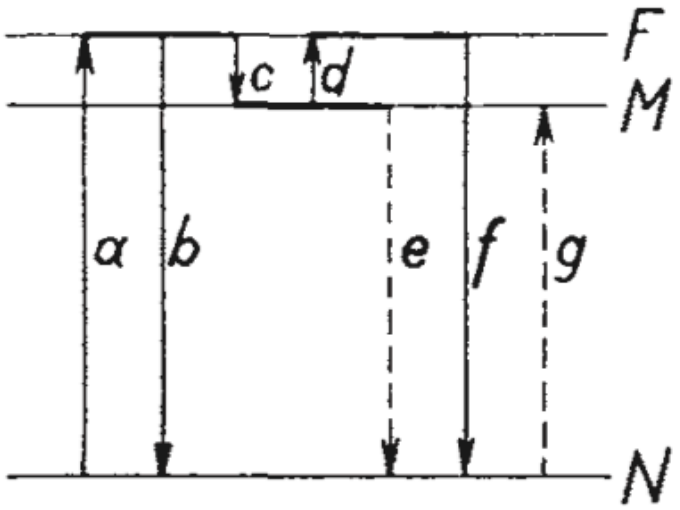

FIG. 1.—Energy levels in a phosphorescent molecule. *a*–absorption, *b*–fluorescence, *c*–transition to metastable level, *d*–thermal excitation, *e* and *f*–phosphorescence, *g*–absorption of very small transition probability.

Figure 2: The first published Jablonski diagram from [22] with the original figure text.

Fluorescence has since had many applications: emergency markers for finding people lost at sea, commercially available lamps, in forensics, biochemistry, many different kinds of optical sensors and labeling [8, 24, 25]. The sensitivity and specificity of which fluorescence can be detected has developed to the point where it is possible to measure fluorescence of single molecules, as described by Tan [9] and Weiss [12].

1.3 The sol-gel process

Already in 1846 Ebelmen published a paper on silica gels [26], however the drying times were one year or longer, making them tedious to work with. The silica gel was again investigated from the late 1800s through the 1920s [27], but no deep understanding of the physical-chemical principles was achieved. Then 50 years ago the use of immobilized enzymes ventured from the laboratory and into industry [28]. The reasons for this were many: highly specific and reversible reactions, temperature ranges of 4-60 °C and the conditions reactions occurs under are not as harsh as other chemical reactions. Enzymes can be encapsulated in an array of methods, however inorganic materials are favorable. This is because inorganic materials do not change morphology based on pH and solvent conditions and they are resistant from biological attacks from contaminations like bacteria. Other advantages are that the inorganic materials can be prepared in many different ways and the pore diameters of the inorganic support can be greatly varied [28-31].

The two most used starting silicate precursors are tetramethoxy orthosilicate (TMOS) and tetraethyl orthosilicate (TEOS), are easily available and cheap [29, 30, 32-34]. However there are some disadvantages with TMOS and TEOS. One of the main drawbacks is that the hydrolysis of TMOS and TEOS release methanol and ethanol, respectively [27, 32, 34]. The release of alcohol can decrease the activity of enzymes, and in the worst consequence denature the protein [35-40]. When the gel dries, shrinking occurs, and this can hinder the enzyme activity greatly [37], still the shrinking can also lead to a framework that holds the enzyme in its active state, an keeps it from unfolding [35]. TMOS and TEOS hydrolysis and condensation is usually either acid or base catalyzed [41]. Strong acids and bases can significantly alter the function of proteins [42], and this is of course not desired. An example of what can happen to enzyme activity after immobilization in TMOS can be read in a paper from 1999 by Badjić and Kostić [43], where they report that only 1-2 % of enzyme activity was retained. There are also examples of encapsulation of GOx in both TMOS [44-46] and TEOS [33], which gave better results. These will be discussed later.

The need for sol-gels that could immobilize biomolecules, lead to the use of "biocompatible sol-gel substrates" such as Poly(glyceryl silicate) (PGS), Diglyceryl silane (DGS), SS (sodium silicate). These are water soluble, and hydrolyze and condensate quickly in water without any catalyst at low temperatures and mild pH-values [32, 37, 40, 47, 48].

The first structure of DGS, and an example of hydrolysis, seen in Figure 3, was proposed in an article by Brook *et al.* [36] in 2004, the same year their patent for polyol-modified silanes was granted [39]. In a paper by Vanderkooy and Brook [49], DGS was described as a mixture of 5,6 ringed isomers with stoichiometric formula $Si(glycerol)_2$.
The following enzymes have been successfully encapsulated in a DGS based sol-gel matrix: Factor Xa [36, 38], dihydrofolate reductase [38, 50], cyclooxygenase-2 [38], γ-glutamyl transpeptidase [38], human serum albumin [40, 51] maltose binding protein [52], horseradish peroxidase [53], firefly luciferase [54] and tyrosine kinase [55]. High enzyme activity retained [38, 40, 55], long-term stability [36, 38, 40], reduced shrinkage [36, 54, 56] and increased thermal stability [40] is reported for DGS based matrices compared to TEOS derived matrices. Of all the biomolecules immobilized in DGS, only DNAzymes were reported [57] to have better activity in a TMOS based matrix, however the DNAzymes were used for metal ion detection, which is quite different from detection of glucose. Many reports have been made on the advantages of sugar modified silanes as precursors for enzyme immobilization matrices [34, 40, 53-56, 58]. Mostly Gluconamidylsilane (GLS) is used together with DGS to give even better results than the DGS did by itself.

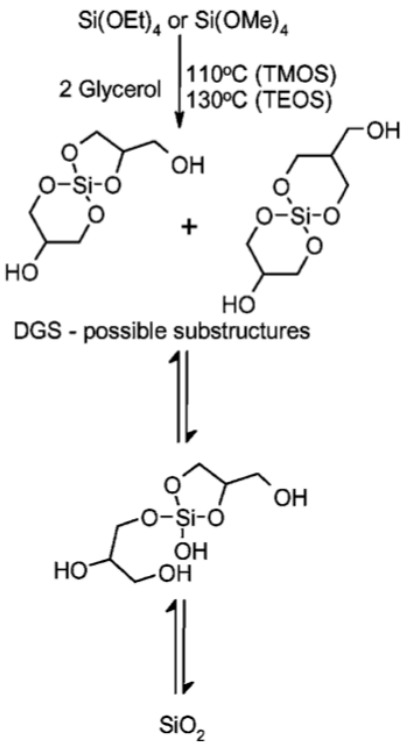

Figure 3: The first proposed structure for DGS by Brook et al. [36]. Here the reaction to obtain DGS is showed together with possible substructures, hydrolysis and condensation to glass.

A low reaction temperature is of course important when working with fragile biomolecules like enzymes. Transparency and homogeneity is important when working with light. By using the sol-gel process a clear, homogenous film can be produced at low temperatures [27, 29, 30]. To optimize the biocompatibility of the sol-gel matrix, changes in pH and the release of alcohols should be reduced. This can be achieved by using DGS as the precursor for the sol-gel matrix [34, 36].

1.4 GOx, and its use in glucose sensors

Since its discovery in 1928 by Müller [59], GOx has become the most used enzyme for analytical purposes [60]. In a paper by Bentley and Neuberger from 1949 [61] the reaction seen in Figure 4 was presented.

$$C_6H_{12}O_6 + O_2 + H_2O = C_6H_{12}O_7 + H_2O_2$$

Figure 4: Simple reaction oxidation of glucose by glucose oxidase from Bentley and Neuberger [61].

This reaction, although correct, is not very descriptive. A more complex version can be seen in Figure 5, which will be used to explain the different sensing methods used today. GOx has two tightly bound flavin adenine dinucleotide (FAD) molecules, which are reduced in the oxidization of β-D-glucose.

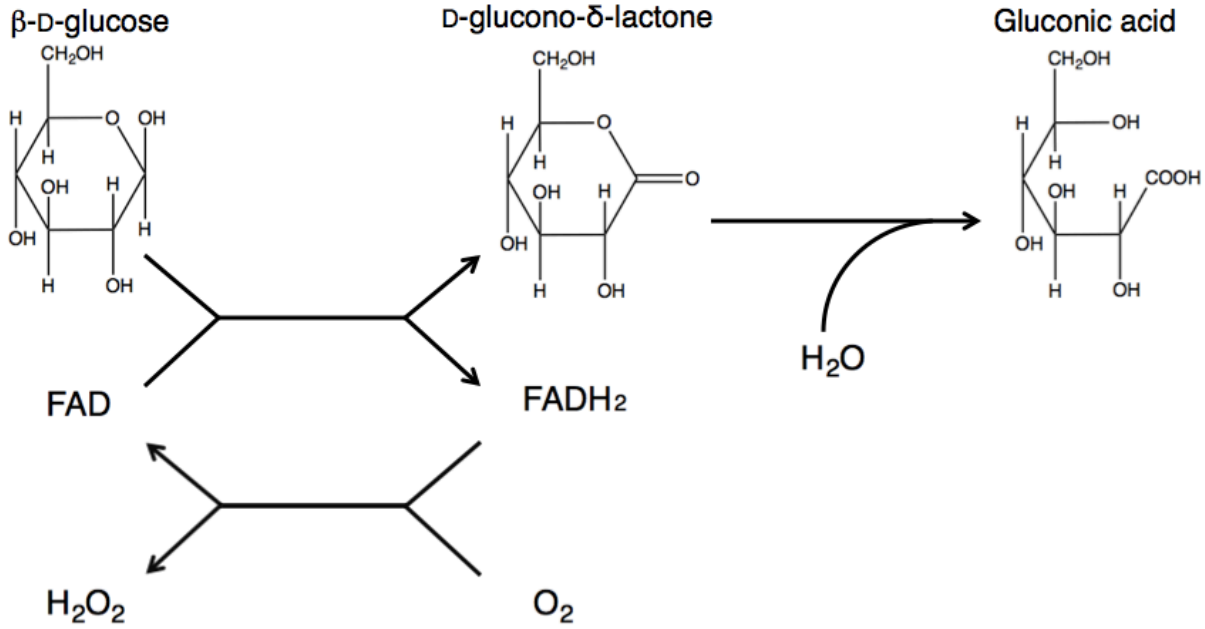

Figure 5: A more complete reaction for oxidation of β-D-glucose in GOx. As seen oxygen, water and glucose is used, and hydrogen peroxide and gluconic acid is produced. FAD and $FADH_2$ concentrations depend on the concentrations of other reactants and products.

As seen in Figure 5 oxygen is consumed in the reaction to oxidize $FADH_2$ to FAD. There are many glucose sensors based on the detection of changes in oxygen concentration [62-69]. H_2O_2 is a product of the re-oxidization of $FADH_2$, and many sensors measure H_2O_2 to determine glucose concentrations [70-76]. Some use the change in pH or gluconic acid concentration that occurs when glucose is oxidized [77-82]. Most glucose sensors are amperometric [83], and many of them utilize GOx [84-90]. Some other electrochemical sensors use GOx immobilized in a sol-gel matrix [91-93]. The electrochemical sensors measure the change in current and potential during the oxidization of glucose [94].

1.4.1 Using GOx fluorescence to measure glucose concentrations

A different way of using GOx to measure the β-D-glucose concentration is its intrinsic fluorescence [6]. There is no doubt that the tryptophan residues in GOx inhibits fluorescence [42, 95, 96], however there has been some debate concerning FAD and its fluorescent properties [33, 97]. Some claim both the reduced and oxidized form of FAD show fluorescence in solution [98], but no fluorescence from FAD bound to GOx is measurable [95, 96, 98]. A guess that two different types of apoenzyme exist, one that is fluorescent and one that is not, has been made [99]. Others write that both forms of FAD inhibit fluorescence in GOx [5, 33, 100]. When glucose is present in the solution some claim the intensity of fluorescence increases [101, 102], and some that it decreases [103, 104]. When GOx is immobilized in a silica gel and glucose is present some write the intensity of fluorescence rises [45], and some that is drops [101, 105].

In 1989 Trettnak and Wolfbeis [102] reported the first optical glucose sensor using the intrinsic fluorescence of GOx, with excitation at 450 nm and measurement > 500 nm. They had trapped a GOx solution between a dialysis membrane and Plexiglas which the excitation and emission light could travel through. Both UV light [106, 107] and visible light [11, 97] can be used to excite FAD. Sierra *et al.* used labeled GOx [96] to get higher intensities while avoid using UV light. Chudobova *et al.* have reported [11] bubbling with N_2 (g) to get a lower detection limit. In Table 1 some different results on range of fluorescence measurements on GOx are provided.

Table 1: Ranges for some glucose sensors in different matrices using fluorescence. *Dependent on concentration of dissolved oxygen, which was regulated from 0.1-100 % to achieve the result shown.

UV or VIS	Range	Matrix	Reference
UV	0.5-20 mM	In solution	[106]
UV	0-1 mM	In solution	[107]
UV	0-20 mM	Gelatine	[107]
VIS	2-10 mM	Nylon net	[11]
VIS	1-8 mM	Gelatine	[97]
VIS	1-5 mM	Agarose	[97]
VIS	0.05-0.5 mM	In solution	[97]

VIS	0.009-100 mM*	TEOS/hydroxyethyl carboxymethyl cellulose	[108]
UV (fiber optic)	0-5 mM	TMOS	[45]
VIS (fiber optic)	0-20 mM	TMOS	[45]
VIS (time-resolved)	0.4-5 mM	TMOS	[46]
VIS (fluorescent dyes)	0.6-5.6 mM	TMOS	[44]

Already in 2014 18 articles [70-72, 109-123] have been published on "Optical glucose sensors", however only one [72] utilize GOx, but is based on H_2O_2-detection, and does not use the intrinsic fluorescence of GOx.

1.5 Aim of this work

The aim of this work was to develop an optical biosensor for glucose using the intrinsic fluorescence of GOx. The enzyme was to be immobilized in a silica matrix and comparisons to the enzyme in solution, with regards to fluorescence intensity, were to be made. Another part of this work was the evaluation of a new and more biocompatible silane for the encapsulation of GOx.

2 Theoretical background

2.1 Fluorescence

The absorption and luminescence of light from a substance can be illustrated in a Jablonski diagram, seen in Figure 6. Fluorescence is the emission of light from a substance. It can occur after a substance has absorbed light, and an electron is excited to an energetically higher state. The electron returns to ground state and emits a photon, this is called fluorescence [8].

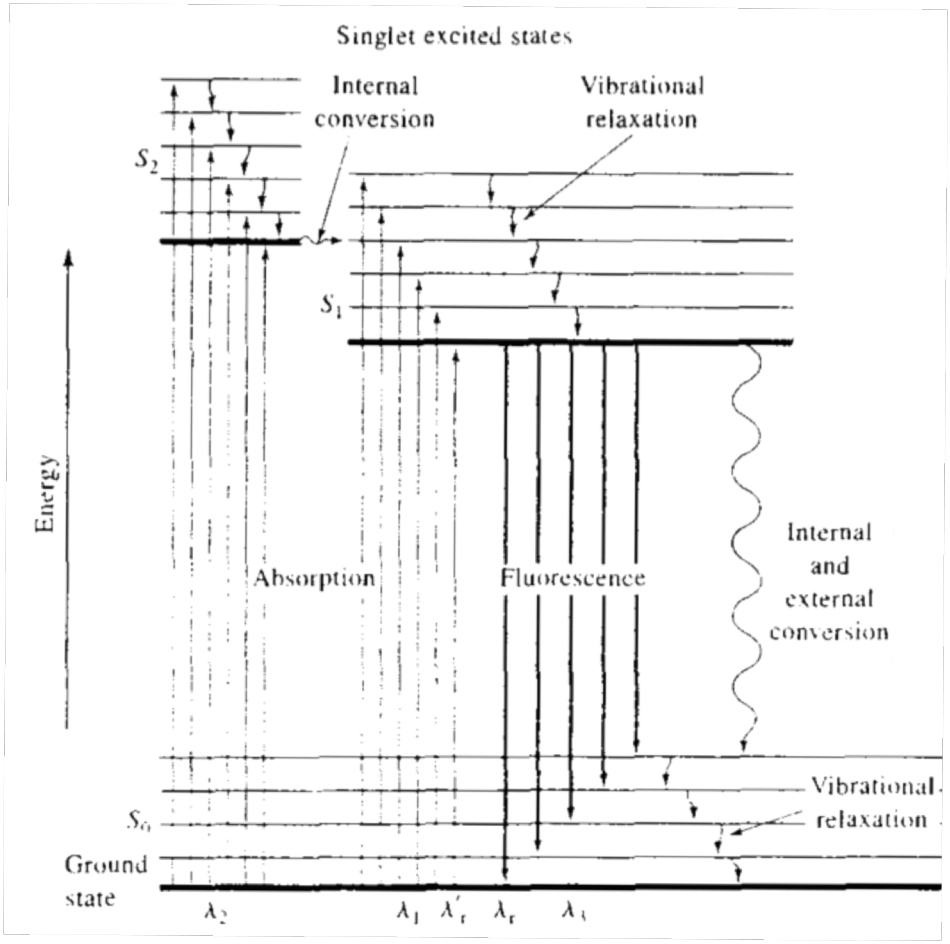

Figure 6: Jablonski diagram from Skoog et al. [124]. To the left absorption can be seen, on the top internal conversion and vibrational relaxation is seen, and in the middle fluorescence is seen.

The excitation of electrons happens within 10^{-15} seconds. At what light energy absorption happens is depended on the substance in question. The energy has to be equal to the energy needed to excite an electron. The electron can be exited to a range of different vibrational levels in different electronic states. S_0 is the notation for ground

state and the higher electronic states are denoted S_1, S_2 and so forth. Usually the electron quickly (10^{-12} seconds) relax to the lowest vibrational level of S_1 by vibrational relaxation and possibly internal conversion. The fluorescence lifetimes are generally close to 10^{-8} seconds. The excited electron is not stable, and returns to S_0 with the possibility of emitting a photon (fluorescence). Internal and external conversion, where the molecule only release heat is also a possible route for returning to ground state. After emission of a photon the electron commonly returns to a higher vibrational state of the ground state, before it quickly (10^{-12} seconds) relaxes to the lowest vibrational state of the ground state.

Because the electron usually undergoes vibrational relaxation between absorption and fluorescence, the energy of the emitted light is lower than that of the absorbed light. This is called the Stokes shift. Since the emission usually occurs to a higher vibrational ground state, the emission spectrum is often a mirror image of the absorption spectrum.

During the fluorescence lifetime quenching can occur, this is a collective term for all factors that decrease the intensity of fluorescence. Quenching results in heat being given off instead of a photon.

At low temperatures the relaxation to the lowest vibrational level of S_1 can be much slower than at room temperature. If the electrons return to ground state before relaxation to S_1 is complete, a blue shift of the emission peak will be seen [8]. It is therefore important to have control of temperature when measuring fluorescence.

Raman scattering is an inelastic scattering of a photon. The photon loses some of its energy, and scatters from the sample with a higher wavelength. For a water sample the wavenumber difference is 3600 cm^{-1}.

2.1.1 How the spectrofluorometer works

A typical spectrofluorometer is shown in Figure 7. Note that this is not the exact spectrofluorometer used for this work.

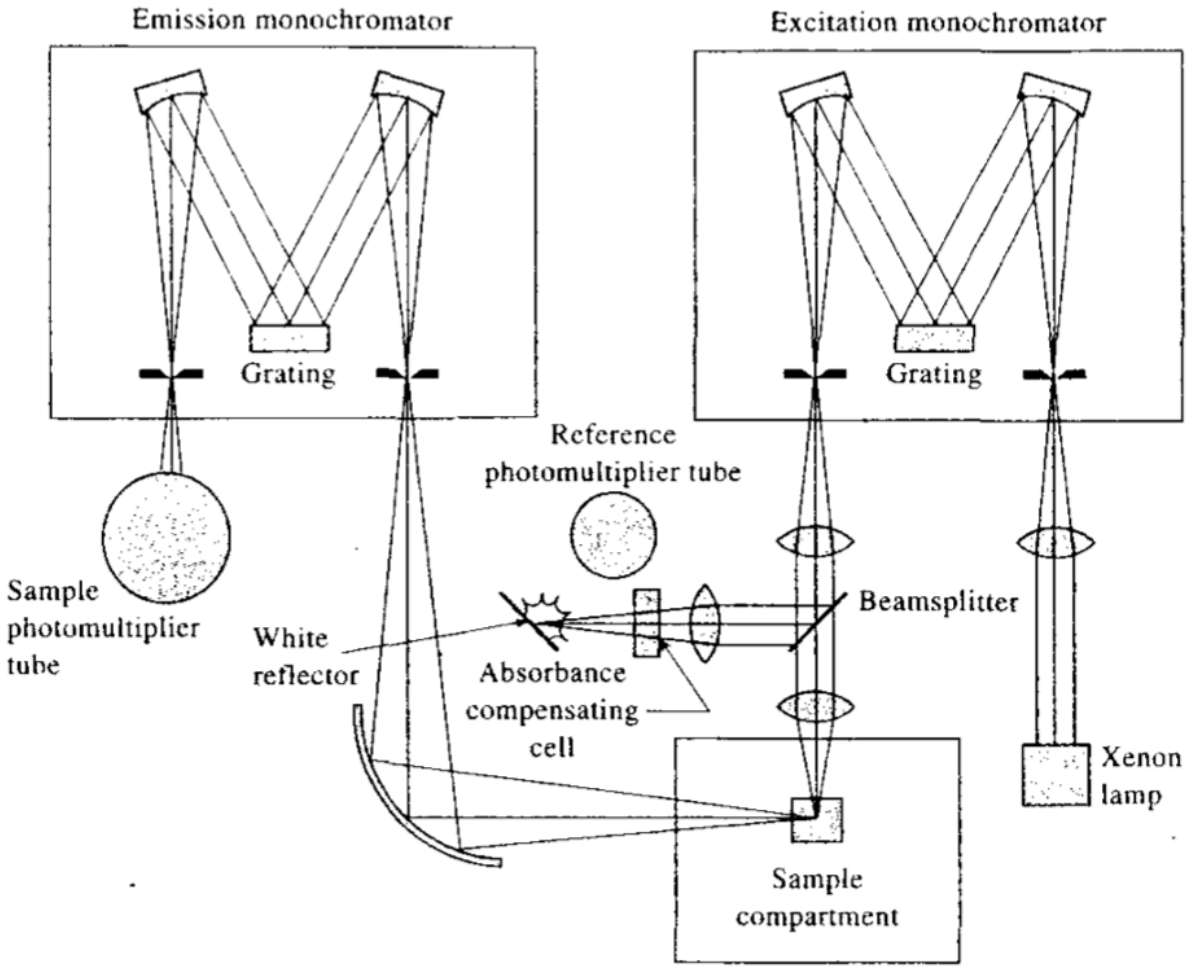

Figure 7: A general overview of a spectrofluorometer from Skoog et al. [124].

A xenon lamp emits light which is passed through a lens and an excitation monochromator which sends through light of a determined wavelength, or scans through different wavelengths at a given scan rate. The monochromatic light then passes through a excitation slit, a lens, and a beam splitter, which splits the light into a reference part of the instrument and the sample compartment. Notice that the detection of light from the sample compartment does not occur at 180°, but at 90°, allowing fluorescence and not absorbance to be measured. The light emitted from the sample passes through an emission slit and an emission monochromator fixed at a specific wavelength or scanning over multiple wavelengths. The monochromatic light is amplified and detected by a photomultiplier tube. In some spectrofluorometers, like the one used, there are also excitation and emission filters. Even though the monochromator is supposed to send out only one wavelength at a time, there are some common errors, like second-order transmission, which allows wavelengths half as long as the wanted

wavelength to pass. Excitation and/or emission filters can be used to remove unwanted wavelengths transmitted through the monochromator.

2.2 GOx and oxidization of β-D-glucose

GOx is a homodimer, each subunit weighing from 65 to 160 kDa, depending on the amount of glycosylation [125, 126]. The GOx used for this work had a total weight of 160 kDa. Each subunit has a tightly fixed FAD as seen in Figure 8. The FAD molecule is not covalently bound to any residues, but kept in place by a 31-residue lid [46].

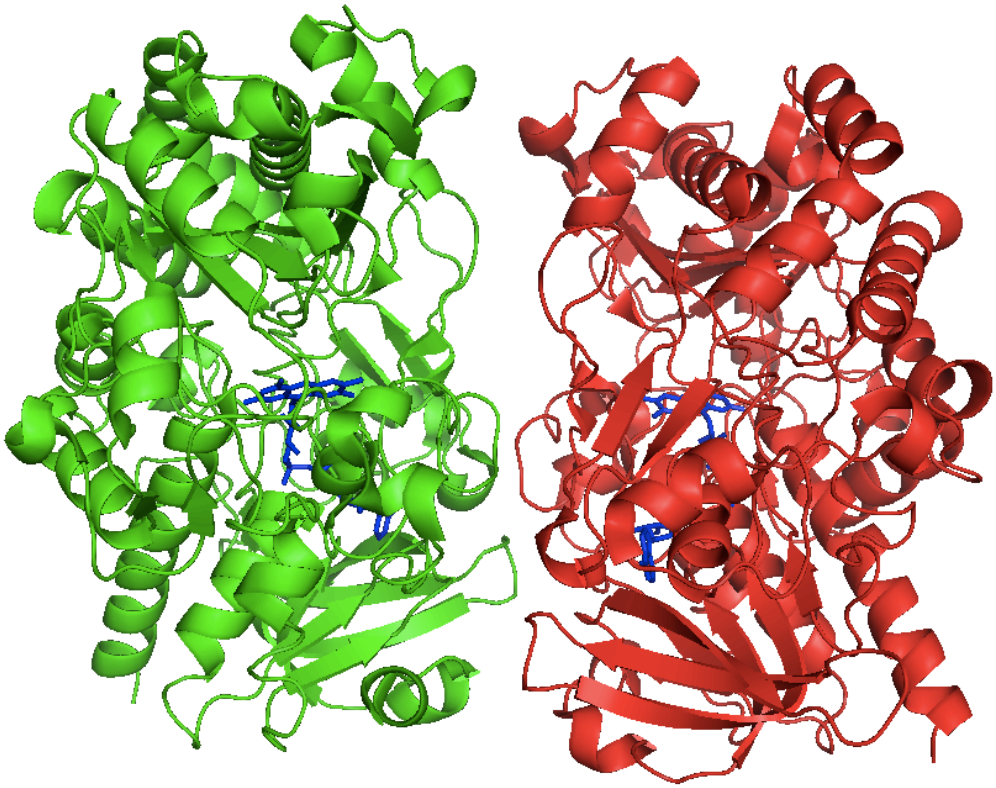

Figure 8: GOx and its tightly bound FAD. One subunit in green, and one in red. The FAD molecules are blue.

Alpha helices, beta sheets and random coils together with glucose in the active site in close proximity to FAD can be seen in Figure 9.

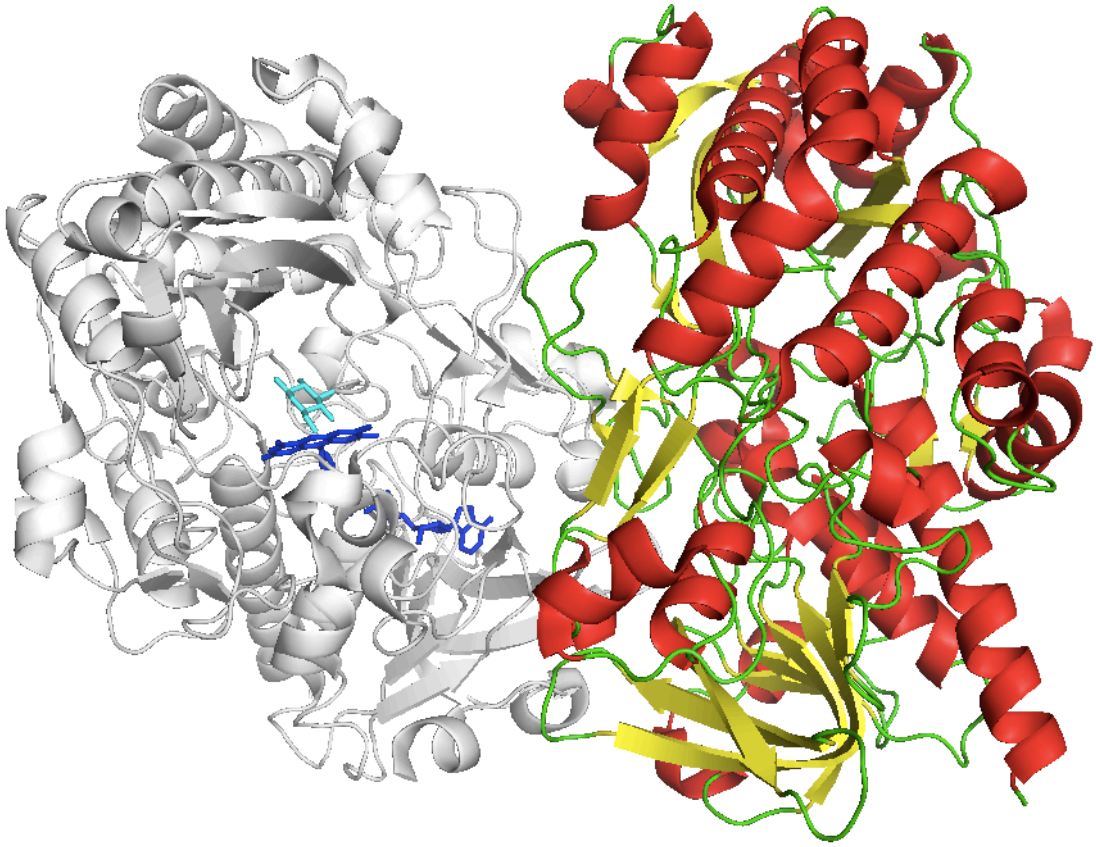

Figure 9: GOx, one gray subunit and one with red alpha helices, yellow beta sheets and green random coils. The cyan molecule seen in the active seat is β-D-glucose, and the blue molecule is FAD.

GOx catalyzes the reaction from β-D-glucose and oxygen to D-glucono-δ-lactone and hydrogen peroxide, utilizing the prosthetic group FAD. During the oxidation of glucose, FAD is reduced to $FADH_2$, and oxidized back to FAD under the presence of oxygen. The re-oxidization of $FADH_2$ produce H_2O_2. D-glucono-δ-lactone reacts with water to form gluconic acid. All reactions mentioned above can be seen in Figure 5. If catalase is present in the enzyme solution, it can catalyze the reaction from H_2O_2 to O_2 and H_2O.

The C1 carbon of glucose places itself between His516 and His559 as seen in Figure 10. The two histidines help stabilize the transition state between β-D-glucose and D-glucono-δ-lactone in the active seat [127]. His516 is central for the oxidization of glucose to take place [128], as it preserves the dipolar links of the active site. Molecular oxygen acts as the electron acceptor.

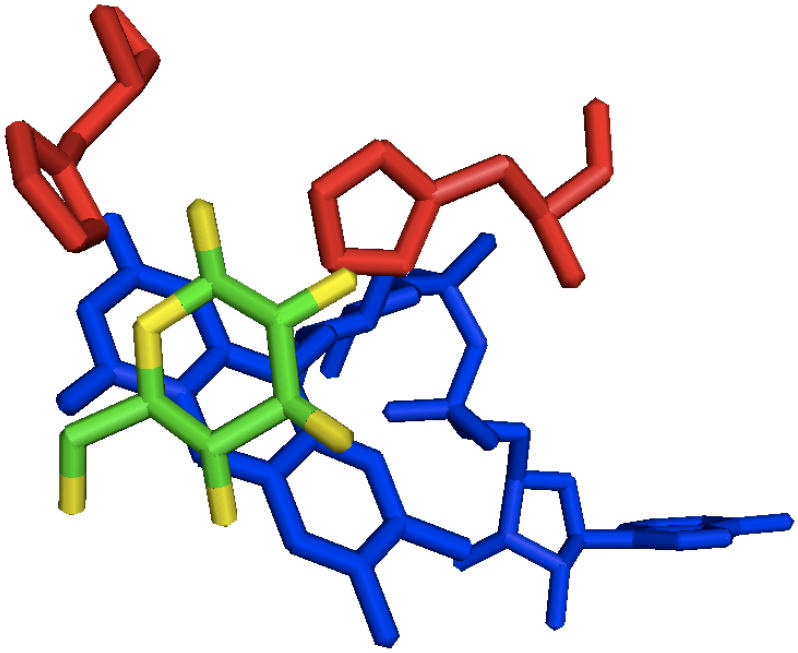

Figure 10: β-D-glucose (green carbons and yellow oxygens) in the active seat of GOx, FAD (blue), and histidines (red), 516 (right) and 559 (left)

The intrinsic fluorescence of GOx stems from tryptophan, tyrosine, phenylalanine and FAD. The amino acids absorb at 257 nm (phenylalanine), 274 nm (tyrosine) and 280 nm (tryptophan). Phenylalanine, tyrosine and tryptophan emit fluorescence at 282, 303 and 348 nm respectively. FAD absorbs with four peaks at 206, 275, 375 and 460 nm, and has an emission maxima around 520 nm [96]. FRET from tryptophan to FAD has been reported [95].

When FAD is in solution the isoalloxazine and adenine rings interact through a stacked confirmation both ground state and excited state [46, 129], this is also true when FAD is bound to GOx [101]. These two forms of FAD have different fluorescent properties, but can interchange in both ground state and excited state. Both species can absorb and emit light, but they have different lifetimes; ~2.8 ns for the open conformation and ~4 ps for the stacked conformation. In open form the FAD molecules are buried deep within each subunit [130], and the aromatic amino acids surrounding FAD quench the fluorescence strongly [99]. Unfolding of GOx leads to the release of FAD, and a immense increase in fluorescence is seen [99]. The addition of ethanol (EtOH) to the enzyme solution has also been reported to denature GOx, and increase the intensity of fluorescence [33]

The activity of an enzyme signifies at what rate it can catalyze the enzyme specific reaction. Activity is often measured in U/g (units per gram). One unit of GOx, will oxidize 1 μmole of β-D-glucose per minute at given pH and temperature [131].

2.3 Sol-gel process

TMOS and other orthosilicates in water can undergo hydrolysis, condensation, aging and drying to form sol-gel matrices [27]. Many of the reactions occurs simultaneously [132], and not as stepwise as it might seem in this explanation.
Hydrolysis and condensation for TMOS is seen in Figure 11.

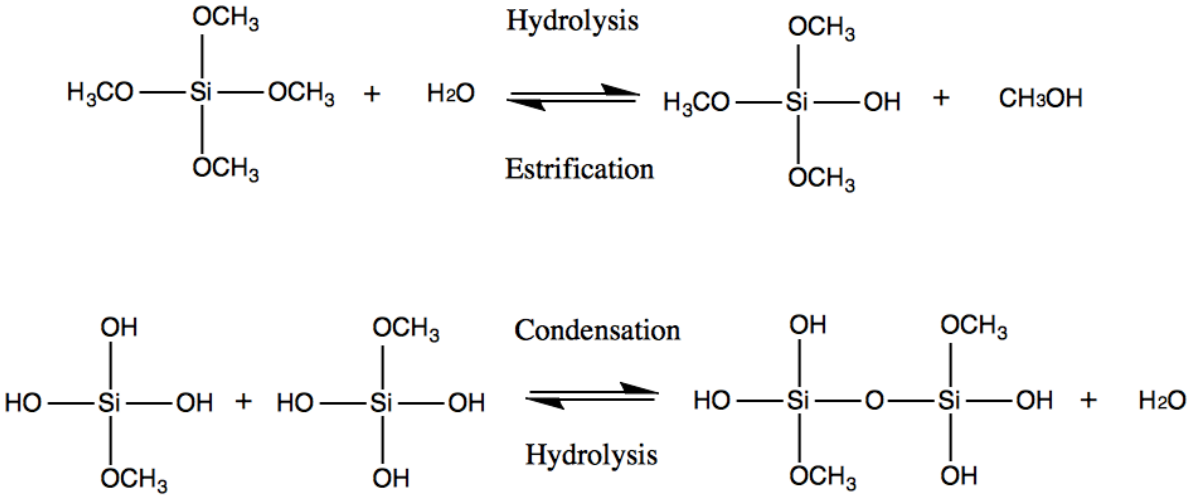

Figure 11: Hydrolysis, esterification and condensation of alkoxy silanes, here demonstrated with TMOS.

The reaction is usually either acid or base catalyzed. If not, the hydrolysis is usually very slow [27]. The water/silane-ratio is also important for the rate of hydrolysis [41]. A water/silane-ratio of 2 is theoretically enough to complete hydrolysis [41], but higher ratios lead to a higher rate of hydrolysis.

The size of the alkoxy group is of great importance for the condensation reaction rate because it can have a steric hindrance effect. The larger the alkoxy group, the slower the hydrolysis [132]. If the water/silane-ratio is large the concentration of $Si(OH)_4$ is low after hydrolysis, which cause a slow condensation [41].

After some polycondensation a structure like the one seen in Figure 12 is obtained. This is a simplification as not all of the oxygen atoms are protonated, except in a strong acid.

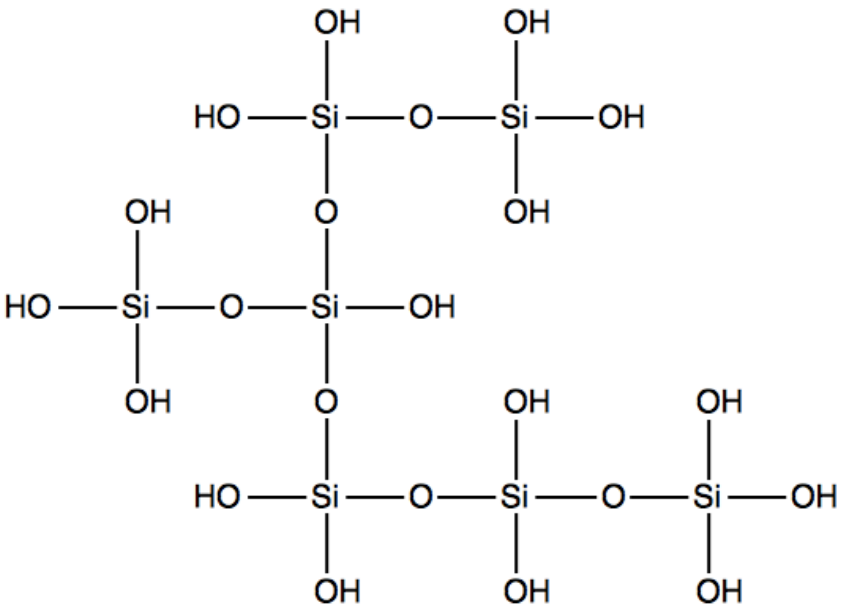

Figure 12: An example of a fully hydrolyzed and polycondensed TMOS.

The rate at which this reaction occurs depends on pH, the concentration of water and orthosilicate. A sol is formed, and the viscosity of the mixture increases. After some time a three dimensional network will be formed, when this happens the viscosity increases abruptly. It is now possible to see that the long-term product of the polycondensation will be a glass-like material (SiO_2). After the gel is solid aging is important. During aging the now solid gel is to allow the condensation to continue, and let the sol-gel based solid build strength to withstand the drying. Shrinking can be observed in the aging phase because polycondensation pulls the structure closed together [133].

After an appropriate time the solid is removed from the liquid and drying starts. The liquid inside the porous solid will now be removed, this can cause great capillary stress, and the solid can crack violently if the aging time was not adequate.

Further steps can be taken to make the solid stronger and more stable, however these involve heating the sol-gel based solid to temperatures that are not suitable for enzymes [133].

For DGS the sol-gel process is much the same, but both the hydrolysis and condensation can occur quickly without the presence of acids or bases [36].

3 Experimental

3.1 Chemicals

Chemical	Purchased from	CAS number	Purity/composition
D-(+)-Glucose	Sigma-Aldrich	50-99-7	≥ 99,5 %
GOx (E.C. 1.1.3.4) 50kU 123,900 U/g	Sigma-Aldrich	9001-37-0	Protein, 65-85 %
GOx (E.C. 1.1.3.4) 50kU 147,900 U/g	Sigma-Aldrich	9001-37-0	Protein, 65-85 %
GOx (E.C. 1.1.3.4) 50kU 228,253 U/g	Sigma-Aldrich	9001-37-0	Protein, 65-85 %
TMOS	Sigma-Aldrich	681-84-5	≥ 99 %
TEOS	ABCR GmbH & Co. KG	78-10-4	99 %
HCl	KeboLab	94-12-29	37 %
NaOH	AzkoNobel	1310-73-2	97-98 %
Fluorescein	Sigma-Aldrich	2321-07-5	≥ 99 %
Glycerol	VWR international	56-81-5	≥ 99.7 %
Triton® X-100	Sigma-Aldrich	9002-93-1	≥ 95 % (Laboratory Grade)
PBS-powder	Sigma-Aldrich	Product Number: P5368	BioPerformance Certified
H_2O	-	-	Double distilled

3.2 Measurements of fluorescence in solutions

Measurements of emission and excitation in solutions were done using a Varian Cary Eclipse Fluorescence Spectrophotometer with the software Cary Eclipse Scan Application v.1.1 (2002) which was always turned on at least 60 minutes before

measurements took place. The cuvette used was a Hellma precision-quartz cuvette, type SUPRASIL 101-QS with a path length of 1.000 cm.

In excitation experiments the setup seen in Table 2 was used. Excitation spectra were obtained by measuring the emission at a fixed wavelength while the excitation monochromator scanned through a range of wavelengths. So light of different wavelengths in turn illuminated the sample while the emission from the sample was measured at a fixed wavelength. For emission spectra the setup seen in Table 3 was used. For emission spectra the following was done; The excitation monochromator was fixed at a wavelength while the emission monochromator allowed an array of wavelengths through. Further details on spectrofluorometer settings can be seen in Appendix A.

Table 2: Settings for the spectrofluorometer for excitation experiments

What	**Setting/Value**
Software	Scan
Scan mode	Excitation
Emission wavelength	530 nm
Start wavelength for emission	250 nm
Stop wavelength for emission	520 nm

Table 3: Settings for the spectrofluorometer for emission experiments

What	**Setting/Value**
Software	Scan
Scan mode	Emission
Excitation wavelength	450 nm
Start wavelength for emission	480 nm
Stop wavelength for emission	600 nm

A java program for more efficiently process the data from experiments done with the spectrofluorometer was written. The reason for writing this program was that it was very time consuming to import all the data from the experiments into Excel, remove all the unnecessary values, find the average of the remaining data and subtract the zero

sample. This process also allowed for big errors, and a lot of annoyance. The program named “CSVXLS” reads .csv-files, finds the average of all the relevant data, asks if the user want values from a zero sample to be subtracted and writes the results to .txt-files. These .txt-files can then easily be imported into Excel to draw graphs or further analyze the data. The Java-code and other details on this program can be seen in Appendix C.

3.2.1 Calibration of temperature and time

To find the time it took for a solution to reach room temperature, which was 22.7 °C, from 0 °C, a temperature and time experiment was carried out. Four plastic vials containing 10 mL H_2O each were placed in an ice bath until the temperature was close to 0 °C, and then placed on the lab counter. The temperature was measured in consequent solutions every minute until the temperature was close to room temperature.

3.2.2 Making solutions for measurements

All GOx and glucose solutions were prepared the same day as the measurements took place. GOx, glucose and PBS solutions were all kept at 0-4 °C until the final hour before measurement, when they were left in room temperature.

GOx and glucose solutions were made by weighing out a specific amount of the enzyme/glucose with a Mettler AE200 Analytical Balance and dissolve it in a given amount of premade phosphate buffered saline (PBS) solution. One bag of PBS-powder made 1 L 0.01 M PBS, with pH 7.4 at 25 °C. To stir the solutions and measure temperatures a RCT IKAMAG® safety control with VT-5 S40 contact thermometer was used. When measurements were done with more than one concentration of glucose, one stock solution was made and the other concentrations diluted from that one. Pipettes used were VWR® Single-Channel, Ultra High-Performance Pipette with a range of 100-1000 µL and Eppendorf Research® with a range of 10-100 µL. It should be noted that the GOx containers bought contained 65-85 % protein. A composition of 75 % has been used for all calculations of concentration.

The mixing time for GOx-solutions and glucose solutions before measurements was between 40 seconds and 2 minutes for different experiments, but was kept constant for each separate measurement series.

3.2.3 Controlling the signal drift

The spectrofluorometer was tested for signal drift by using four identical PBS-solutions and four identical GOx-solutions in plastic vials. Determination of the signal drift was done by measuring the emission intensity at 530 nm, while the sample was excited at 450 nm. The solutions were treated similarly, but with some hours between the measurement of first and last sample, see Table 4 for details.

Table 4: Treatment of the solutions used for signal drift testing.

Solution and order of experiments	**Time the solution was in room temperature before the measurement was done**	**Time after last measurement**
PBS	1 h 21 min	-
GOx solution	1 h 20 min	30 min
GOx solution	1 h 26 min	36 min
PBS	1 h 10 min	14 min
GOx solution	56 min	86 min (two other experiments were done in between)
PBS	54 min	26 min
GOx solution	1 h 3 min	63 min (two other experiments were done in between)
PBS	55 min	22 min

3.2.4 Experiment on degassing of oxygen in solution

An experiment using nitrogen bubbling to remove oxygen from the solution was performed. This was done by pouring the appropriate solution in the cuvette and bubbling N_2 (g) into it by using frit purging for approximately 5 minutes. After bubbling the cuvette was quickly put into the spectrofluorometer and measured.

3.2.5 Assessment of background signal

By irradiating PBS in the cuvette at different wavelengths (435, 450 and 465 nm), but otherwise using the same settings as in Table 3, the background signal was examined.

3.3 In-lab-test of fluorescence

To make an in-lab-test of the fluorescence from GOx and fluorescein an Arduino UNO single-board microcontroller was used to make a RGB-light emitting diode (LED) emit light to mimic 450 nm. This was done by using the Macintosh built-in App "Digital Color Meter" V.4.4. and the spectrum in Figure 13 to determine the RGB-values for 450 nm. See Appendix D for programming of the RGB-LED.

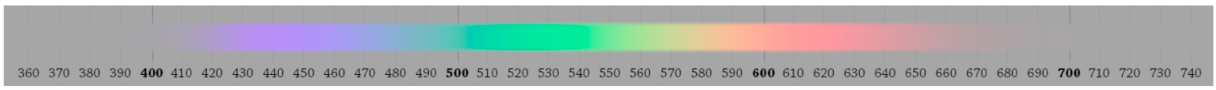

Figure 13: The visible spectrum used to find the RGB values of 450 nm [134].

In Figure 14 the Arduino UNO R3 can be seen with the breadboard, 330 ohm resistors, jumper wires and the RGB-LED (YSL-R596CR3G4B5C-C10) mimicking 450 nm. All parts are from "SparkFun Inventor's Kit for Arduino V3". The red wire is connected to the red pin, the blue wire to the blue pin, and the white to the green pin of the RGB-LED. The black wire is connected to ground. The USB seen leaving the picture at the left side is connected to a computer, and can also be connected to another power source.

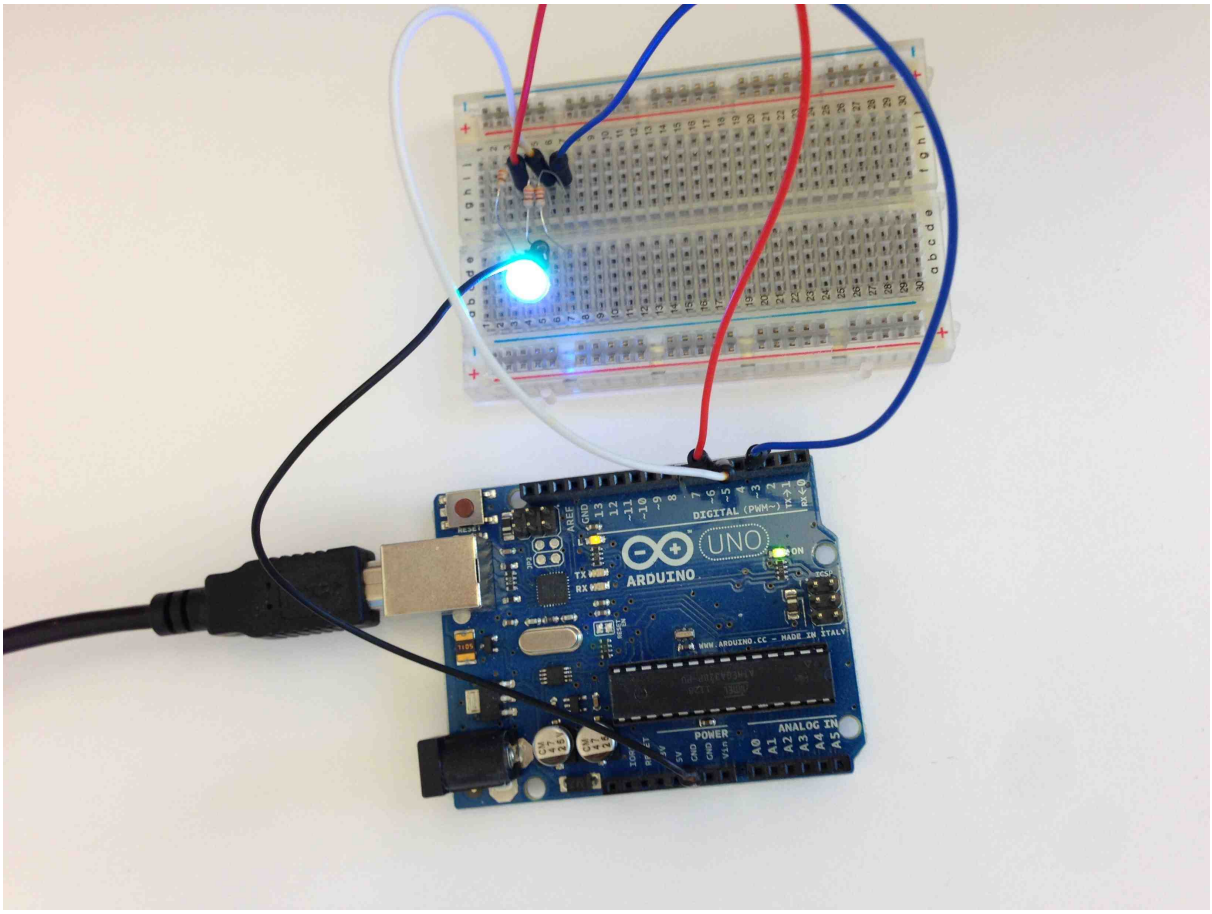

Figure 14: The Arduino with all the wiring done to make the RGB-LED emit light mimicking 450 nm.

3.4 Microcopy

All microscopy was done using an Olympus BX51TF microscope with PixeLINK Megapixel FireWire Camera Model Pl-A662. It was used with the software Linksys32 V. 1.6.1. All scales seen in the bottom right of the pictures were made by using the software's measurement function.

3.5 Synthesis and analysis of DGS

3.5.1 Synthesis of DGS

Using the recipe from Brook *et al.* [39], DGS was produced by weighing out 20.8 g (0.1 mole) TEOS and 18.5 g (0.2 mole) glycerol on a Mettler AE200 Analytical Balance, and stirring them in a round-bottomed flask placed in an oil bath. The oil bath was heated on

a Heidolph MR 3001 K with the temperature feedback probe set at 130 °C. The round-bottomed flask was fitted with a reflux condenser and a drying tube. After 43 hours a short path distillation head was fitted on the round-bottomed flask and EtOH was distilled of (a nuclear magnetic resonance (NMR)-spectrum was taken of the byproduct) while the oil bath still held 130 °C. After 1 h and 25 min traces of EtOH were evaporated in a Townson + Mercer (Altincham England) vacuum oven with the vacuum pump Speedivac ED 35 at around 140 °C for 2 h and 20 min. The flask was removed, the product was crushed, transferred to another glass container and placed in a desiccator under reduced pressure.

3.5.2 Analysis of DGS

Solid state NMR was done on a Ultra shield Bruker 500 WB Plus with Avance III apparatus, with an operation frequency of 500 MHz. The software used was Topspin v.3.0. Theoretical spectra were made in MestReNova BETA. Liquid state NMR was done on Bruker DPX 200, and Bruker AVII 400 instruments, controlled with Topspin 1.3 and Topspin 2.1 respectively. Infrared spectroscopy of DGS was done on a Bruker IFS 66v/S spectrometer. Mass spectrometry of DGS was done on a Bruker Apex 47e instrument.

3.6 Sol-gel derived thin-films

Cover glasses Ø 15 mm, thickness No. 1 purchased from Menzel GmbH & Co KG, cover glasses Ø 13 mm, Borosilicate glass thickness No. 1 purchased from VWR international and a 96 well polystyrene cell culture plate array from Greiner bio-one was used to apply the sol-gel based film on/in.

3.6.1 Experimental design with sol-gel derived films based on TMOS

Experimental design was used to determine what the best way of making TMOS based films was, using a modified version of the recipe from Portaccio *et al.* [45]. In Table 5 the different experiments and the variables examined can be seen, and in Table 6 the amounts used for all experiments can be seen. The three factors used to decide which

matrix was best were: transparency, cracks and other problems. All films got a score from zero (worst) to five (best).

Table 5: Treatment table used in experimental design, the films either contained acid or base, included Triton® X-100 or not, and was applied on glass or polystyrene.

Experiment number	Catalyst	Triton® X-100	Applied on
1	Acid	With	Glass
2	Acid	With	Polystyrene
3	Acid	Without	Glass
4	Acid	Without	Polystyrene
5	Base	With	Glass
6	Base	With	Polystyrene
7	Base	Without	Glass
8	Base	Without	Polystyrene

Table 6: Amounts and concentrations for the experimental design.

Chemical	Amount
TMOS	516.7 µL
H_2O	150 µL
Triton® X-100	30 µL
HCl (40 mM)	10 µL
NaOH (40 mM)	10 µL

3.6.2 The recipe used for TMOS based films

The substances in Table 7 were weighed out using a Mettler AE200 Analytical Balance or pipetted out using VWR® Single-Channel, Ultra High-Performance Pipette with a range of 100-1000 µL and Eppendorf Research® with a range of 10-100 µL and stirred for 1 hour in an ice bath on a RCT IKAMAG® safety control. The mixture was then stirred with PBS 1:1 (v/v), for 5 minutes before the sol was applied onto glass plates or into wells in the plate array.

Table 7: Modified sol-gel recipe using TMOS from Portaccio et al. [45]

Chemical	Weight/Volume
TMOS	2000 µL
H_2O	600 µL
HCl (40 mM)	40 µL
Triton-X-100	0.137_6 g

3.6.3 Making sol-gel films with DGS

A recipe patented by Brook *et al.* [36] was used to make sol-gel derived films with DGS. See Table 8 for the substances weighed using a Mettler AE200 Analytical Balance or pipetted out using VWR® Single-Channel, Ultra High-Performance Pipette with a range of 100-1000 µL.

Table 8: Recipe for sol-gel films with DGS from [36].

Chemical	Amount
DGS	0.20 g
H_2O	600 µL

DGS was sonicated with ice-cold ddH_2O, in a Brandson 3510 ultrasonic bath at 0 °C for 10 minutes. When the DGS was dissolved, the mixture was filtered and stirred with PBS 1:1 (v/v) for 5 minutes. The sol was then applied onto glass plates or into the wells of the plate array. The PBS-solution contained different concentrations of GOx or Fluorescein. A Sartorius M-pact AX2202 weight was used to weigh fluorescein.

3.7 Experimental setup with optical fibers

The 3D printer used was a 3D Touch BFB-3000 Plus. Figures were drawn in SketchUp Make V.13.0.4811, and converted using Axon 2 V.2.1.0.

The experimental setup used to measure fluorescence in sol-gel plates can be seen in Figure 15, and a setup for plate array with a groove plate as can be seen in Appendix H.

The reflection probe QR200-REF-UV-VIS with reference leg from Ocean Optics was used to measure the fluorescence in the 96 well polystyrene cell culture plate array from Greiner bio-one. The probe contains six illumination fibers around one read fiber, and all fibers have a core diameter of 200 µm. An optical fiber of the type F600-UV/VIS-SR was used between the xenon lamp from Avantes named AvaLight-Xe and the emission filter, which was a band pass filter from Semrock with part number: FF01-448/20. An optical fiber of the type FC-UV/NIR200-2 was used between the excitation filter; a long pass filter from Semrock with part number: FF01-496/LP, and the Avantes spectrophotometer, AvaSpec-2048-USB2. Both filter holders were Avantes FH-INL (In-Line Filter Holder), and the power supply for the light source and spectrophotometer passed through an UPS of make Cyperpower BR850ELCD. All this equipment was placed on an optical table. The software used was Avasoft 7.3.1 with the settings seen in Table 9.

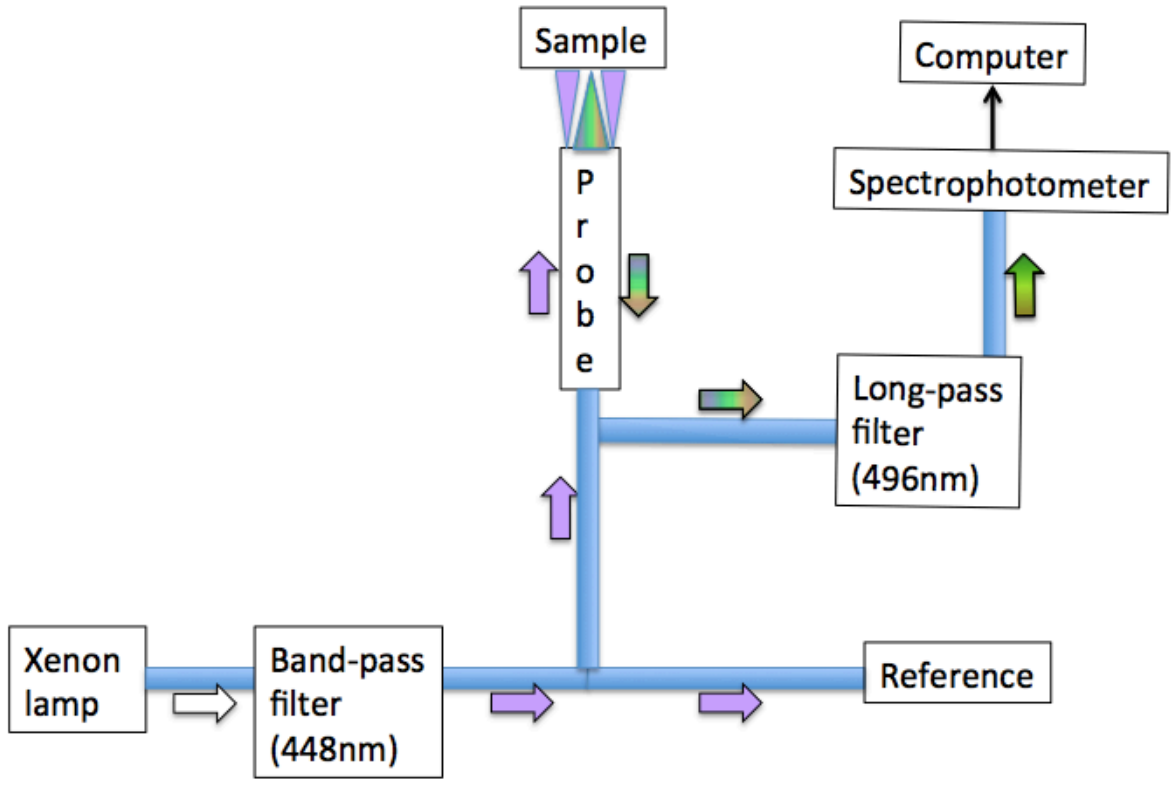

Figure 15: Setup for measurements with optical fibers. The probe has six illumination fibers, but the light from only two can be seen in this figure. The arrows indicate light direction and what wavelengths of light travels trough the specific part of the fiber.

Table 9: Settings in the Avasoft software.

What	Setting/Value
Average of	1 scan
Integration time	10 000 ms
Number of flashes	1000 flashes

10 spectra were recorded for each sample, and the average was calculated in Microsoft Excel. The setting used gives the maximum number of flashes per second for the Xe-lamp used, which is 100 Hz.

The optimal distance from the probe to the sample was located using 1 mM fluorescein immobilized in a DGS-matrix. Avasoft was running with the settings seen in Table 10. The probe was moved closer and further away from the plate array until the maximum intensity was discovered. Then the probe was secured at that position. Then both the excitation and emission filter houses were adjusted so that the maximum intensity was seen.

Table 10: Settings in the Avasoft software for optimizing the distance between the probe and plate array.

What	Setting/Value
Average of	1 scan
Integration time	1000 ms
Number of flashes	100 flashes

To measure the fluorescence, first the probe was placed under a well with a DGS derived film, the light from the xenon lamp was switched off, and the whole setup was covered so no light entered from above. The value obtained from this setup was saved as a dark reference. Then measurements were performed, and the plate array was moved around to measure in all the appropriate wells, with the dark values automatically subtracted from the intensities measured. After all the wells with GOx were measured, PBS was placed in one well with GOx immobilized in DGS and measured. Then different glucose concentrations were placed in the other GOx-DGS wells and measured.

4 Results and discussion

4.1 Measurements of fluorescence in solutions

Before attempting to make an optical biosensor with GOx immobilized in a sol-gel matrix, some preliminary testing had to be done. The first test was to check how long a solution at 0 °C took to reach room temperature. The second important test was to see if GOx inhibited an intrinsic fluorescence, if it is possible to use the reported excitation maxima at 450 nm, and whether the intensity of the fluorescence of GOx increased or decreased when oxidizing β-D-glucose, since this has been a matter of debate in the literature.

Shown in Figure 16 are the results of the temperature and time experiment. The solutions started at 0 °C and approached room temperature (22.7 °C).

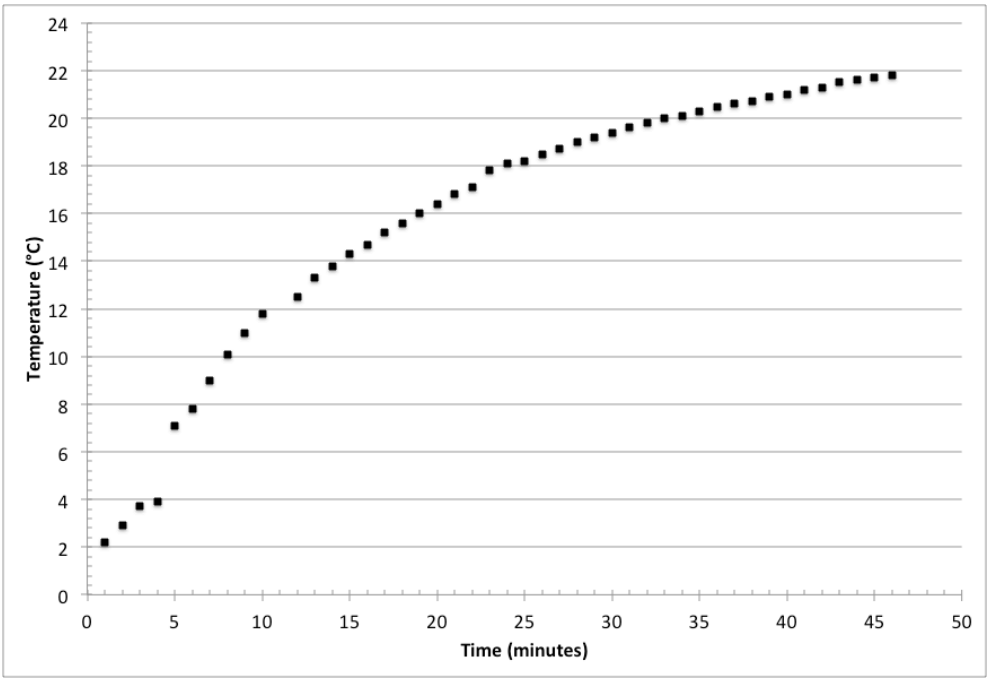

Figure 16: The time it took for 10 mL H_2O to reach room temperature in a plastic vial.

The first of the plastic vial was placed on the magnetic stirrer, which held a lower temperature than the lab counter, so the first four measurement points in the graph in Figure 16 can be disregarded. It was determined from the graph that 60 minutes in room temperature was a sufficient time to stabilize the temperature in the solutions.

This result was used for all measurements done in solutions with the spectrofluorometer, as they were all left out for 60 minutes before they were mixed and measured. One reason for letting the temperature increase from 0 °C was the temperature dependency of fluorescence written about in the theoretical background. The reason for keeping the solutions at 0 °C in the first place is to hinder denaturation of the enzyme.

The solutions were mixed a given time before the measurements took place. This was so that the solutions could become homogenous, and an equilibrium could be reached. The specific mixing time changed somewhat during the two years of study, but was kept between 40 seconds and 2 minutes.

As seen in Figure 17 the enzyme shows fluorescence at 530 nm with varying intensities when excited at wavelengths from 250 nm to 520 nm. FAD and $FADH_2$ tightly bound to GOx display a clear difference in excitation intensities. 530 nm was chosen as the wavelength to examine excitation because of many reports on wavelengths around 530 nm being effective [46, 97, 101, 102].

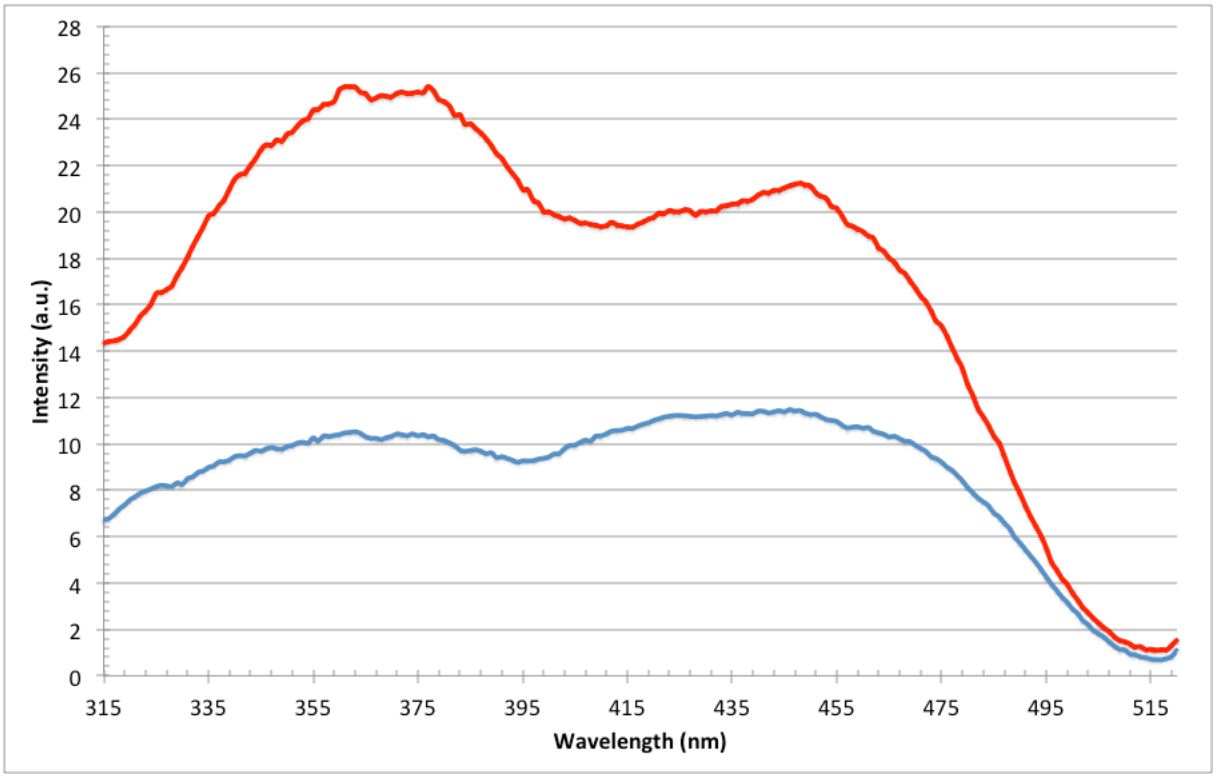

Figure 17: Excitation intensity of GOx (536.5 U/mL PBS) without glucose (■) and with 2 mM glucose (■), measured at 530 nm.

Using the parameters from Table 2, or the detailed version in Table 14, Appendix A, the spectrum in Figure 17 was obtained. A detailed version of this spectrum can be seen in Appendix B. In Figure 17 it is apparent that the maximum excitation of GOx without glucose can be achieved at approximately 450 nm, while the maximum excitation of GOx with glucose can be reached at around 370 nm, when measuring excitation intensity at 530 nm. In other words FAD has an excitation maximum at 450 nm, and $FADH_2$ has an excitation maximum at 370 nm, which is similar to the absorption maxima which Ghisla *et al.* [98] (355 and 452 nm for "reduced" and "oxidized" GOx respectively) and Sierra *et al.* reported (375 and 460 nm for FAD and $FADH_2$ in general).

Based on the spectra above a wavelength of 450 nm was chosen to excite the FAD in GOx. One major reason for choosing 450 nm over 370 nm is that 450 nm is in the visible part of the electromagnetic spectrum. Many biological substances absorb UV light [5, 106], and when to ultimate goal is to create a glucose sensor for *in vivo* use [5, 102], this wavelength did not seem like a logical choice. Another advantage is that one does not need the cuvettes, optical fibers and other glassware to be made of expensive quartz.

When measuring the fluorescence while the sample was excited at 450 nm the spectrum seen in Figure 18 was attained. As seen FAD and $FADH_2$ emits light with a single peak at approximately 530 nm, with a clear difference in intensity. This result indicates that the intensity of fluorescence is increased when GOx reacted with glucose in solution, contrary to what Eftink [103] and Yoshimoto *et al.* [104] reported, but identical to what Trettnak and Wolfbeis [102] and Harnett *et al.* [101] reported.

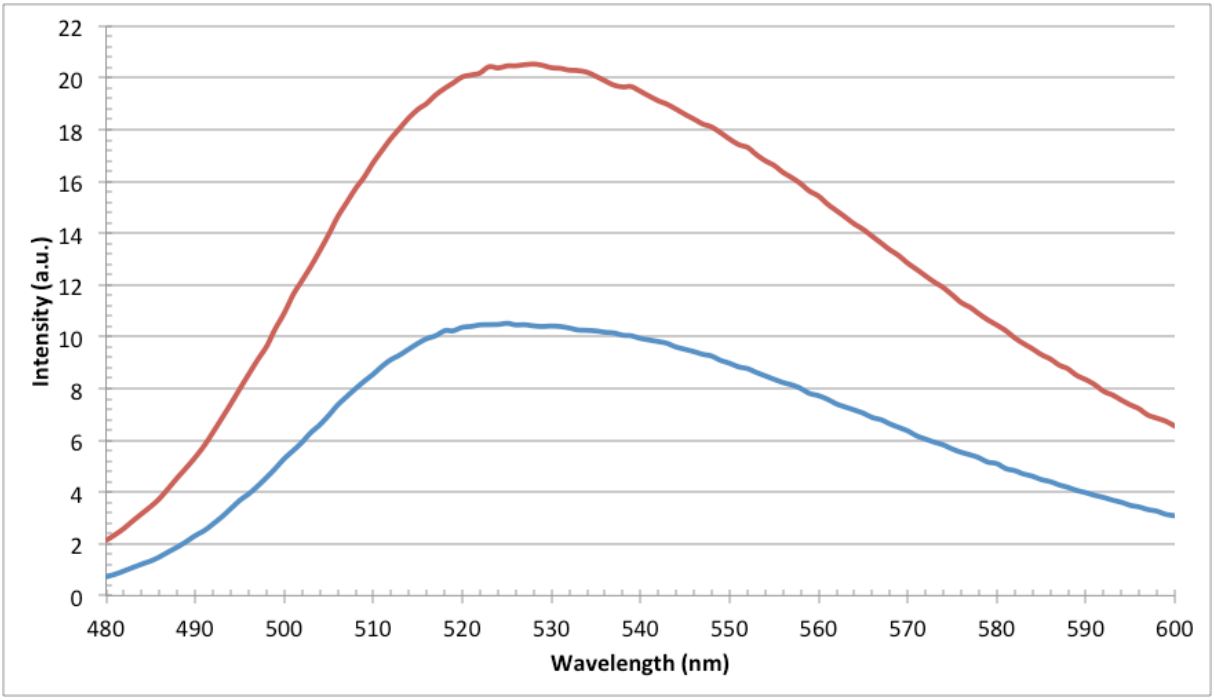

Figure 18: Emission spectrum of GOx (536.5 U/mL PBS) without glucose (■) and with 2 mM glucose (■), both in PBS solution. Excitation at 450 nm.

4.1.1 Control of signal drift in the spectrofluorometer

Signal drift in the spectrofluorometer could greatly impede the analysis of the attained spectra, therefore a test was commissioned. The results for control of signal drift with zero sample (PBS) and GOx can be seen in Figure 19. Emission intensities at 530 nm, when the sample was excited at 450 nm were measured. No strong signal drift was observed, however there might be some weak signal drift between the last two measurements for both zero sample and GOx. Error bars are present for both lines and are only around 1 % for each point. The solutions were not out in room temperature the exact same length before measurement, this can of course also affect the result, but there is no clear correlation between the time in room temperature before

measurement and intensity. For the remainder of this work it was assumed that the spectrofluorometer did not show any signal drift.

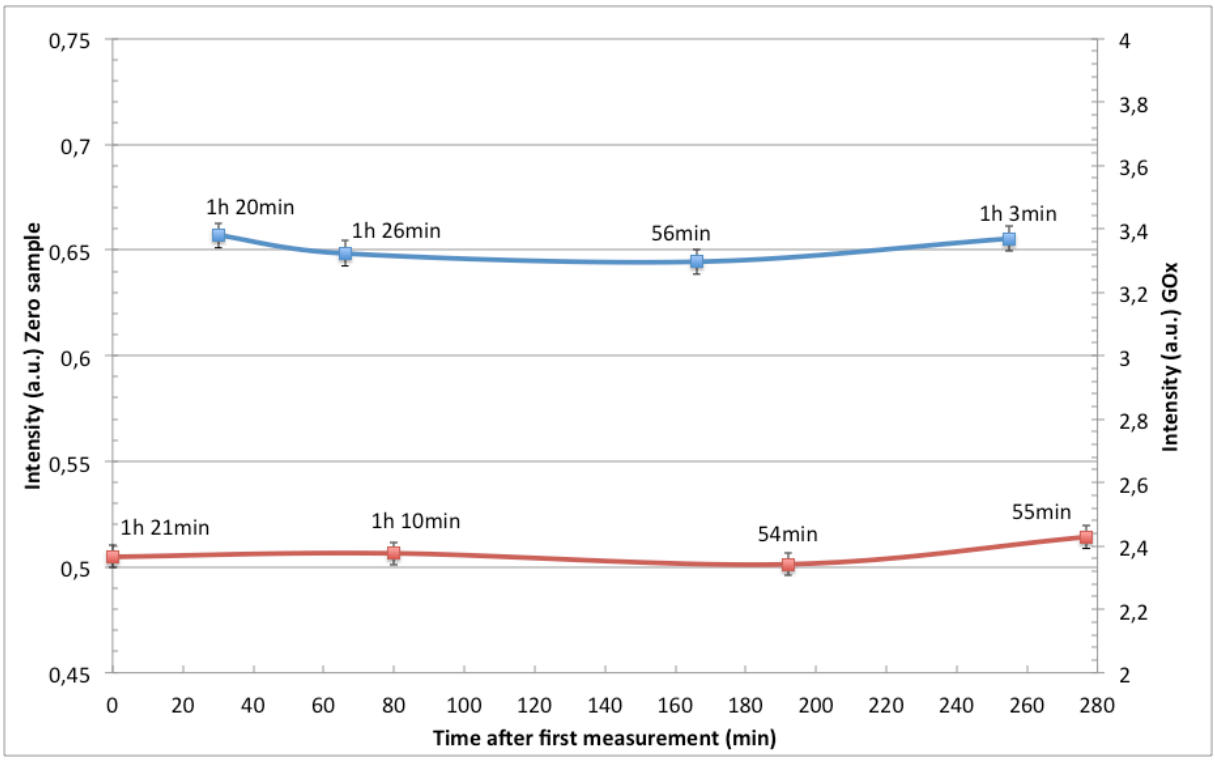

Figure 19: Signal drift control with zero sample (■) (PBS – left axis) and GOx (■) (right axis) (46.5U/mL PBS). The time the solution was out of ice bath is noted above each point. The intensity was measured at 530 nm. Excitation 450 nm.

4.1.2 Degassing of oxygen from solution

A report [11] has been made on the benefits on degassing oxygen from the GOx solution by bubbling it with nitrogen to decrease the detection limit. See Figure 20 and Figure 21 for the results for bubbling nitrogen into the cuvette before measuring with the spectrofluorometer.

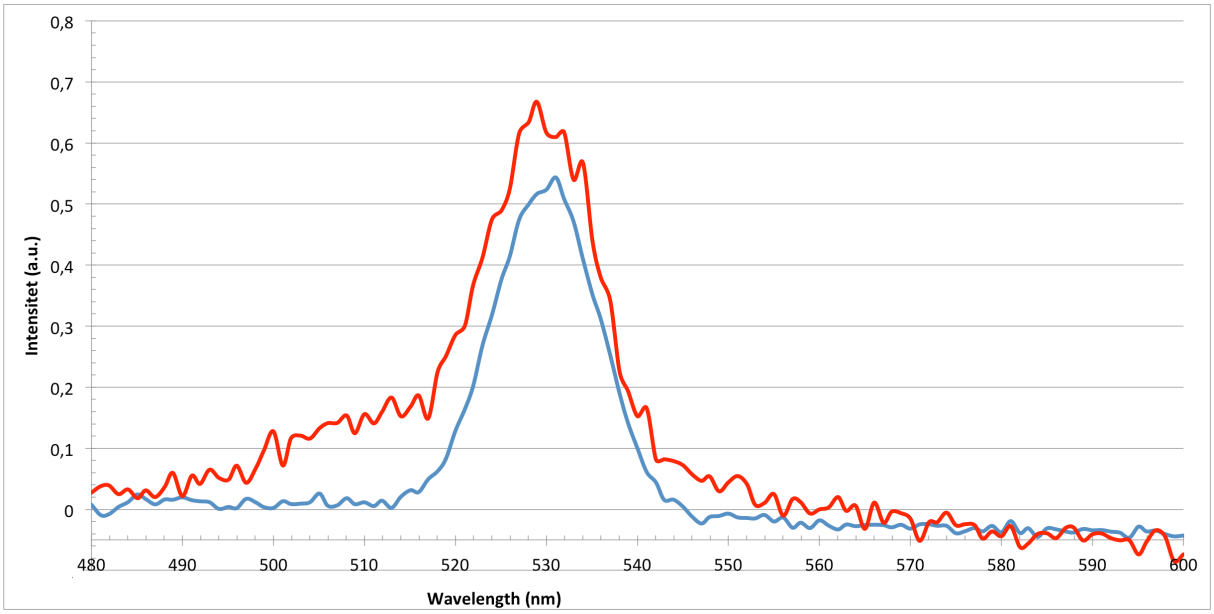

Figure 20: Emission spectrum of zero sample (PBS). Excitation at 450 nm. Untreated zero sample (■) and zero sample degassed with N_2(g) (■).

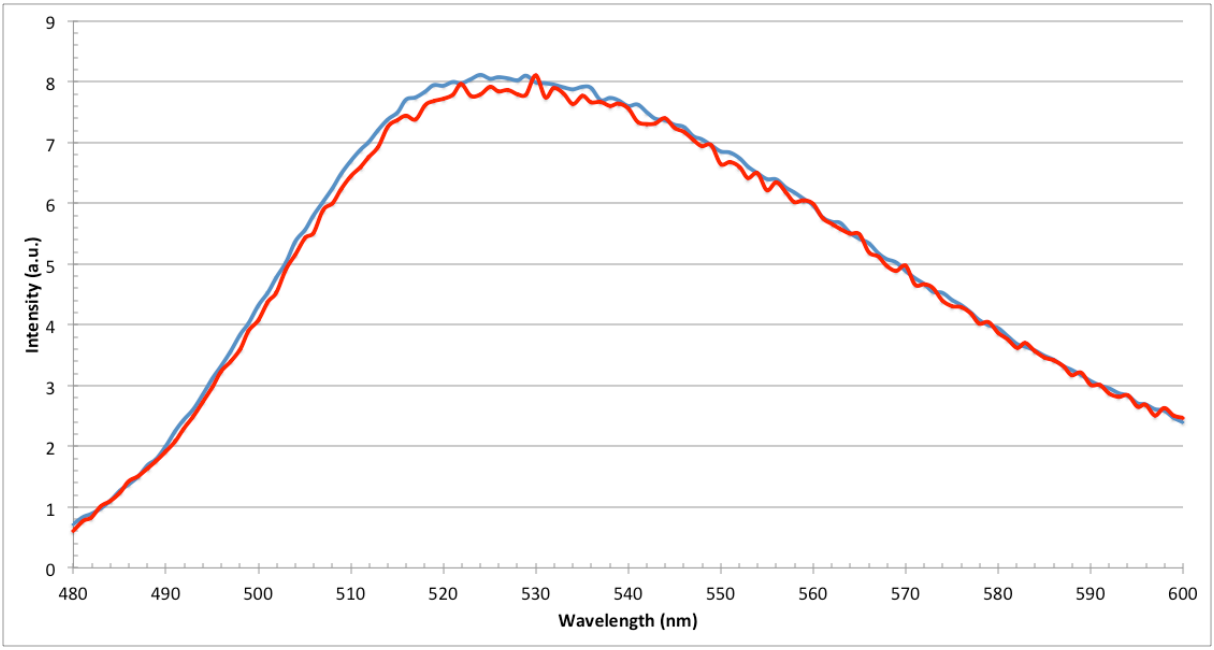

Figure 21: Emission spectrum of GOx (23 U/mL PBS). Excitation at 450 nm. Untreated GOx (■) and GOx degassed with N_2(g) (■).

It seems that the intensity of the Raman scattering increased since the difference between the peak intensities is about 20 %. It must however be mentioned that the graph for the untreated PBS is an average of 20 scans, whereas the graph for the nitrogen bubbled PBS is the average of only 2 scans, so the results after N_2 (g) bubbling are not reliable. It is however strange that the intensity of Raman scattering apparently

change after nitrogen bubbling. If there still were tiny bubbles in the solution at the measurement time, or dust in the zero sample, this could explain the strange result. The reason that only two scans were obtained was that it was very hard to control the rate of which nitrogen was bubbled into the system, as the gas valve was very sensitive. It was therefore difficult to know it the same amount of nitrogen had been bubbled through the solutions. The time between degassing the solution and measurement is important, because the solution after being bubbled with nitrogen is not in equilibrium. If more scans were to be taken of the degassed PBS and/or GOx solutions, a setup with the possibility of degassing the sample with high precision while it was measured was probably needed. Or a sealed system where the nitrogen concentration stayed stable throughout the measurement. In Figure 21 the nitrogen bubbled GOx appears to have a slight decrease, however the difference is only about 1 %, which is not greater than the standard deviation for the GOx measurements. As for the zero sample, the graph for the degassed GOx is the average of only two measurements. Due to the results and problems with degassing of the samples, nitrogen bubbling was not looked further into in this work.

4.1.3 Assessment of background spectrum

The results from the first experiment using the fluorescence spectrophotometer showed a contorted spectrum, see Figure 34 in Appendix E. The activity of GOx was very low, only 4.2 U/mL, so it was assumed that something else was sending light into the detector. A background spectrum of the zero sample was therefore subsequently subtracted from all the spectra with GOx in PBS.

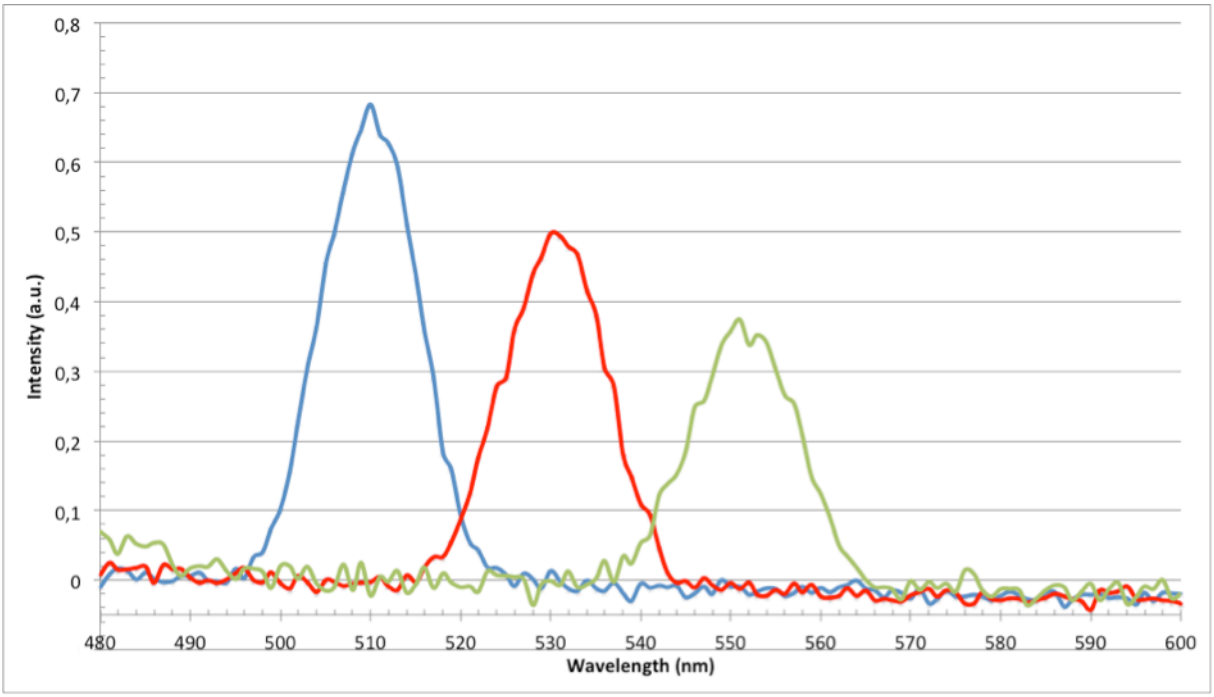

Figure 22: Intensity spectrum of zero sample (PBS solution). Excitation with three different wavelengths: 435 nm (■), 450 nm (■) and 465 nm (■).

In a later experiment, the results of which can be seen in Figure 22, it was discovered that the peak seen around 530 nm in reality is Raman scattering. The spectra captured before the discovery of Raman scattering are still correct because the background spectrum was subtracted. In Figure 23, a spectrum of GOx emission with and without the Raman scattering peak can be seen. It is evident why a background spectrum must be subtracted. In the spectrum in Figure 23 the peak intensity is around 10 % higher with the Raman peak than without.

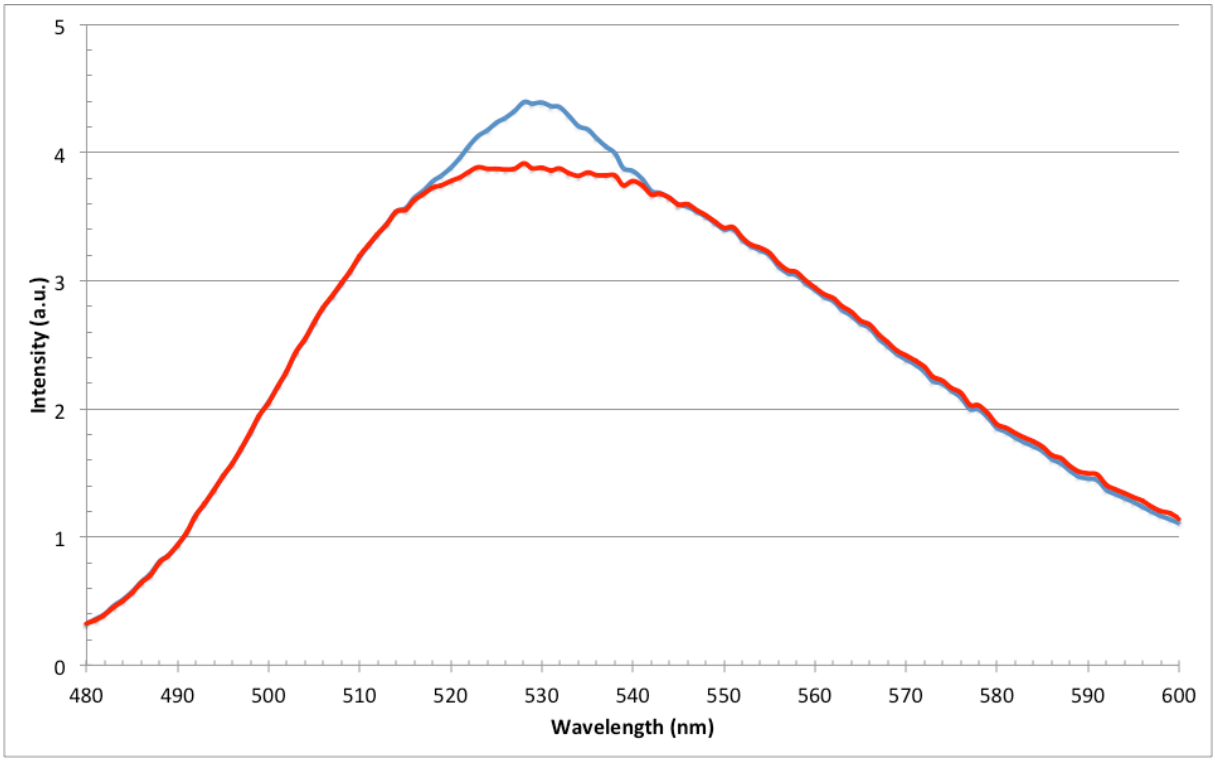

Figure 23: Emission spectrum of GOx (46.5 U/mL PBS) without subtraction of background spectrum (■), and with subtraction of background spectrum (■).

4.1.4 Linear range for glucose concentration measurements

The linear range of glucose concentration possible to measure with GOx in solution was to be determined. Many emission spectra were obtained with different glucose concentrations in GOx solutions with equal activity. The intensities at 530 nm were used to plot the results seen in Figure 24. A zoomed in version can be seen in Figure 25. It is clear that the intensity of GOx change when it is oxidizing glucose, however the linear range was not determined as the glucose concentrations either gave maximum or minimum intensity. A small increase can possibly be seen between 0 and 0.625 mM glucose, but it is not clear. If the point at 0.75 is omitted a graph which looks like the one Lepore *et al.* [97] reported could be seen. However the standard deviation for this point is only 0.17 arbitrary units, so it seems it can not be removed.

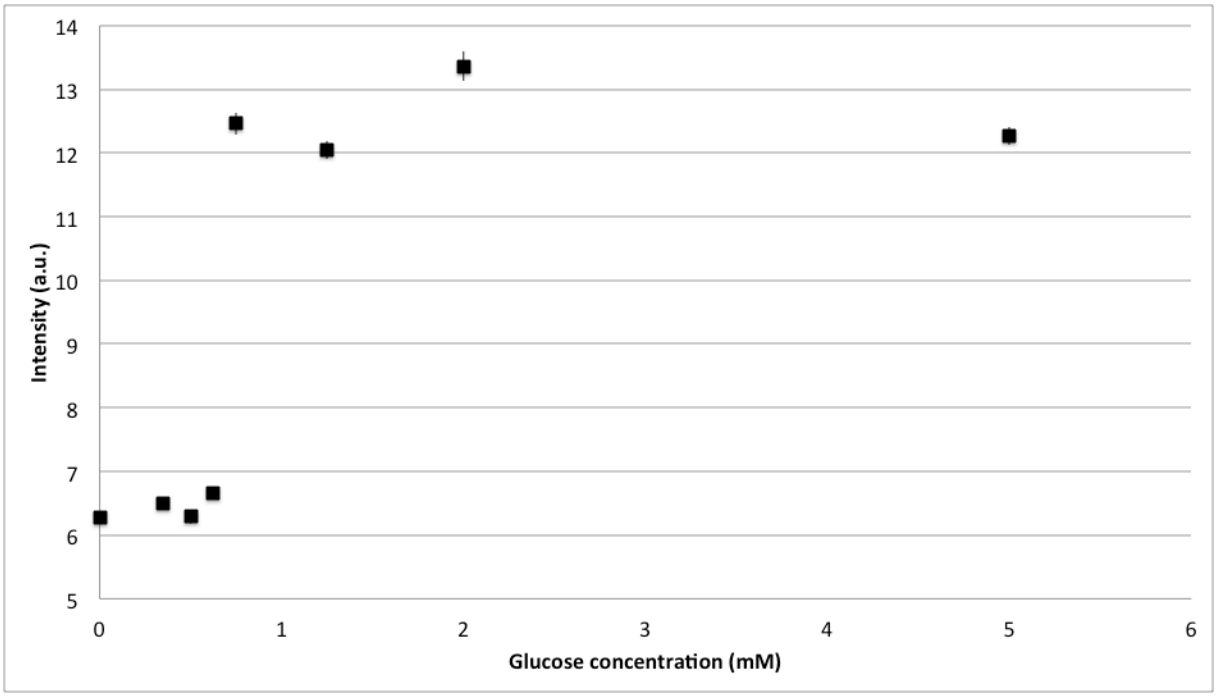

Figure 24: Emission intensity at 530 nm for GOx (856 U/mL PBS) with different concentrations of glucose.

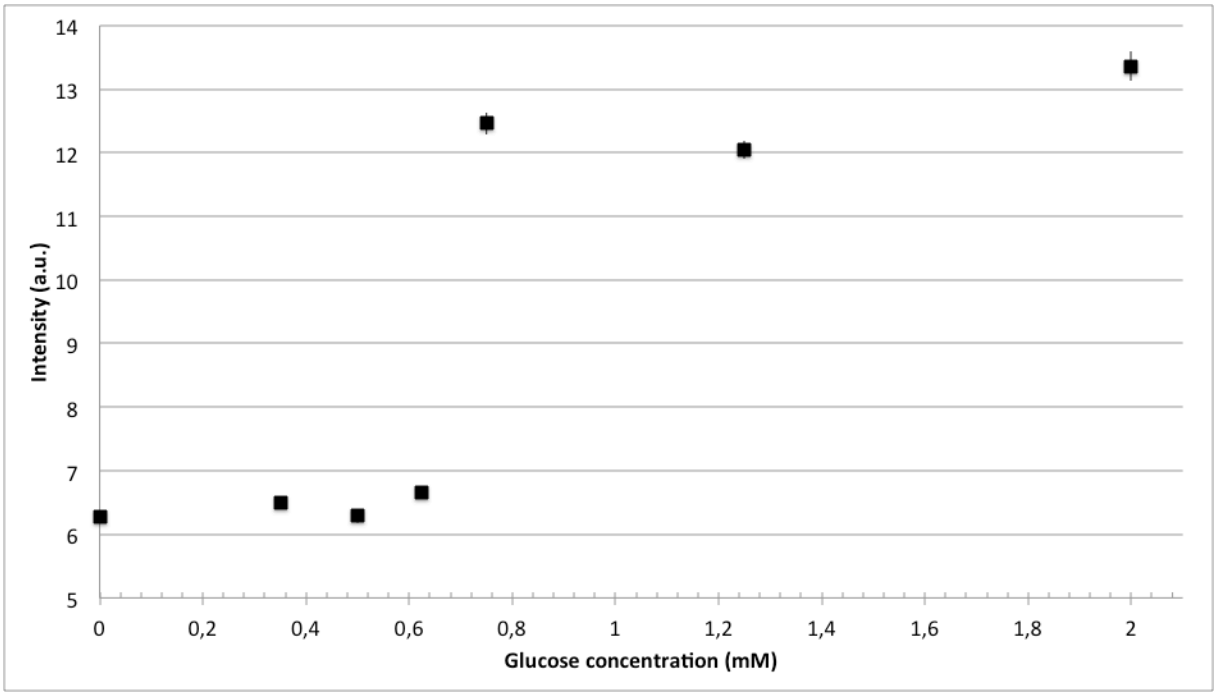

Figure 25: Emission intensity at 530 nm for GOx (856 U/mL PBS) with different concentrations of glucose, zoomed in version.

4.1.5 In-lab-test of fluorescence

To make an in-lab-test of fluorescence an Arduino microcontroller was used. The RGB values determined by "Digital Color Meter" were: Red = 54, Green = 80 and Blue = 137. The led was used to excite a 2 mM fluorescein solution in Figure 26. The green light seen around the light from the LED and at the meniscus is fluorescence.

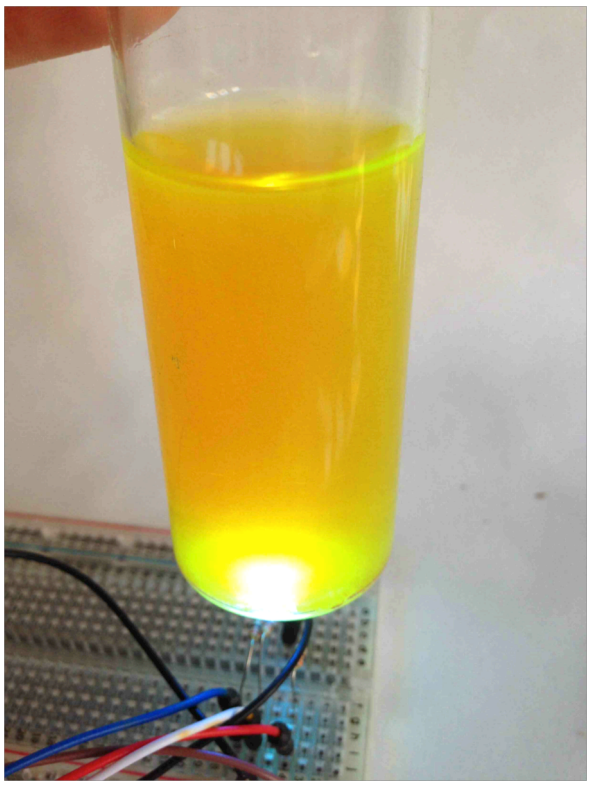

Figure 26: In-lab-test of fluorescence using an RGB-LED to excite a 2 mM fluorescein solution.

The in-lab-test worked for fluorescein, for GOx however the led and/or the fluorescence from GOx was to weak to be seen with the human eye.

4.2 Glucose sensing with immobilized GOx

4.2.1 Experimental design with sol-gel derived films based on TMOS

To determine the best way to make a TMOS based immobilization matrix experimental design was used. The results indicated that acid was a better catalyst than base when wanting a transparent film, as previously reported by Portaccio *et al.* [45], and that base

is a better catalyst when whole films are wanted. The results also indicate that the addition of Triton ® X-100 does not affect transparency, but if the sol-gel is applied onto glass plates the transparency was greater than when it was applied to polystyrene. The experimental design did not lead to any usable sol-gel based films.

Table 11: Variables used and grades given for the eight different experiments.

Experiment number	Catalyst	Triton® X-100	Applied on	Transparency	Cracks	Other problems
1	Acid	With	Glass	5	1	5
2	Acid	With	Polystyrene	5	3	5
3	Acid	Without	Glass	5	1	5
4	Acid	Without	Polystyrene	4	0	1
5	Base	With	Glass	2	5	2
6	Base	With	Polystyrene	0	5	0
7	Base	Without	Glass	3	5	3
8	Base	Without	Polystyrene	0	5	0

4.2.2 Making sol-gel films using TMOS

Even though the results from the experimental design were not decisive, acid catalysis and Triton ® X-100 were used in the TMOS based films. The use of TMOS did not give any good results, and the use of TMOS was terminated before making films with immobilized GOx. There are many examples of researchers using TMOS based films [44, 46, 135], however in this work they did not seem to work. The finding of a new biocompatible precursor for the silica matrix, made TMOS seem obsolete.

4.2.3 Sol-gel films on glass plate

Sol-gel films were applied to glass plates before the plate array was used. An advantage of using the glass plates was that it was easy to see what the film looked like from all angles. To measure GOx immobilized in a sol-gel matrix onto a glass plate, the whole glass plate could have been put at the bottom of a cuvette, and an optical fiber could easily excite the GOx from below or above. A major disadvantage was the reaction

between the sol and the glass, which lead to surface tension when the film dries. When the tension after some time became larger than the forces holding the film together, cracks formed. In some films the cracking was so extreme that parts of the film were found several centimeters from the glass plate. To avoid cracking PBS was used to cover the gel, but the PBS dissolved of the gel if it was added to soon. And no clear timeframe for the gelation was found for TMOS; it could sometimes be only 30 minutes, and other times it could take a few hours.

4.2.4 Sol-gel based films in the plate array

After some testing with applying sol-gel onto glass plates and seeing a lot of problems, a new method was used. Examination of applying the sol-gel into a 96 well plate array with a polystyrene bottom was done. Experiments were done with both TMOS and DGS derived films, and both seemed to crack far less than they did on glass plates. The reason can be that the sol does not react with the polystyrene in the plate array, but reacts with the glass plate as discussed above.

4.2.5 Making sol-gel films using DGS

4.2.5.1 Production of DGS

DGS is not commercially available. The production of DGS was done by refluxing TEOS and glycerol at 130 °C. There were some inaccuracies in the temperature, a temperature of 118 °C was observed, and a temperature of 132 °C was also observed. In average the temperature was probably a few degrees to low. However this was compensated by letting the mixture react for some hours more than originally planned.

During distillation of the mixture the vapor held a temperature between 78 and 80 °C. An NMR-spectrum of the byproduct was attained, and the spectrum looks very much like that of EtOH (see Figure 47, Appendix J).

The recipe said to vacuum distill both glycerol and TEOS before the reaction, but a previous test with NMR-analysis of both TEOS and glycerol before and after vacuum-distillation proved this to be unnecessary.

After the product had been dried in the vacuum oven it was observed that all the liquid had evaporated. The product of the DGS synthesis was white/glassy crystals, which were easily crumpled to small crystals/powder before storage in the desiccator.

It was observed that the substance closest to the flask was more glassy than the substance in the middle of the flask. It is possible that the stirring was not powerful enough, and the solution closer to the oil bath was heated more than the mixture in the middle of the flask. This could have lead to DGS condensing to longer Si-O-chains, which was later confirmed by ^{29}Si solid state-NMR (ssNMR) seen in Appendix I. The produced DGS dissolved quite easily in water confirming that is was not fully polymerized.

4.2.5.2 Structure of DGS

The structure of DGS was not determined. However the NMR, infrared (IR) and mass spectrometry (MS)-spectra seen in Appendix I gave some insights to what the structure could be. The structure proposed in papers seem strange. It seems unlikely that it is energetically favorable for one of the glycerols to make a five-ring with the silicon and oxygens. Two six-membered rings seem more plausible because of less stress in the molecule.

The ^{29}Si ssNMR (MAS) spectrum (seen in Figure 45, Appendix J) implied that some of the DGS had hydrolyzed and condensed, since peaks for Q^0, Q^1 and Q^2 are seen at -82.9, -88.6 and -96.1 ppm respectively. In the patent from Brook *et al.* [39] it is reported three peaks with chemical shift and percentage of composition for Q^0, Q^1 and Q^2: -82.4 (97%), -95.6 (1 %) and -103.7 (1 %) ppm respectively. The ^{29}Si ssNMR (MAS) of the DGS produced in this work was not quantitative, so no calculations can be made regarding the composition. The peak for Q^0 is seen at the same chemical shift, but the peaks for Q^1 and Q^2 have a substantial shift difference, however both seem to be within the chemical shifts where Q^1 and Q^2 are found [41].

From the ^{13}C ssNMR (MAS) (seen in Figure 46, Appendix J) what appears to be four separate peaks can be seen (75.6, 72.9, 65.5 and 63.9 ppm). This leads to the conclusion that there are four chemically different carbon atoms. Brook *et al.* [39] reported three peaks in their ^{13}C ssNMR (MAS) spectrum (72.7, 63.6 and 51.9 ppm). In the theoretical spectra seen in Appendix I, no peaks near 51.9 ppm are seen, and where this peak stems from remains unknown. The two other peaks from Brook *et al.* and the peaks for the DGS produced in this work seem similar. Since the peaks are not discrete, an assumption that there are more than one isomer of DGS was made. Another possibility is that the reacted DGS, where two more DGS molecules have polymerized, are responsible for the widening of the peaks.

The IR-data was almost identical to the data from Brook *et al.* [39] indicating that the same functional groups were present in the created substance. The obtained IR-spectrum had the peaks (3401, 2942, 2889, 1638, 1465, 1408, 1056, 930 and 864 cm^{-1}), Brook et al. reported the following peaks (3365m, 2941m, 2887m, 1650w, 1461m, 1417m, 1191s, 1110s, 1051s, 994m, 926m and 859w cm^{-1}). The intensities of the peaks in the attained spectrum can be seen in Figure 49, Appendix J. Some of the peaks were assigned to functional groups, as seen in Table 12, the rest were not appointed.

Table 12: The IR peaks of DGS, and what functional group they probably stem from.

Peak (cm^{-1})	**Functional group the peak was assigned to**
3401	O-H
2942	sp^3-hybridized carbon (stretch)
1465	CH_2 (bend)
1056	C-O / Si-O and/or Si-O-Si

The MS-data imply that there are a lot of molecules with higher molecular weight than DGS, which has a molecular weight of 208 g/mole. No significant peaks are seen between 203 and 221 m/z. However the MS was run using water and methanol to solve the sample, and since the rate of hydrolysis and condensation of DGS is high in the presence of water, it seems likely that the DGS has reacted to form particles. It is therefore decided that the MS-results can be disregarded.

The important thing to note is that the structure of DGS does not really matter. The main reason for using DGS is so that no MeOH or EtOH is released during hydrolysis of the orthosilicate. After TEOS and glycerol had fully reacted all EtOH (^{1}H NMR in Figure 47, Appendix J) was distilled and dried off, so all that is left is the enzyme friendly glycerol and some form of silica that hydrolyze and condensate to form glass.

4.2.5.3 Sol-gel with DGS

Making sol-gel derived films with DGS was far easier than using TMOS. The reaction time was shorter and gelation happened significantly faster. A probable cause of the quick hydrolysis and condensation is the high water solubility of DGS, which allows the DGS to be miscible in water. It is also likely that the concentration of glycerol in solution affects the esterification rate [132]. Since there are only two alkoxy molecules per SiO_2 molecule, the esterification will probably be slower than if there were four alkoxy groups per SiO_2. Another important factor is that the ratio between H_2O and DGS (70:1) was very different than the ratio between H_2O and TMOS (14:1). The ratio between H_2O and DGS implicates a very high reaction rate for hydrolysis, compared to the H_2O/TMOS-ratio.

The use of DGS to immobilize biological substances is reported to be far better than using TMOS and TEOS [36], but since no TMOS based films with immobilized GOx were made, no comparison of the TMOS and DGS based films can be done in regard to immobilization. However the films produced with TMOS cracked a lot during drying, and the gelation could take some hours. For DGS the gelation time could be as short as five minutes, which is the same as Smith *et al.* [136] reported, and less cracking was seen for the DGS derived films, than for the TMOS based films. Judging from the sometime extreme cracking of the TMOS films, the release of MeOH, and the low pH values required for hydrolysis and condensation, it appears that the DGS film is far more suitable for immobilization of GOx for an optical biosensor.

In Figure 27 a microscopy picture of a DGS-based matrix in the plate array can be seen. It is clear that the film is optically transparent, but not homogenous. This film was not

filtered before application to see how much the filtration altered the film. In Figure 28 a DGS based film in the plate array can be seen. The particles seen are probably fluorescein aggregates in small water pockets. The film in Figure 28 was used to find the optimal distance between the probe and the plate array. This goes to show that a fluorophore in an inhomogeneous film can still emit light. Whether the intensity of the fluorescence was decreased as a result of the inhomogeneous film is not known. In Figure 29 a DGS based matrix with immobilized GOx can be seen. It is apparent that the film is neither translucent or homogeneous. This film was used with the setup for plate array measurement with groove plate and pipes.

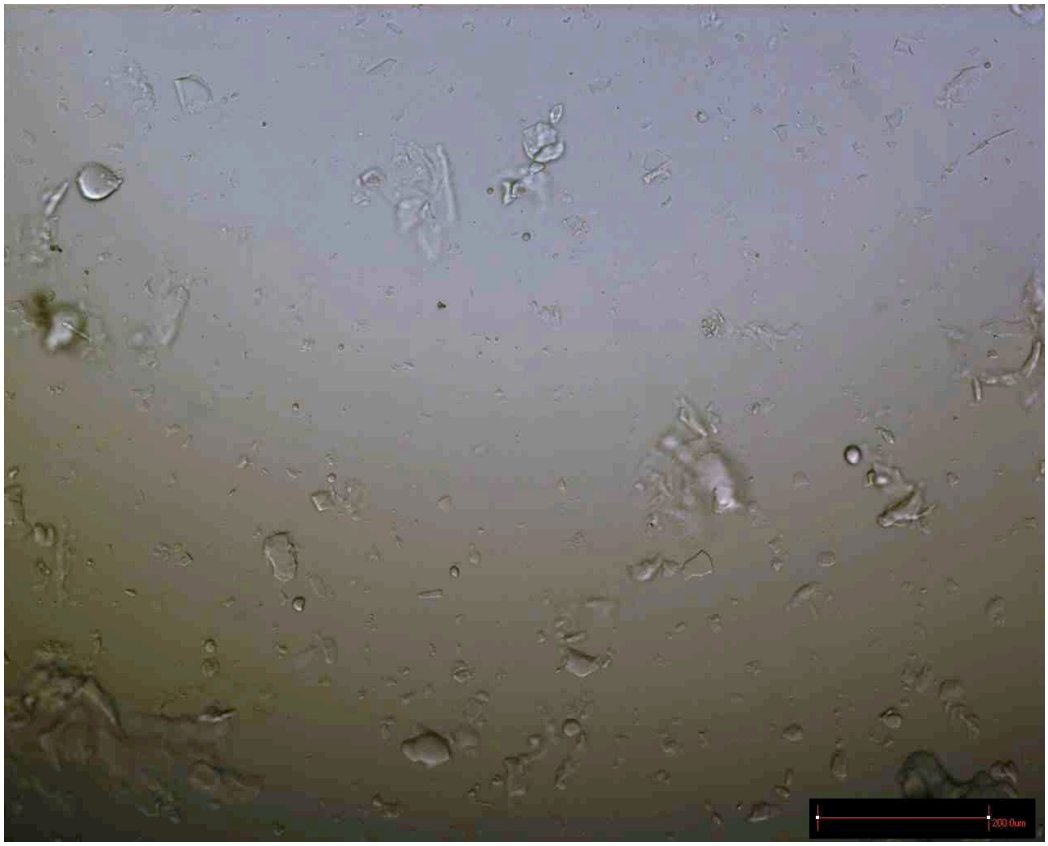

Figure 27: Microscope picture of an unfiltered DGS based film in plate array.

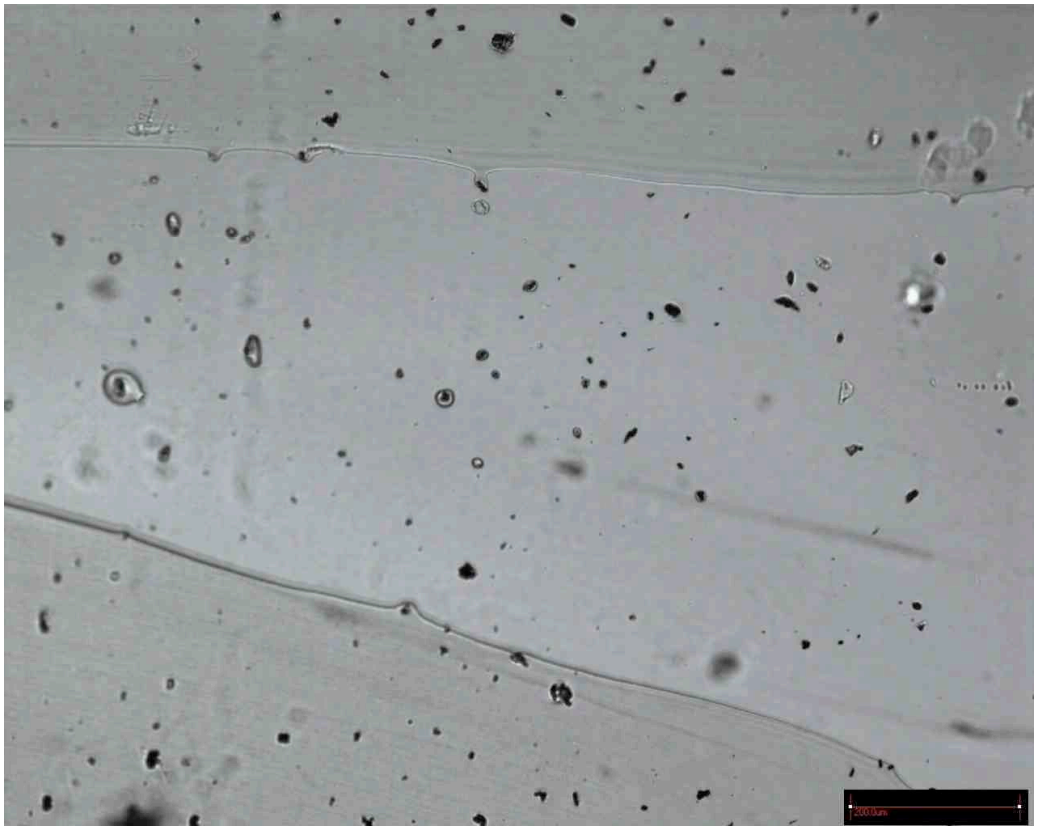

Figure 28: DGS based film with 1mM fluorescein in plate array.

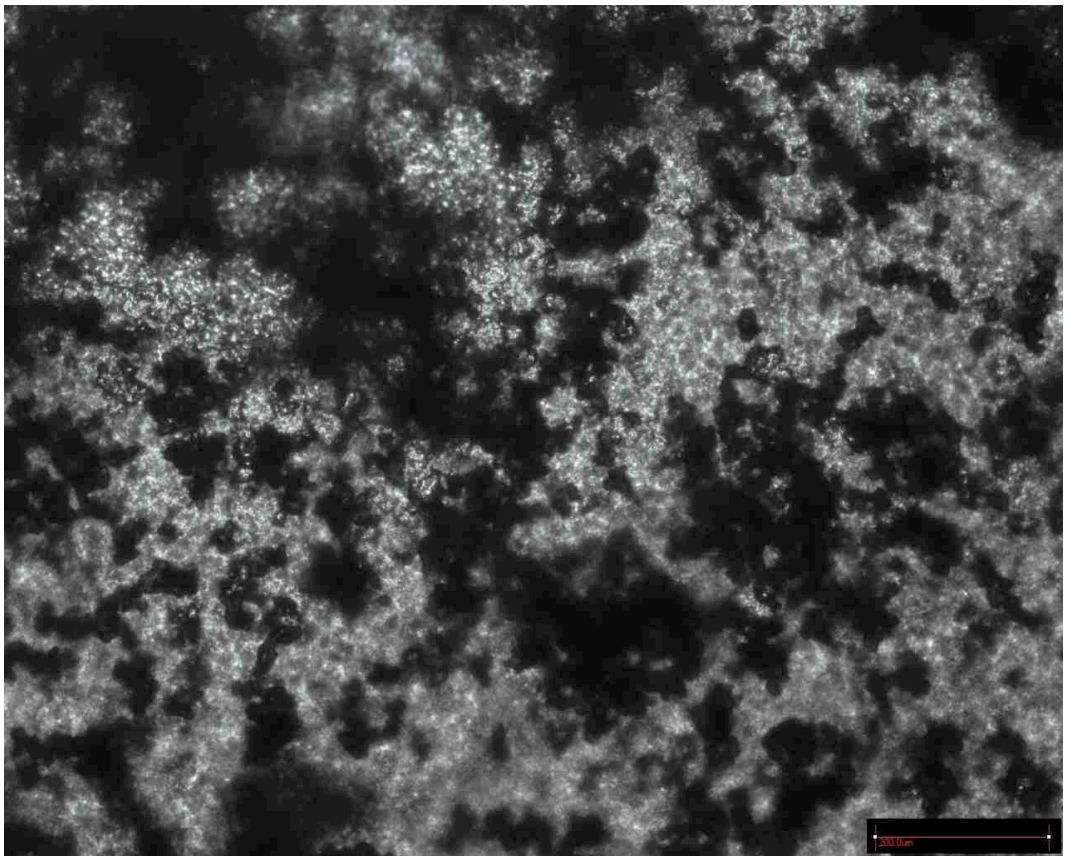

Figure 29: DGS based film with GOx (0.049 g/mL sol or 11094 U/mL sol) in plate array.

4.2.6 Measuring fluorescence in the plate array

A way to measure fluorescence in the plate array was needed. Since no micro plate reader was available, the solution was to make my own setup. The setup was to be used with optical fibers and a probe of known dimensions. The sol-gel based films were to be immobilized in a plate array (see Appendix F). There were three main ideas:

1. To use a microtable with a specially milled piece of metal (see Appendix G)
2. To use a holder for the plate array and a separate holder for the fiber
3. To use a holder that could hold both the plate and the fiber (see Appendix H)

The first idea was disregarded after some time because the microtable only had a range of 25 mm, and after some experimenting, it was found that the setup would be useless. Some time was spent on the second idea as it seemed easier to adjust distance, angles and so on with two separate parts. However the third idea was regarded as the best after the setup seen in Appendix H was investigated.

Two ways to make the components after they were designed using the 3D-drawing program SketchUp was though of:

1. Use the 3D printer that was available at Oslo University College
2. Let the chemistry departments own instrument workshop make it

First method 1 was tested, but the 3D printer used was not accurate enough to make the components right. Another problem was that the printer sometimes stopped feeding material through the printers nozzle, but did not recognize this problem itself. This lead to unfinished products that could not be used. The drawings were given to the chemistry departments instrument workshop so they could make the experimental setup. 3D drawings of the experimental setup can be seen in Appendix H.

The finished setup was used with optical components described in the experimental chapter. To decide on which excitation and emission filters were to be used, the excitation spectrum seen in Figure 17, and the emission spectrum seen in Figure 18, was

used. In Figure 30 the filter transmission spectra can be seen together with the excitation and emission spectra.

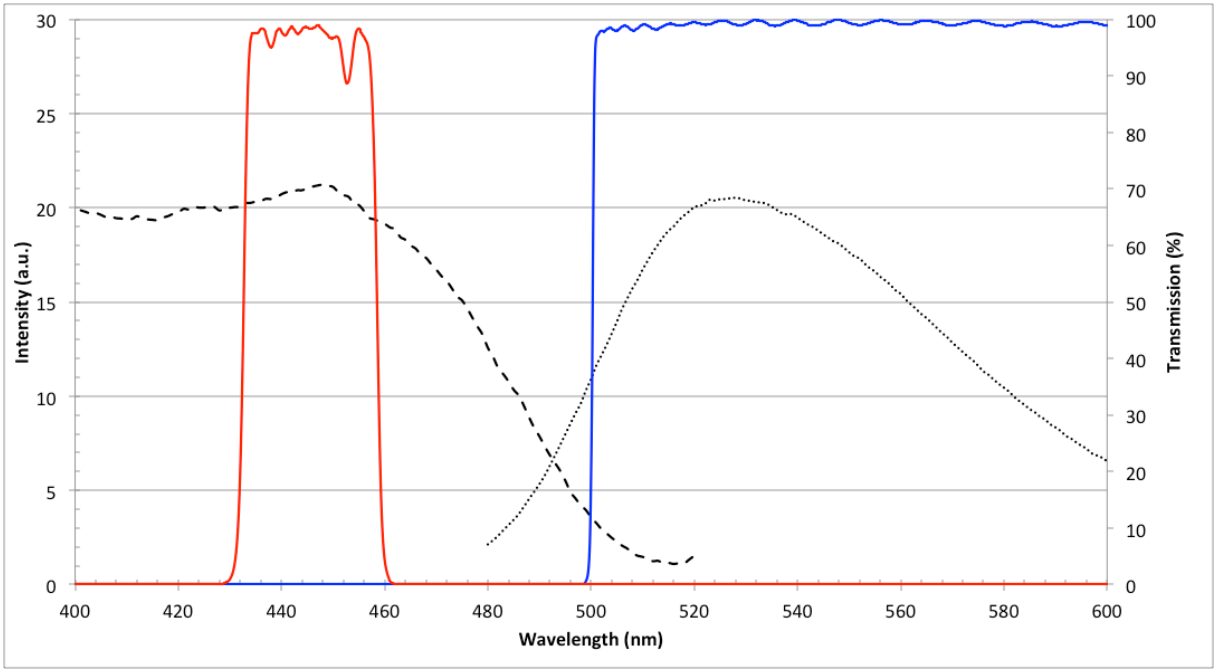

Figure 30: Filters used seen together with the excitation (–––) and emission (···) spectra of GOx (536.5 U/mL PBS) with 2mM glucose (intensity on left axis). The filters were a 448 nm band pass filter (■) and a 496 nm long pass filter (■) (transmission on right axis).

To measure the best distance between the probe and the DGS-film, a film with fluorescein was used. Fluorescein was chosen because it shows a much higher fluorescence than GOx at approximately the same wavelength, which allowed the distance regulation to be done faster and more accurate. The optimal distance was found to be 2 mm between the probe and the film, and therefore 1 mm between the probe and the plate array since it has a 1 mm thick polystyrene layer (See Appendix F).

Measurement of GOx fluorescence in a DGS based matrix was successful, as seen in Figure 31. A slight decrease in intensity is seen for most wavelengths when 200 µL of PBS was added. It is possible that this is only a random occurrence. Both spectra are an average of 10, yet the one with the PBS is far less smooth. This measurement was done a DGS film from the same batch as the one seen in Figure 29. The high GOx activity/mL sol was used because very low signals were detected from films with equal concentration and activity as the ones in solution.

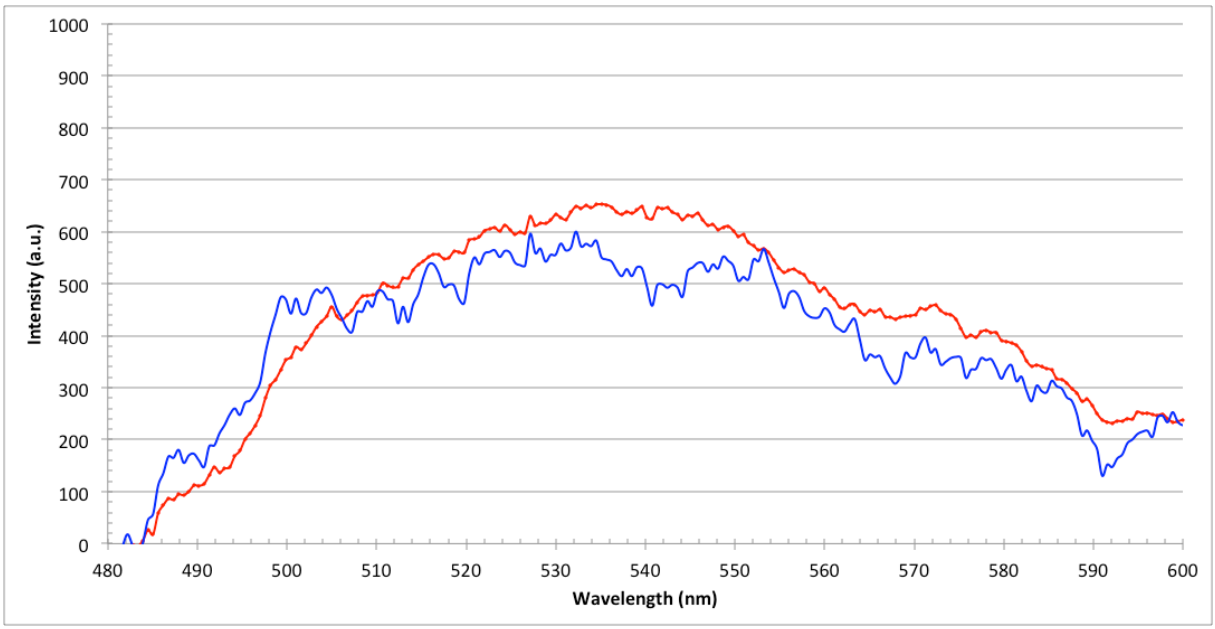

Figure 31: Emission spectrum of GOx (11094 U/mL sol) in DGS-matrix with 200 µL PBS (■) and without (■).

When pouring 200 µL of 10 mM glucose solution onto the GOx immobilized in DGS, a slight increase in intensity was seen for most wavelengths (see Figure 32). As for the graph with PBS added in Figure 31, the graph with added glucose solution is much less smooth. The increased intensity does not seem to be a real effect, as the signal fluctuated a lot during measurements.

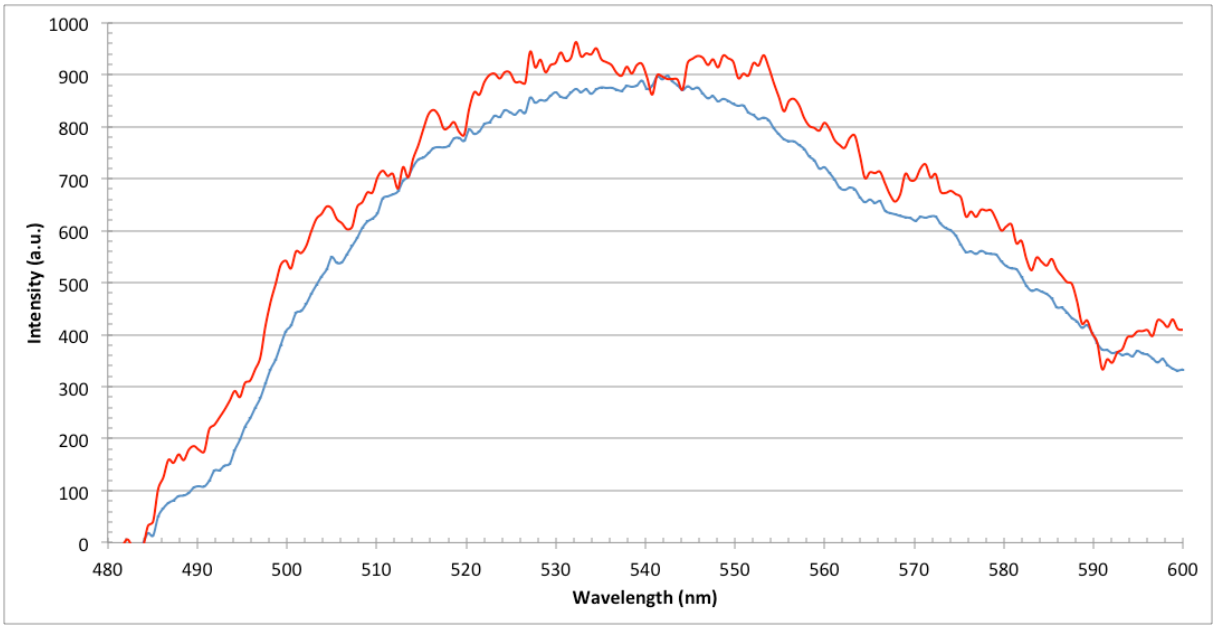

Figure 32: Emission spectrum of GOx (11094 U/mL sol) in DGS-matrix with 200 µL 10 mM glucose (■) and without (■).

The signal fluctuated a lot between each measurement. This can probably not be a result of voltage differences from the power source, as an UPS was used. Fluctuations is probably a result of too low signals [137]. It is possible that the signal could have been stabilized by the use of a reference photodiode, as seen in the experimental setup in Figure 15. Because the measurements with glucose in the sol-gel derived films were not successful, the reference photodiode was not used.

There are some possibilities regarding the low signal strength: the fiber diameter was not big enough, all filters and junctions waste a lot of light, and GOx is maybe not strongly fluorescent when immobilized.

The spectrophtotometer used was maybe not sensitive enough to measure the weak signal from GOx. When used to measure the fluorescence of fluorescein it gave good results, however fluorescein is much stronger fluorescent than FAD in GOx.

5 Conclusion and future outlook

5.1 Conclusion

Using TMOS to make sol-gel derived films is a much used method, and has proved to be effective for some biological systems. However most enzymes are fragile, and the release of alcohols can be of great harm to the enzyme by reducing its catalytic capability or in the extreme denature and destroy it completely. Hence it seems like a good idea to use other silanes for the encapsulation of enzymes.

Using enzymes for quantitative measurements can be difficult. The enzymes can become denatured and loose most of their activity, or be stabilized by the immobilization matrix and have an increased activity. The intensity of fluorescence from GOx increased when oxidizing glucose in solution, however it was difficult to measure the fluorescence in a sol-gel derived film. This was because the signal was weak, either because of the experimental setup or GOx itself reacting negatively to immobilization.

DGS is a new and interesting silane which may provide a more gentle way to encapsulate enzymes. To the authors knowledge this is the first report on GOx being immobilized in a DGS based sol-gel matrix.

The structure of DGS was not determined by ssNMR, NMR, IR or MS. One of the structures proposed in papers looks energetically unfavorable. However the main purpose of using DGS compared to TMOS or TEOS is the release of the enzyme-friendly glycerol instead of the enzyme-unfriendly MeOH or EtOH. The structure does not matter to much as glycerol and SiO_2 are the only components left in the product after EtOH is distilled of.

The experimental setup with optical fibers used with the groove plate and pipes seemed to work fine. The process of finding the best way to measure fluorescence using a plate array was challenging, but the results seem good. This can only be said because of

distance testing with fluorescein, as the immobilized GOx showed a very weak fluorescence.

It may seem that this method for measurement of glucose concentration is not ideal. Maybe the measurement of oxygen used in the reaction or the amount of H_2O_2 produced are better ways to determine the glucose concentration, than the fluorescence of FAD and $FADH_2$.

5.2 Future Outlook

If further work was to be done on glucose sensing using GOx immobilized in a DGS derived matrix, some other methods would have been chosen. The experimental setup can probably be used with other fluorescent systems.

There are many papers on the positive effect of sugar-modified silanes have on enzymes immobilized in DGS matrix. The effect GLS has on the DGS matrix would have been interesting to examine.

Measurements in solution would have been done to determine the linear range GOx can sense glucose concentrations in.

More experiments with GOx immobilized in DGS derived matrices would have been done to get an optically clear an homogenous film.

It will be interesting to follow the development of glucose sensors in the future as much money and time is invested in this field around the world.

6 References

[1] J. E. Shaw, R. A. Sicree and P. Z. Zimmet *"Global estimates of the prevalence of diabetes for 2010 and 2030"* Diabetes Res Clin Pract, 87 (1): *4-14* **(2010)**

[2] G. Danaei, M. M. Finucane, Y. Lu, G. M. Singh, M. J. Cowan, C. J. Paciorek, J. K. Lin, F. Farzadfar, Y.-H. Khang, G. A. Stevens, M. Rao, M. K. Ali, L. M. Riley, C. A. Robinson and M. Ezzati *"National, regional, and global trends in fasting plasma glucose and diabetes prevalence since 1980: systematic analysis of health examination surveys and epidemiological studies with 370 country-years and 2·7 million participants"* The Lancet, 378 (9785): *31-40* **(2011)**

[3] J. Pickup *"Developing Glucose Sensors for in-Vivo Use"* Trends in Biotechnology, 11 (7): *285-291* **(1993)**

[4] J. C. Pickup, F. Hussain, N. D. Evans and N. Sachedina *"In vivo glucose monitoring: the clinical reality and the promise"* Biosens Bioelectron, 20 (10): *1897-1902* **(2005)**

[5] M. S. Steiner, A. Duerkop and O. S. Wolfbeis *"Optical methods for sensing glucose"* Chem Soc Rev, 40 (9): *4805-4839* **(2011)**

[6] J. C. Pickup, F. Hussain, N. D. Evans, O. J. Rolinski and D. J. Birch *"Fluorescence-based glucose sensors"* Biosens Bioelectron, 20 (12): *2555-2565* **(2005)**

[7] F. S. Ligler and C. A. R. Taitt *"Optical biosensors: present and future"*: **(2002)**

[8] J. Lakowicz, R. *"Principles Of Fluorescence Spectroscopy"*: **(2006)**

[9] W. H. Tan *"Optical measurements on the nanometer scale"* Trac-Trends in Analytical Chemistry, 17 (8-9): *501-513* **(1998)**

[10] D. W. Lübbers and N. Opitz *"[The pCO2-/pO2-optode: a new probe for measurement of pCO2 or pO in fluids and gases (authors transl)]"* Zeitschrift fur Naturforschung. Section C: Biosciences, 30 (4): *532-533* **(1974)**

[11] I. Chudobová, E. Vrbová, M. Kodíček, J. Janovcová and J. Káš *"Fibre optic biosensor for the determination of d-glucose based on absorption changes of immobilized glucose oxidase"* Analytica Chimica Acta, 319 (1-2): *103-110* **(1996)**

[12] S. Weiss *"Fluorescence spectroscopy of single biomolecules"* Science, 283 (5408): *1676-1683* **(1999)**

[13] L. C. Clark, Jr. and C. Lyons *"Electrode systems for continuous monitoring in cardiovascular surgery"* Ann N Y Acad Sci, 102 (1): *29-45* **(1962)**

[14] Y. S. I. Inc. *"New Products"* Analytical chemistry, 47 (8): *787A-791A* **(1975)**

[15] M. Shichiri, R. Kawamori, Y. Yamasaki, N. Hakui and H. Abe *"Wearable Artificial Endocrine Pancreas with Needle-Type Glucose Sensor"* Lancet, 2 (8308): *1129-1131* **(1982)**

[16] M. J. Tierney, J. A. Tamada, R. O. Potts, R. C. Eastman, K. Pitzer, N. R. Ackerman and S. J. Fermi *"The GlucoWatch biographer: a frequent automatic and noninvasive glucose monitor"* Ann Med, 32 (9): *632-641* **(2000)**

[17] *Web page* http://research.microsoft.com/en-us/collaboration/stories/functionalcontactlens.aspx Accessed: **27.04.2014**

[18] H. Yao, Y. Liao, A. R. Lingley, A. Afanasiev, I. Lahdesmaki, B. P. Otis and B. A. Parviz *"A contact lens with integrated telecommunication circuit and sensors for wireless and continuous tear glucose monitoring"* Journal of Micromechanics and Microengineering, 22 (7): *1-10* **(2012)**

[19] *Web page* http://googleblog.blogspot.no/2014/01/introducing-our-smart-contact-lens.html Accessed: **25.02.2014**

[20] J. F. W. Herschel *"On a Case of Superficial Colour Presented by a Homogeneous Liquid Internally Colourless"* Philosophical Transactions of the Royal Society of London, 135: *143-145* **(1845)**

[21] G. G. Stokes *"On the Change of Refrangibility of Light"* Philosophical Transactions of the Royal Society of London, 142: *463-562* **(1852)**

[22] A. Jabłoński *"Efficiency of Anti-Stokes Fluorescence in Dyes"* Nature, 131 (3319): *839-840* **(1933)**

[23] A. Jabłoński *"Über den Mechanismus der Photolumineszenz von Farbstoffphosphoren"* Zeitschrift für Physik, 94 (1-2): *38-46* **(1935)**

[24] B. Kuswandi, R. Andres and R. Narayanaswamy *"Optical fibre biosensors based on immobilised enzymes"* Analyst, 126 (8): *1469-1491* **(2001)**

[25] P. C. Jeronimo, A. N. Araujo and B. S. M. M. M. Conceicao *"Optical sensors and biosensors based on sol-gel films"* Talanta, 72 (1): *13-27* **(2007)**

[26] J. Ebelmen *"Recherches sur les combinaisons des acides borique et silicique avec les éthers"*: **(1846)**

[27] L. L. Hench and J. K. West *"The Sol-Gel Process"* Chemical reviews, 90 (1): *33-72* **(1990)**

[28] H. H. Weetall *"Enzymes Immobilized on Inorganic Supports"* Trends in Biotechnology, 3 (11): *276-280* **(1985)**

[29] H. Podbielska *"Sol-gel technology for biomedical engineering"* Bulletin of the Polish Academy of Sciences. Technical sciences, 53 (3): *261* **(2005)**

[30] A. C. Pierre *"The sol-gel encapsulation of enzymes"* Biocatalysis and biotransformation, 22 (3): *145-170* **(2004)**

[31] L. M. Ellerby, C. R. Nishida, F. Nishida, S. A. Yamanaka, B. Dunn, J. S. Valentine and J. I. Zink *"Encapsulation of proteins in transparent porous silicate glasses prepared by the sol-gel method"* Science, 255 (5048): *1113-1115* **(1992)**

[32] W. Jin and J. Brennan *"Properties and applications of proteins encapsulated within sol–gel derived materials"* Analytica Chimica Acta, 461 (1): *1-36* **(2002)**

[33] M. Przybyt, E. Miller and T. Szreder *"Thermostability of glucose oxidase in silica gel obtained by sol-gel method and in solution studied by fluorimetric method"* J Photochem Photobiol B, 103 (1): *22-28* **(2011)**

[34] M. A. Brook, Y. Chen, K. Guo, Z. Zhang and J. D. Brennan *"Sugar-modified silanes: precursors for silica monoliths"* Journal of Materials Chemistry, 14 (9): *1469-1479* **(2004)**

[35] R. Bhatia, C. J. Brinker, A. Gupta and A. Singh *"Aqueous Sol–Gel Process for Protein Encapsulation"* Chemistry of materials, 12 (8): *2434-2441* **(2000)**

[36] M. A. Brook, Y. Chen, K. Guo, Z. Zhang, W. Jin, A. Deisingh, J. Cruz-Aguado and J. D. Brennan *"Proteins entrapped in silica monoliths prepared from glyceroxysilanes"* Journal of Sol-Gel Science and Technology, 31 (1-3): *343-348* **(2004)**

[37] I. Gill and A. Ballesteros *"Encapsulation of Biologicals within Silicate, Siloxane, and Hybrid Sol–Gel Polymers: An Efficient and Generic Approach"* Journal of the American Chemical Society, 120 (34): *8587-8598* **(1998)**

[38] T. Besanger, Y. Chen, A. Deisingh, R. Hodgson, W. Jin, S. Mayer, M. Brook and J. Brennan *"Screening of Inhibitors Using Enzymes Entrapped in Sol–Gel-Derived Materials"* Analytical chemistry, 75 (10): *2382-2391* **(2003)**

[39] M. A. Brook, Brennan, John D., Chen, Yang *"Polyol-modified silanes as precursors for silica"* (20040034203): **(2004)**

[40] X. Sui, J. Cruz Aguado, Y. Chen, Z. Zhang, M. Brook and J. Brennan *"Properties of Human Serum Albumin Entrapped in Sol–Gel-Derived Silica Bearing Covalently Tethered Sugars"* Chemistry of materials, 17 (5): *1174-1182* **(2005)**

[41] C. J. Brinker and G. W. Scherer *"CHAPTER 3 - Hydrolysis and Condensation II: Silicates"* Sol–Gel Science: *96-233* **(1990)**

[42] G. A. Petsko and D. Ringe *"Protein structure and function"*: **(2004)**

[43] J. D. Badjić and N. M. Kostić *"Effects of Encapsulation in Sol–Gel Silica Glass on Esterase Activity, Conformational Stability, and Unfolding of Bovine Carbonic Anhydrase II"* Chemistry of materials, 11 (12): *3671-3679* **(1999)**

[44] S. de Marcos, J. de Marcos, J. F. Galindo, J. Sierra, J. R. Galbán, S. Castillo and M. de *"An optical glucose biosensor based on derived glucose oxidase immobilised onto a sol–gel matrix"* Sens Actuators B Chem, 57 (1-3): *227-232* **(1999)**

[45] M. Portaccio, M. Lepore, B. Della Ventura, O. Stoilova, N. Manolova, I. Rashkov and D. G. Mita *"Fiber-optic glucose biosensor based on glucose oxidase immobilised in a silica gel matrix"* Journal of Sol-Gel Science and Technology, 50 (3): *437-448* **(2009)**

[46] R. Esposito, B. Della Ventura, S. De Nicola, C. Altucci, R. Velotta, D. G. Mita and M. Lepore *"Glucose sensing by time-resolved fluorescence of sol-gel immobilized glucose oxidase"* Sensors (Basel), 11 (4): *3483-3497* **(2011)**

[47] Z. Zheng, Y. Chen, R. J. Hodgson, M. A. Brook and J. D. Brennan *"Macroporous silica monoliths derived from glyceroxysilanes: Controlling gel formation and pore structure"* Macromolecular symposia, 226: *253-261* **(2005)**

[48] I. Gill *"Bio-doped Nanocomposite Polymers: Sol–Gel Bioencapsulates"* Chemistry of materials, 13 (10): *3404-3421* **(2001)**

[49] A. Vanderkooy and M. A. Brook *"Polyvinylpyrrolidone molecular weight controls silica shell thickness on Au nanoparticles with diglycerylsilane as precursor"* ACS Appl Mater Interfaces, 4 (8): *3980-3986* **(2012)**

[50] R. Hodgson, Y. Chen, Z. Zhang, D. Tleugabulova, H. Long, X. Zhao, M. Organ, M. Brook and J. Brennan *"Protein-Doped Monolithic Silica Columns for Capillary Liquid Chromatography Prepared by the Sol–Gel Method: Applications to Frontal Affinity Chromatography"* Analytical chemistry, 76 (10): *2780-2790* **(2004)**

[51] N. M. Eleftheriou and J. D. Brennan *"Probing the dynamics of domain III of human serum albumin entrapped in sol–gel derived silica using a Sudlow's site II specific fluorescent ligand"* Journal of Sol-Gel Science and Technology, 50 (2): *184-193* **(2009)**

[52] A. Dattelbaum, G. Baker, J. Fox, S. Iyer and J. Dattelbaum *"PEGylation of a Maltose Biosensor Promotes Enhanced Signal Response When Immobilized in a Silica Sol–Gel"* Bioconjugate chemistry, 20 (12): *2381-2384* **(2009)**

[53] T. Y. Lin, C. H. Wu and J. D. Brennan *"Entrapment of horseradish peroxidase in sugar-modified silica monoliths: toward the development of a biocatalytic sensor"* Biosens Bioelectron, 22 (9-10): *1861-1867* **(2007)**

[54] J. Cruz Aguado, Y. Chen, Z. Zhang, N. Elowe, M. Brook and J. Brennan *"Ultrasensitive ATP Detection Using Firefly Luciferase Entrapped in Sugar-Modified*

Sol–Gel-Derived Silica" Journal of the American Chemical Society, 126 (22): *6878-6879* **(2004)**

[55] J. A. Cruz-Aguado, Y. Chen, Z. Zhang, M. A. Brook and J. D. Brennan *"Entrapment of Src protein tyrosine kinase in sugar-modified silica"* Anal Chem, 76 (14): *4182-4188* **(2004)**

[56] Y. Chen, Z. Zhang, X. Sui, J. Brennan and M. Brook *"Reduced shrinkage of sol–gel derived silicas using sugar-based silsesquioxane precursors"* Journal of Materials Chemistry, 15 (30): *3132* **(2005)**

[57] Y. Shen, G. Mackey, N. Rupcich, D. Gloster, W. Chiuman, Y. Li and J. D. Brennan *"Entrapment of fluorescence signaling DNA enzymes in sol-gel-derived materials for metal ion sensing"* Anal Chem, 79 (9): *3494-3503* **(2007)**

[58] X. Sui, T.-Y. Lin, D. Tleugabulova, Y. Chen, M. Brook and J. Brennan *"Monitoring the Distribution of Covalently Tethered Sugar Moieties in Sol–Gel-Based Silica Monoliths with Fluorescence Anisotropy: Implications for Entrapped Enzyme Activity"* Chemistry of materials, 18 (4): *887-896* **(2006)**

[59] D. Müller *"Studien über ein neues Enzym Glykoseoxydase. I"* Biochem. Z, 199: *136-170* **(1928)**

[60] J. Raba and H. A. Mottola *"Glucose Oxidase as an Analytical Reagent"* Critical Reviews in Analytical Chemistry, 25 (1): *1-42* **(1995)**

[61] R. Bentley and A. Neuberger *"The Mechanism of the Action of Notatin"* Biochemical Journal, 45 (5): *584-590* **(1949)**

[62] W. Trettnak, M. J. P. Leiner and O. S. Wolfbeis *"Optical sensors. Part 34. Fibre optic glucose biosensor with an oxygen optrode as the transducer"* The Analyst, 113 (10): *1519* **(1988)**

[63] B. P. Schaffar and O. S. Wolfbeis *"A fast responding fibre optic glucose biosensor based on an oxygen optrode"* Biosens Bioelectron, 5 (2): *137-148* **(1990)**

[64] B. A. Dremel, S. Y. Li and R. D. Schmid *"On-line determination of glucose and lactate concentrations in animal cell culture based on fibre optic detection of oxygen in flow-injection analysis"* Biosens Bioelectron, 7 (2): *133-139* **(1992)**

[65] O. S. Wolfbeis, I. Oehme, N. Papkovskaya and I. Klimant *"Sol-gel based glucose biosensors employing optical oxygen transducers, and a method for compensating for variable oxygen background"* Biosens Bioelectron, 15 (1-2): *69-76* **(2000)**

[66] X. J. Wu, M. M. F. Choi and D. Xiao *"A glucose biosensor with enzyme-entrapped sol-gel and an oxygen-sensitive optode membrane"* Analyst, 125 (1): *157-162* **(2000)**

[67] K. Y. Cheng, J. C. Wang, C. Y. Lin, W. R. Lin, Y. A. Chen, F. J. Tsai, Y. C. Chuang, G. Y. Lin, C. W. Ni, Y. T. Zeng and M. L. Ho *"Electrochemical synthesis, characterization of*

Ir-Zn containing coordination polymer, and application in oxygen and glucose sensing" Dalton Trans, 43 (17): *6536-6547* **(2014)**

[68] Z. Zhou, L. Qiao, P. Zhang, D. Xiao and M. M. Choi *"An optical glucose biosensor based on glucose oxidase immobilized on a swim bladder membrane"* Anal Bioanal Chem, 383 (4): *673-679* **(2005)**

[69] R. M. Bukowski, V. P. Chodavarapu, A. H. Titus, A. N. Cartwright and F. V. Bright *"Phase fluorometric glucose biosensor using oxygen as transducer and enzyme-doped xerogels"* Electronics Letters, 43 (4): *202-204* **(2007)**

[70] Q. Zhao, S. Chen, H. Huang, L. Zhang, L. Wang, F. Liu, J. Chen, Y. Zeng and P. K. Chu *"Colorimetric and ultra-sensitive fluorescence resonance energy transfer determination of H2O2 and glucose by multi-functional Au nanoclusters"* Analyst, 139 (6): *1498-1503* **(2014)**

[71] X. Shan, L. Chai, J. Ma, Z. Qian, J. Chen and H. Feng *"B-doped carbon quantum dots as a sensitive fluorescence probe for hydrogen peroxide and glucose detection"* Analyst, 139 (10): *2322-2325* **(2014)**

[72] Q. Chang *"Optical determination of glucose and hydrogen peroxide using a nanocomposite prepared from glucose oxidase and magnetite nanoparticles immobilized on graphene oxide"* Mikrochimica acta, 181 (5-6): *527* **(2014)**

[73] Y. Zhang, Y. J. Zhang, X. D. Xia, X. Q. Hou, C. T. Feng, J. X. Wang and L. Deng *"A quantitative colorimetric assay of H2O2 and glucose using silver nanoparticles induced by H2O2 and UV"* Chinese Chemical Letters, 24 (12): *1053-1058* **(2013)**

[74] J. Sun, J. Ge, W. Liu, M. Lan, H. Zhang, P. Wang, Y. Wang and Z. Niu *"Multi-enzyme co-embedded organic-inorganic hybrid nanoflowers: synthesis and application as a colorimetric sensor"* Nanoscale, 6 (1): *255-262* **(2014)**

[75] S. X. Xu, H. L. Qi, S. Y. Zhou, X. F. Zhang and C. X. Zhang *"Mediatorless amperometric bienzyme glucose biosensor based on horseradish peroxidase and glucose oxidase cross-linked to multiwall carbon nanotubes"* Microchimica Acta, 181 (5-6): *535-541* **(2014)**

[76] O. S. Wolfbeis, M. Schaferling and A. Durkop *"Reversible optical sensor membrane for hydrogen peroxide using an immobilized fluorescent probe, and its application to a glucose biosensor"* Microchimica Acta, 143 (4): *221-227* **(2003)**

[77] X. J. Gao, W. Y. Yang, P. F. Pang, S. T. Liao, Q. Y. Cai, K. F. Zeng and C. A. Grimes *"A wireless magnetoelastic biosensor for rapid detection of glucose concentrations in urine samples"* Sensors and Actuators B-Chemical, 128 (1): *161-167* **(2007)**

[78] P. F. Pang, W. Y. Yang, S. J. Huang, Q. Y. Cai and S. Z. Yao *"Measurement of glucose concentration in blood plasma based on a wireless magnetoelastic biosensor"* Analytical Letters, 40 (5): *897-906* **(2007)**

[79] W. Y. Yang, P. F. Pang, X. J. Gao, Q. Y. Cai, K. F. Zeng and C. A. Grimes *"Detection of lactose in milk samples using a wireless multi-enzyme biosensor"* Sensor Letters, 5 (2): *405-410* **(2007)**

[80] S. Hotta, K. Miyano, H. Aoki, N. Fujiwara, A. Masui, D. Yano, K. Sano, K. Yamanaka, C. Kimura and T. Sugino *"Use of Porous Ion Exchange Film for Glucose Sensing"* Polymer Engineering and Science, 49 (5): *960-963* **(2009)**

[81] S. Seker, Y. E. Arslan and Y. M. Elcin *"Electrospun Nanofibrous PLGA/Fullerene-C60 Coated Quartz Crystal Microbalance for Real-Time Gluconic Acid Monitoring"* Ieee Sensors Journal, 10 (8): *1342-1348* **(2010)**

[82] K. Tohda *"Development of Optical Sugar Sensors as Implantable Devices for Interstitial Glucose Monitoring"* Bunseki Kagaku, 62 (10): *903-914* **(2013)**

[83] P. U. Abel and T. von Woedtke *"Biosensors for in vivo glucose measurement: can we cross the experimental stage"* Biosensors & bioelectronics, 17 (11-12): *1059-1070* **(2002)**

[84] J. M. Harris, G. P. Lopez and W. M. Reichert *"Silica-dispersed glucose oxidase for glucose sensing: in vitro testing in serum and blood and the effect of condensation pH"* Sens Actuators B Chem, 174: *373-379* **(2012)**

[85] K. Xu, G. Q. Xu, J. Lv, J. W. Cui and Y. C. Wu *"Pt nanoparticles modified Au nanowire array for amperometric and potentiometric detection of glucose"* Journal of Solid State Electrochemistry, 17 (9): *2381-2389* **(2013)**

[86] J. Cui, S. B. Adeloju and Y. Wu *"Integration of a highly ordered gold nanowires array with glucose oxidase for ultra-sensitive glucose detection"* Anal Chim Acta, 809: *134-140* **(2014)**

[87] K. Edagawa, Y. Fuchiwaki and M. Yasuzawa *"In Vivo Evaluation of Fine Needle Amperometric Glucose Sensors Implanted in Rabbit's Blood Vessel"* Journal of the Electrochemical Society, 161 (2): *B3111-B3115* **(2014)**

[88] Z. R. Marand, N. Shahtahmassebi, M. R. Housaindokht, G. H. Rounaghi and I. Razavipanah *"Construction of an Amperometric Glucose Biosensor by Immobilization of Glucose Oxidase on Nanocomposite at the Surface of FTO Electrode"* Electroanalysis, 26 (4): *840-848* **(2014)**

[89] W. Yang, T. Bai, L. R. Carr, A. J. Keefe, J. Xu, H. Xue, C. A. Irvin, S. Chen, J. Wang and S. Jiang *"The effect of lightly crosslinked poly(carboxybetaine) hydrogel coating on the performance of sensors in whole blood"* Biomaterials, 33 (32): *7945-7951* **(2012)**

[90] C. C. Huang, Q. A. Wang, C. T. Gu and H. B. Shao *"Determination of serum glucose using flow injection analysis and highly selective glucose sensor based on composite films"* Electrochimica Acta, 65: *90-96* **(2012)**

[91] S. Yang, Y. Lu, P. Atanossov, E. Wilkins and X. Long *"Microfabricated glucose biosensor with glucose oxidase entrapped in sol-gel matrix"* Talanta, 47 (3): *735-743* **(1998)**

[92] W. Z. Jia, K. Wang, Z. J. Zhu, H. T. Song and X. H. Xia *"One-step immobilization of glucose oxidase in a silica matrix on a Pt electrode by an electrochemically induced sol-gel process"* Langmuir, 23 (23): *11896-11900* **(2007)**

[93] G. Chang, Y. Tatsu, T. Goto, H. Imaishi and K. Morigaki *"Glucose concentration determination based on silica sol-gel encapsulated glucose oxidase optical biosensor arrays"* Talanta, 83 (1): *61-65* **(2010)**

[94] A. J. Bard and L. R. Faulkner *"Electrochemical methods: fundamentals and applications"* 2: **(1980)**

[95] A. Haouz, C. Twist, C. Zentz, A. M. de Kersabiec, S. Pin and B. Alpert *"Forster energy transfer from tryptophan to flavin in glucose oxidase enzyme"* Chemical Physics Letters, 294 (1-3): *197-203* **(1998)**

[96] J. Sierra, J. Galban, S. de Marcos and J. Castillo *"Fluorimetric–enzymatic determination of glucose based on labelled glucose oxidase"* Analytica Chimica Acta, 368 (1-2): *97-104* **(1998)**

[97] A. Lepore, M. Portaccio, E. De Tommasi, P. De Luca, U. Bencivenga, P. Maiuri and D. G. Mita *"Glucose concentration determination by means of fluorescence emission spectra of soluble and insoluble glucose oxidase: some useful indications for optical fibre-based sensors"* Journal of Molecular Catalysis B-Enzymatic, 31 (4-6): *151-158* **(2004)**

[98] S. Ghisla, V. Massey, J. M. Lhoste and S. G. Mayhew *"Fluorescence and optical characteristics of reduced flavines and flavoproteins"* Biochemistry, 13 (3): *589-597* **(1974)**

[99] B. E. P. Swoboda *"The relationship between molecular conformation and the binding of flavin-adenine dinucleotide in glucose oxidase"* Biochimica et biophysica acta. Protein structure, 175 (2): *365-379* **(1969)**

[100] A. Ramanavicius, N. Ryskevic, A. Kausaite-Minkstimiene, U. Bubniene, I. Baleviciute, Y. Oztekin and A. Ramanaviciene *"Fluorescence study of glucose oxidase self-encapsulated within polypyrrole"* Sensors and Actuators B-Chemical, 171: *753-759* **(2012)**

[101] A. M. Hartnett, C. M. Ingersoll, G. A. Baker and F. V. Bright *"Kinetics and thermodynamics of free flavins and the flavin-based redox active site within glucose oxidase dissolved in solution or sequestered within a sol-gel-derived glass"* Analytical chemistry, 71 (6): *1215-1224* **(1999)**

[102] W. Trettnak and O. S. Wolfbeis *"Fully Reversible Fibre-Optic Glucose Biosensor Based on the Intrinsic Fluorescence of Glucose-Oxidase"* Analytica Chimica Acta, 221 (2): *195-203* **(1989)**

[103] M. R. Eftink *"The Use of Fluorescence Methods to Monitor Unfolding Transitions in Proteins"* Biophysical Journal, 66 (2): *482-501* **(1994)**

[104] M. Yoshimoto, M. Sato, S. Wang, K. Fukunaga and K. Nakao *"Structural stability of glucose oxidase encapsulated in liposomes to inhibition by hydrogen peroxide produced during glucose oxidation"* Biochemical Engineering Journal, 30 (2): *158-163* **(2006)**

[105] G. Zoldák, A. Zubrik, A. Musatov, M. Stupák and E. Sedlák *"Irreversible thermal denaturation of glucose oxidase from Aspergillus niger is the transition to the denatured state with residual structure"* Journal of biological chemistry, 279 (46): *47601-47609* **(2004)**

[106] J. F. Sierra, J. Galban and J. R. Castillo *"Determination of glucose in blood based on the intrinsic fluorescence of glucose oxidase"* Analytical chemistry, 69 (8): *1471-1476* **(1997)**

[107] P. de Luca, M. Lepore, M. Portaccio, R. Esposito, S. Rossi, U. Bencivenga and D. Mita *"Glucose Determination by Means of Steady-state and Time-course UV Fluorescence in Free or Immobilized Glucose Oxidase"* Sensors (Basel), 7 (11): *2612-2625* **(2007)**

[108] X. J. Wu and M. M. F. Choi *"An optical glucose biosensor based on entrapped-glucose oxidase in silicate xerogel hybridised with hydroxyethyl carboxymethyl cellulose"* Analytica Chimica Acta, 514 (2): *219-226* **(2004)**

[109] M. Batumalay, H. A. Batumalay, W. Rahman, Y. S. Kam, F. Ong, R. Ahmad, S. W. Zakaria, H. Harun, M. Ahmad and Batumalay *"Evaluation of the tapered PMMA fiber sensor response due to the ionic interaction within electrolytic solutions"* Journal of modern optics, 61 (2): *154-160* **(2014)**

[110] M. Eriksson and Z. Iqbal *"Two measurement modes for mobile phone optical sensing"* Sensors and Actuators B-Chemical, 195: *63-70* **(2014)**

[111] X. Gao, X. Li, Q. Wan, Z. Li and H. Ma *"Detection of glucose via enzyme-coupling reaction based on a DT-diaphorase fluorescence probe"* Talanta, 120: *456-461* **(2014)**

[112] Y. He, X. Wang, J. Sun, S. Jiao, H. Chen, F. Gao and L. Wang *"Fluorescent blood glucose monitor by hemin-functionalized graphene quantum dots based sensing system"* Anal Chim Acta, 810: *71-78* **(2014)**

[113] M. L. Ho, J. C. Wang, T. Y. Wang, C. Y. Lin, J. F. Zhu, Y. A. Chen and T. C. Chen *"The construction of glucose biosensor based on crystalline iridium(III)-containing*

coordination polymers with fiber-optic detection" Sensors and Actuators B-Chemical, 190: *479-485* **(2014)**

[114] F. Hu, Y. Y. Huang, G. X. Zhang, R. Zhao and D. Q. Zhang *"A highly selective fluorescence turn-on detection of hydrogen peroxide and D-glucose based on the aggregation/deaggregation of a modified tetraphenylethylene"* Tetrahedron letters, 55 (8): *1471-1474* **(2014)**

[115] T. Kumagai, Y. Tottori, R. Miyata and H. Kajioka *"Glucose sensor with a Sagnac interference optical system"* Appl Opt, 53 (4): *720-726* **(2014)**

[116] T. Kumeria, M. M. Rahman, A. Santos, J. Ferre-Borrull, L. F. Marsal and D. Losic *"Structural and optical nanoengineering of nanoporous anodic alumina rugate filters for real-time and label-free biosensing applications"* Anal Chem, 86 (3): *1837-1844* **(2014)**

[117] Y. Ling, N. Zhang, F. Qu, T. Wen, Z. F. Gao, N. B. Li and H. Q. Luo *"Fluorescent detection of hydrogen peroxide and glucose with polyethyleneimine-templated Cu nanoclusters"* Spectrochim Acta A Mol Biomol Spectrosc, 118: *315-320* **(2014)**

[118] I. N. Pulidindi and A. Gedanken *"Carbon nanoparticles based non-enzymatic glucose sensor"* International journal of environmental analytical chemistry, 94 (1): *28-35* **(2014)**

[119] H. Sakalak, M. Ulasan, S. T. Camli and M. S. Yavuz *"One-pot synthesis of sub-100 nm scale boronic acid functionalized nanoparticles for fluorescent diol sensing"*: *PMSE-275* **(2014)**

[120] R. Verma and B. D. Gupta *"A novel approach for simultaneous sensing of urea and glucose by SPR based optical fiber multianalyte sensor"* Analyst, 139 (6): *1449-1455* **(2014)**

[121] Q. Wang, H. J. Song, Y. Hu, Y. Y. Su and Y. Lv *"Accelerated reducing synthesis of Ag@CDs composite and simultaneous determination of glucose during the synthetic process"* RSC Advances, 4 (8): *3992-3997* **(2014)**

[122] L. Zhang, Z. Y. Zhang, R. P. Liang, Y. H. Li and J. D. Qiu *"Boron-doped graphene quantum dots for selective glucose sensing based on the "abnormal" aggregation-induced photoluminescence enhancement"* Anal Chem, 86 (9): *4423-4430* **(2014)**

[123] W. Zhang, D. Ma and J. Du *"Prussian blue nanoparticles as peroxidase mimetics for sensitive colorimetric detection of hydrogen peroxide and glucose"* Talanta, 120: *362-367* **(2014)**

[124] D. A. Skoog, F. J. Holler and T. A. Nieman *"Principles of instrumental analysis"*: **(1998)**

[125] P. R. Kommoju, Z. W. Chen, R. C. Bruckner, F. S. Mathews and M. S. Jorns *"Probing Oxygen Activation Sites in Two Flavoprotein Oxidases Using Chloride as an Oxygen Surrogate"* Biochemistry, 50 (24): *5521-5534* **(2011)**

[126] A. Kohen, T. Jonsson and J. P. Klinman *"Effects of Protein Glycosylation on Catalysis: Changes in Hydrogen Tunneling and Enthalpy of Activation in the Glucose Oxidase Reaction†"* Biochemistry, 36 (9): *2603-2611* **(1997)**

[127] M. Meyer, G. Wohlfahrt, J. Knablein and D. Schomburg *"Aspects of the mechanism of catalysis of glucose oxidase: a docking, molecular mechanics and quantum chemical study"* J Comput Aided Mol Des, 12 (5): *425-440* **(1998)**

[128] J. P. Roth, R. Wincek, G. Nodet, D. E. Edmondson, W. S. McIntire and J. P. Klinman *"Oxygen isotope effects on electron transfer to O2 probed using chemically modified flavins bound to glucose oxidase"* Journal of the American Chemical Society, 126 (46): *15120-15131* **(2004)**

[129] A. J. Visser *"Kinetics of stacking interactions in flavin adenine dinucleotide from time-resolved flavin fluorescence"* Photochem Photobiol, 40 (6): *703-706* **(1984)**

[130] H. J. Hecht, H. M. Kalisz, J. Hendle, R. D. Schmid and D. Schomburg *"Crystal Structure of Glucose Oxidase from Aspergillus niger Refined at 2·3 Å Reslution"* Journal of Molecular Biology, 229 (1): *153-172* **(1993)**

[131] *Web page* http://www.sigmaaldrich.com/catalog/product/sigma/g7141?lang=en&region=NO Accessed: **01.03.2014**

[132] J. D. Wright and N. A. J. M. Sommerdijk *"Sol-gel materials: chemistry and applications"* 4: **(2000)**

[133] B. C. Dave, B. Dunn, J. S. Valentine and J. I. Zink *"Sol-Gel Encapsulation Methods for Biosensors"* Analytical chemistry, 66 (22): *A1120-A1127* **(1994)**

[134] *Web page* http://upload.wikimedia.org/wikipedia/commons/c/c4/Rendered_Spectrum.png Accessed: **17.02.2014**

[135] R. Esposito, I. Delfino and M. Lepore *"Time-resolved flavin adenine dinucleotide fluorescence study of the interaction between immobilized glucose oxidase and glucose"* J Fluoresc, 23 (5): *947-955* **(2013)**

[136] A. M. E. Smith, J. Fortuna, E. Forsberg, J. Brennan and A. Smith *"An automated materials screening approach for the development of sol–gel derived monolithic silica enzyme reactor columns"* RSC Advances, 4 (31): *15952* **(2014)**

[137] J. Fraden *"Handbook of Modern Sensors: Physics, Designs, and Applications"*: **(2010)**

[138] *Web page*
http://www.greinerbioone.com/en/row/articles/catalogue/article/37_11/13229/ Accessed: **23.09.2013**

7 Appendix

Appendix A Detailed overview of all spectrofluorometer settings

In this appendix a detailed overview of the settings used on the spectrofluorometer can be seen. Where nothing else is mentioned the average of 20 scans was calculated.

Table 13: Detailed settings for the spectrofluorometer for emission experiments

What	**Setting/Value**
Software	Scan
Scan mode	Emission
Excitation wavelength	450 nm
Start wavelength for emission	480 nm
Stop wavelength for emission	600 nm
Excitation slit	5 nm
Emission slit	5 nm
Scan control	Medium
Scan rate	600 nm/min
Data interval	1 nm
Averaging time	0.1000 s
PMT voltage	Medium
Excitation filter	Auto
Emission filter	Open

Table 14: Detailed settings for the spectrofluorometer for excitation experiments

What	**Setting/Value**
Software	Scan
Scan mode	Excitation
Emission wavelength	530 nm
Start wavelength for emission	250 nm
Stop wavelength for emission	520 nm
Excitation slit	5 nm

Emission slit	5 nm
Scan rate	600 nm/min
Data interval	1 nm
Averaging time	0.1000 s
PMT voltage	Medium
Excitation filter	Auto
Emission filter	Open

Appendix B Detailed excitation spectrum

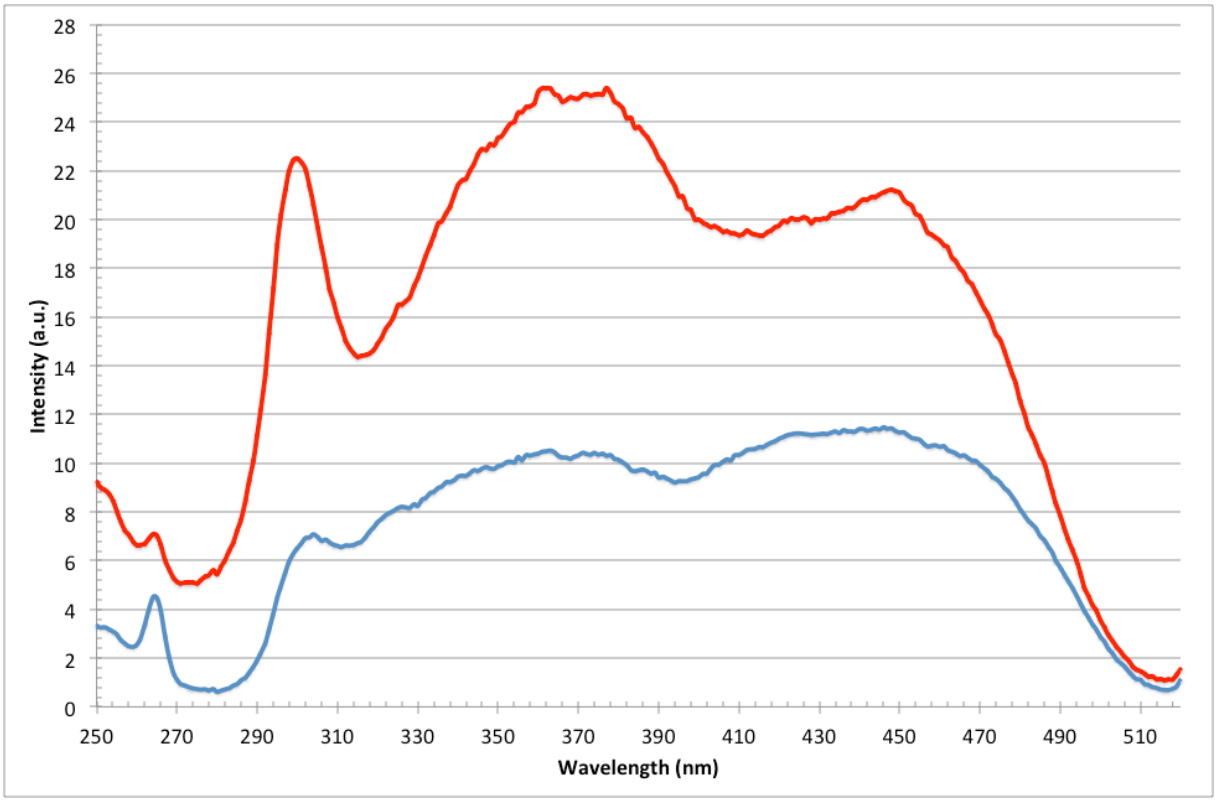

Figure 33: Excitation intensity of GOx (536.5 U/mL PBS) without glucose (■) and with 2 mM glucose (■), measured at 530 nm, using the parameters from Table 14.

The small peaks both spectra exhibit at 265 nm can be ignored, as they arise from a second order transmittance from the excitation monochromator. A background spectrum has been subtracted, however pure PBS scatters less light than GOx in PBS, so the peaks can still be seen.

Appendix C Programming .csv-files to .txt-files

This appendix contains a Java program written to read .csv-files find the average intensity for all the wavelengths in the file. The program first calculates the average of the zero samples for each wavelength, ask the user if he/she wants to subtract the zero sample and does so if the user selects “yes”. This is done by finding the average intensity for each wavelength from the .csv-file with the measurement and then subtract the average for the same wavelength from the zero sample. The resulting two arrays, one with the wavelengths and one with the intensities are written in a .txt-file.

The code was written in Xcode version 4.6.3 in January 2014 using the programming language Java.

```
import java.util.*;
import java.io.*;
import javax.swing.*;

/**
 A program for reading .csv-files, calculating the average of intensities for different
wavelengths, subtracting the average of a zero-sample and writing the results in a .txt-file

 @author Alexander Bjørndal

 */

public class CSVXLS {
    public static void main (String [] args) throws FileNotFoundException {
        try {
            Mainsystem s = new Mainsystem();
        } catch (IOException e ) {
            System.out.println("Something went wrong trying to read the file");
        }
    }
}

/**
 Class with all the methods
 */
class Mainsystem {
    Scanner scanner;
    int numberOfLines = 0;
    int numberOfExperiments = 0;
    boolean csvFile = false;
```

```
    boolean shouldPBSBeSubtracted = false;
    double [][] rawValues;
    double [] averageIntensitiesArray;
    double [] averagePBSArray;
    double [] wavelengths;
    String [] stringAveragePBSArray;
    String [][] resultValues;
    String csvFilename;
    String txtFilename;

    /**
     Constructor
     prompts the user for a .csv-file then calls all the methods needed before writing to a
.txt-file
     @throws IOException
     */

    public Mainsystem() throws IOException {
        csvFilename= "Measurements/";
        while (!csvFile) {
                JFileChooser fileChooser = new JFileChooser(csvFilename);
                int returnValue = fileChooser.showOpenDialog(fileChooser);
                if (returnValue == JFileChooser.APPROVE_OPTION) {
                    csvFilename= fileChooser.getSelectedFile().getName();
                    csvFilename= "Measurements/" + csvFilename;
                }
                csvFile = csvFileType(csvFilename);
        }
        numberOfLines = findLength(csvFilename);
        wavelengths = findWavelengths(csvFilename, numberOfLines);
        readFromFile(csvFilename, numberOfLines, numberOfExperiments);
        averageIntensitiesArray = average(rawValues, numberOfLines, numberOfExperiments/2);
        shouldPBSBeSubtracted = checkIfSubtractPBS();
        if(shouldPBSBeSubtracted) {
            txtFilename= findPBStxtFile();
            readFromTxtFile(txtFilename, numberOfLines);
            averageIntensitiesArray = subtractPBS(averagePBSArray, averageIntensitiesArray);
        }
        changePeriodWithComma(wavelengths, averageIntensitiesArray);
        writeToFile(csvFilename, resultValues, shouldPBSBeSubtracted);
    }

    /**
     Checks whether the user wants to subtract a PBS spectrum from a .txt-file
     @return boolean
     */
    public boolean checkIfSubtractPBS() {
        int reply = JOptionPane.showConfirmDialog(null, "Do you want to subtract a previously
calculated PBS-spectrum.txt?", "Subtract a .txt-file?", JOptionPane.YES_NO_OPTION);
        if (reply == JOptionPane.YES_OPTION) {
```

```
            return true;
        } else {
            return false;
        }
    }

    /**
     Subtracts the PBS spectrum from averageIntensitiesArray

     @param averagePBSArray The PBS values from the .txt-file
     @param averageIntensitiesArray The average of the intensities for given wavelengths
     @return averageIntensitiesArray The average of the intensities for given wavelengths
     */
    public double [] subtractPBS(double [] averagePBSArray, double [] averageIntensitiesArray)
{
        for (int b = 0; b < numberOfLines; b++) {
            averageIntensitiesArray[b] = averageIntensitiesArray[b] - averagePBSArray[b];
        }
        return averageIntensitiesArray;
    }

    /**
     Reads a .txt-file and saves the second column in averagePBSArray

     @param txtFilename Filename for the .txt-file
     @param numberOfLines Number of lines with wavelengths and intensities
     @throws IOException
     */

    public void readFromTxtFile(String txtFilename, int numberOfLines) throws IOException {
        Scanner scanner3 = new Scanner (new File(txtFilename));
        stringAveragePBSArray = new String [numberOfLines];
        scanner3.nextLine();
        for (int p = 0; p < numberOfLines-2; p++) {
            String newLine2 = scanner3.nextLine();
            String [] splitLine2 = newLine2.split(";");
            stringAveragePBSArray[p] = splitLine2[1];
        }
        averagePBSArray = changeCommaWithPeriod(stringAveragePBSArray, numberOfLines);
    }

    /**
     Prompts the user to find a .txt-file

     @return txtFilename Filename for the .txt-file
     */

    public String findPBStxtFile() {
        boolean txtFile = false;
        txtFilename = "Measurements/txt/";
```

```
        while (!txtFile) {
            JFileChooser fileChooser = new JFileChooser(txtFilename);
            int returnValue2 = fileChooser.showOpenDialog(fileChooser);
            if (returnValue2 == JFileChooser.APPROVE_OPTION) {
                txtFilename = fileChooser.getSelectedFile().getName();
                txtFilename = "Measurements/txt/" + txtFilename;
            }
            txtFile = txtFileType(txtFilename);
        }
        return txtFilename;
    }

    /**
     Writes a .txt-file in the Measurements/txt/ directory

     @param csvFilename Filename for the .csv-file
     @param resultValues Array with all the wavelengths and average of intensities
     @param shouldPBSBeSubtracted The boolean representing if the user wants to subtract a
PBS-spectrum or not
     */
    public void writeToFile (String csvFilename , String [][] resultValues, boolean
shouldPBSBeSubtracted) {
        try {
            int cutCsv = csvFilename.indexOf('.');
            csvFilename= csvFilename.substring((13),(cutCsv));
            BufferedWriter writeOut;
            if (shouldPBSBeSubtracted) {
                writeOut = new BufferedWriter(new FileWriter("Measurements/txt/" + csvFilename
+ "_average_minusPBS.txt"));
                writeOut.write(csvFilename+ "minus PBS\n");
            } else {
                writeOut = new BufferedWriter(new FileWriter("Measurements/txt/" + csvFilename
+ "_average.txt"));
                writeOut.write(csvFilename + "\n");
            }
            for (int c = 0; c < resultValues[0].length-2 ; c++) {
                writeOut.write(resultValues[0][c] + ";" + resultValues[1][c] + "\n");
            }
            writeOut.close();
        } catch (IOException f) {
            System.out.println("Something went wrong while writing to file");
        }
    }

    /**
     Exchanges all periods with commas for two given double arrays, and stores them in one
common two dimentional double array

     @param wavelengths Array with all the wavelengths
     @param averageIntensitiesArray The average of the intensities for given wavelengths
```

```
     @return resultValues Array with all the wavelengths and average of intensities

     */
    public String [][] changePeriodWithComma(double [] wavelengths, double []
averageIntensitiesArray) {
        resultValues = new String [2][wavelengths.length];
        for (int s = 0; s < wavelengths.length; s++) {
            resultValues[0][s] = Double.toString(wavelengths[s]);
            resultValues[1][s] = Double.toString(averageIntensitiesArray[s]);
            resultValues[0][s] = resultValues[0][s].replace(".",",");
            resultValues[1][s] = resultValues[1][s].replace(".",",");
        }
        return resultValues;
    }

    /**
    Exchanges all the commas with periods for a given string array, and writes the results in
a double array

     @param stringAveragePBSArray The PBS values from the .txt-file in string format
     @param numberOfLines Number of lines with wavelengths and intensities
     @return averagePBSArray The PBS values from the .txt-file
     */
    public double [] changeCommaWithPeriod (String [] stringAveragePBSArray, int
numberOfLines) {
        averagePBSArray = new double [numberOfLines];
        for (int q = 0; q <= stringAveragePBSArray.length-1; q++) {
            if(stringAveragePBSArray[q] != null) {
                averagePBSArray[q] =
Double.parseDouble(stringAveragePBSArray[q].replace(",","."));
            }
        }
        return averagePBSArray;
    }

    /**
     Reads all the intensities from a given .csv-file and stores them in @param rawValues

     @param csvFilename Filename for the .csv-file
     @param numberOfLines Number of lines with wavelengths and intensities
     @param numberOfExperiments The number of intensities or runs for a given experiment
     @throws IOException

     */
    public void readFromFile(String csvFilename, int numberOfLines, int numberOfExperiments)
throws IOException {
        Scanner scanner2 = new Scanner(new File(csvFilename));
        rawValues = new double [numberOfLines-2][numberOfExperiments];
        String newLine = scanner2.nextLine();
        String [] splitLine = newLine.split(",");
```

```
            scanner2.nextLine();
            for (int k = 0; k < numberOfLines-2; k++) {
                newLine = scanner2.nextLine();
                splitLine = newLine.split(",");
                int z = 0;
                for (int l = 1; l < numberOfExperiments; l+=2) {
                    rawValues[k][z++] = Double.parseDouble(splitLine[l]);
                }
            }
        }

        /**
         Calculates the average of all the intensities in the .csv-file

         @param rawValues Raw data from the .csv-file
         @param numberOfLines Number of lines with wavelengths and intensities
         @param numberOfExperiments The number of intensities or runs for a given experiment
         @return averageIntensitiesArray The average of the intensities for given wavelengths
         */
        public double [] average (double [][] rawValues, int numberOfLines, int
numberOfExperiments) {
            averageIntensitiesArray = new double [numberOfLines];
            for (int m = 0; m < numberOfLines-2; m++){
                double sum = 0;
                for (int n = 0; n < numberOfExperiments; n++) {
                    sum += rawValues[m][n];
                }
                averageIntensitiesArray[m] = sum/numberOfExperiments;
            }
            return averageIntensitiesArray;
        }

        /**
         Finds the length and number of experiments of the interesting data in the .csv-file
         The .csv-file contains a lot of information that needs to be ignored. The first line that
is usable for detecting were the ignorable data begins is the one that starts with
"Collection". However four of the lines previous to this line can be ignored, hence this
method returns numberOfLines-4

         @param csvFilename Filename for the .csv-file
         @return numberOfLines Number of lines with wavelengths and intensities
         @throws IOException
         */
        public int findLength (String csvFilename) throws IOException {
            scanner = new Scanner(new File(csvFilename));
            boolean readOn = true;
                while (scanner.hasNextLine() && readOn) {
                    numberOfLines++;
                    String line = scanner.nextLine();
                    if (line.startsWith("Collection")) {
```

```
                    readOn = false;
                }
                if (numberOfLines == 2) {
                    String [] numberOfExperimentsString = line.split(",");
                    numberOfExperiments = numberOfExperimentsString.length;
                }
            }
            return numberOfLines-4;
    }

    /**
     Reads through the .cvs-file to find the wavelengths, and stores them in @param
wavelengths

     @param csvFilename Filename for the .csv-file
     @param numberOfLines Number of lines with wavelengths and intensities
     @throws IOException
     @return wavelengths Array with all the wavelengths
     */
    public double [] findWavelengths (String csvFilename, int numberOfLines) throws
IOException {
        scanner = new Scanner(new File(csvFilename));
        wavelengths = new double [numberOfLines];
        scanner.nextLine();
        scanner.nextLine();
        for (int counter = 0; counter < numberOfLines-2; counter++) {
            String wholeLine = scanner.nextLine();
            String [] wholeLineSplit = wholeLine.split(",");
            wavelengths[counter] = Double.parseDouble(wholeLineSplit[0]);
        }
        return wavelengths;
    }

    /**
     Checks if the user given file is a .csv-file, and tells the user if it is not

     @param csvFilename Filename for the .csv-file
     */
    public boolean csvFileType(String csvFilename) {
        if (csvFilename.endsWith(".csv")) {
            return true;
        } else {
            JOptionPane.showMessageDialog(null, "That is not a .csv-file");
            return false;
        }
    }

    /**
     Checks if the user given file is a .txt-file, and tells the user if it is not
```

```
     @param txtFilename Filename for the .txt-file
     */
    public boolean txtFileType(String txtFilename) {
        if (txtFilename.endsWith(".txt")) {
            return true;
        } else {
            JOptionPane.showMessageDialog(null, "That is not a .txt-file");
            return false;
        }
    }
}
```

Appendix D Programming a RGB-led

The code was written in the software Arduino version 1.0.5 the 17.02.2014, below is the written program as written in the Arduino software.

```
// Program to make an RGB-led mimic light at 450 nm

// Alexander Bjørndal
// 17.02.2014

// Initializing the ints
const int RED_LED_PIN = 6;
const int GREEN_LED_PIN = 5;
const int BLUE_LED_PIN = 3;
int redIntensity = 54;
int greenIntensity = 80;
int blueIntensity = 137;

void setup() {
 // No setup needed
}

// Sets and loops the intensity for the different circuits coupled to the R,G and B leds
void loop() {
 analogWrite(GREEN_LED_PIN, greenIntensity);
 analogWrite(BLUE_LED_PIN, blueIntensity);
 analogWrite(RED_LED_PIN, redIntensity);
}
```

Appendix E The first emission spectrum

The results from the first measurement done on the spectrofluorometer can be seen in Figure 34. The spectrum is contorted by Raman scattering, and the signal is weak. Note that the signal is negative. That is because the spectrofluorometer was not "zeroed".

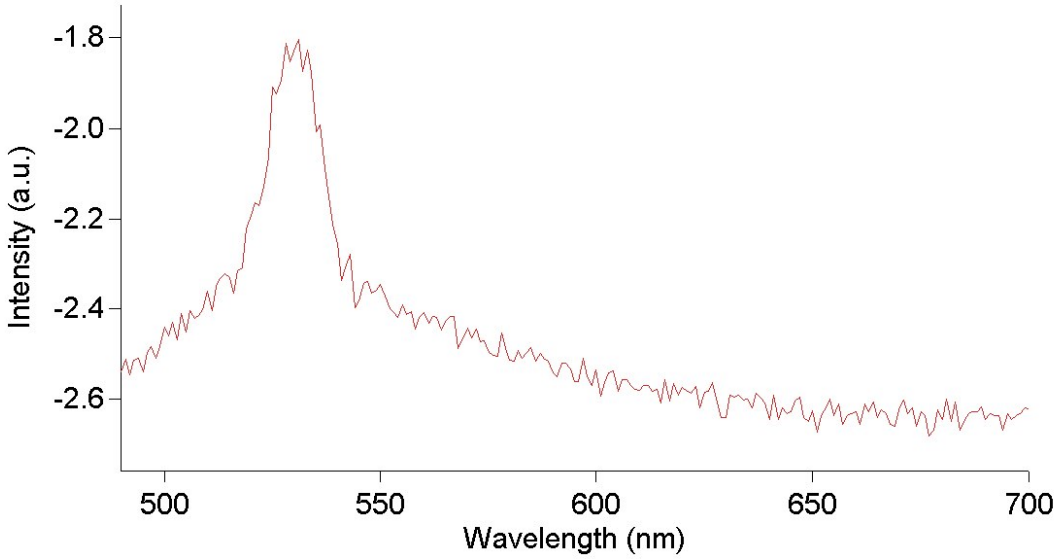

Figure 34: Emission spectrum of GOx (4.2 U/g). Excitation at 450 nm.

Appendix F The plate array

A plate array of the type 96 Well Microplate, PS, µClear® , Chimney Well from greiner bio-one was used. A 3D drawing, seen in Figure 35, was made in SketchUp to test experimental setups with the 3D drawings of both the "Setup for plate array measurement with microtable" (Appendix G), and "Setup for plate array measurement with groove plate and pipes" (Appendix H). In Figure 36 the technical drawings from greiner bio-one can be seen.

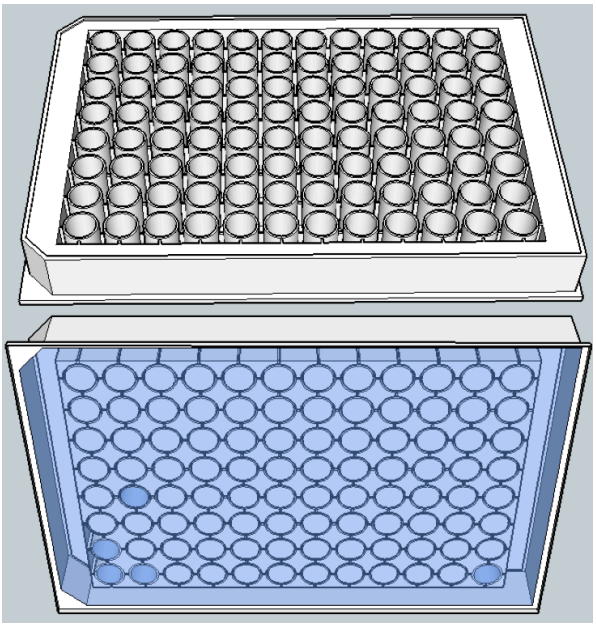

Figure 35: Plate array drawn in SketchUp, seen from above (top) and below (bottom).

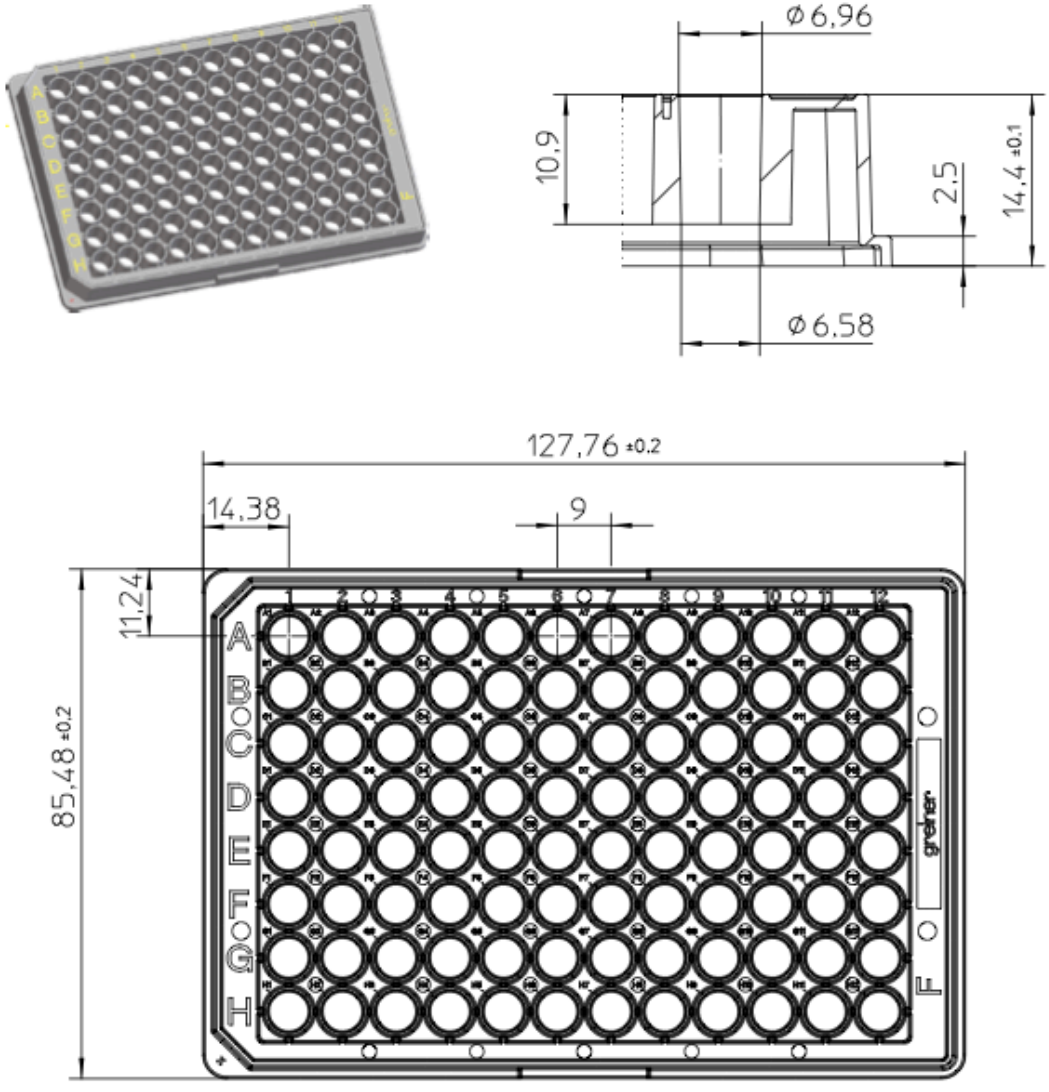

Figure 36: Technical drawing of the plate array from greiner bio-one [138].

Appendix G Setup for plate array measurement with microtable

To measure in the plate array, without buying an expensive plate reader, a setup had to be made. The first idea was to use a Klinger/Micro-Controle MR80.25 Linear Stage that was available in the lab with a milled piece of metal. The range of the microtable was only 25 mm and the distance between the center points of two adjacent wells in the plate array is 9 mm, so this setup would require a lot of moving of the plate array to be used.

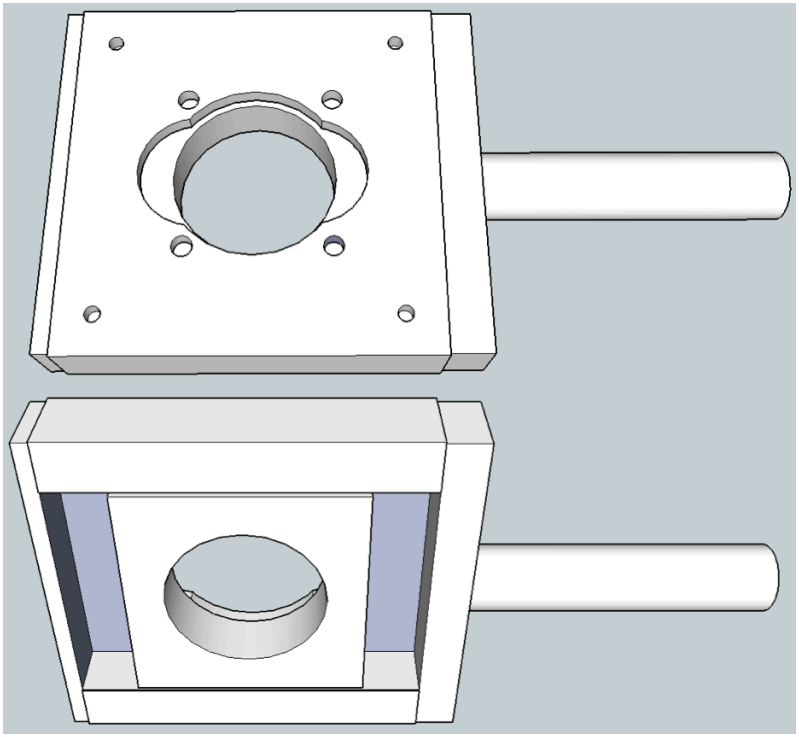

Figure 37: Microtable from SketchUp. Seen from above (top), and below (bottom).

Appendix H Setup for plate array measurement with groove plate and pipes

The setup for measuring fluorescence in a plate array with an optical probe consists of four parts: an inner pipe, an outer pipe, a supporting pipe and a groove plate. The inner pipe contains the optical probe, and is glued to the groove plate. The outer pipe contains

the inner pipe and has a wing screw which holds the optical probe in place inside the inner pipe. The outer pipe also has a thumb screw to fasten the inner pipe. The outer pipe is fastened on top of the supporting pipe with a wing screw. Both the outer and the supporting pipe has a slit to let the optical fiber curve at a natural angle towards the table.

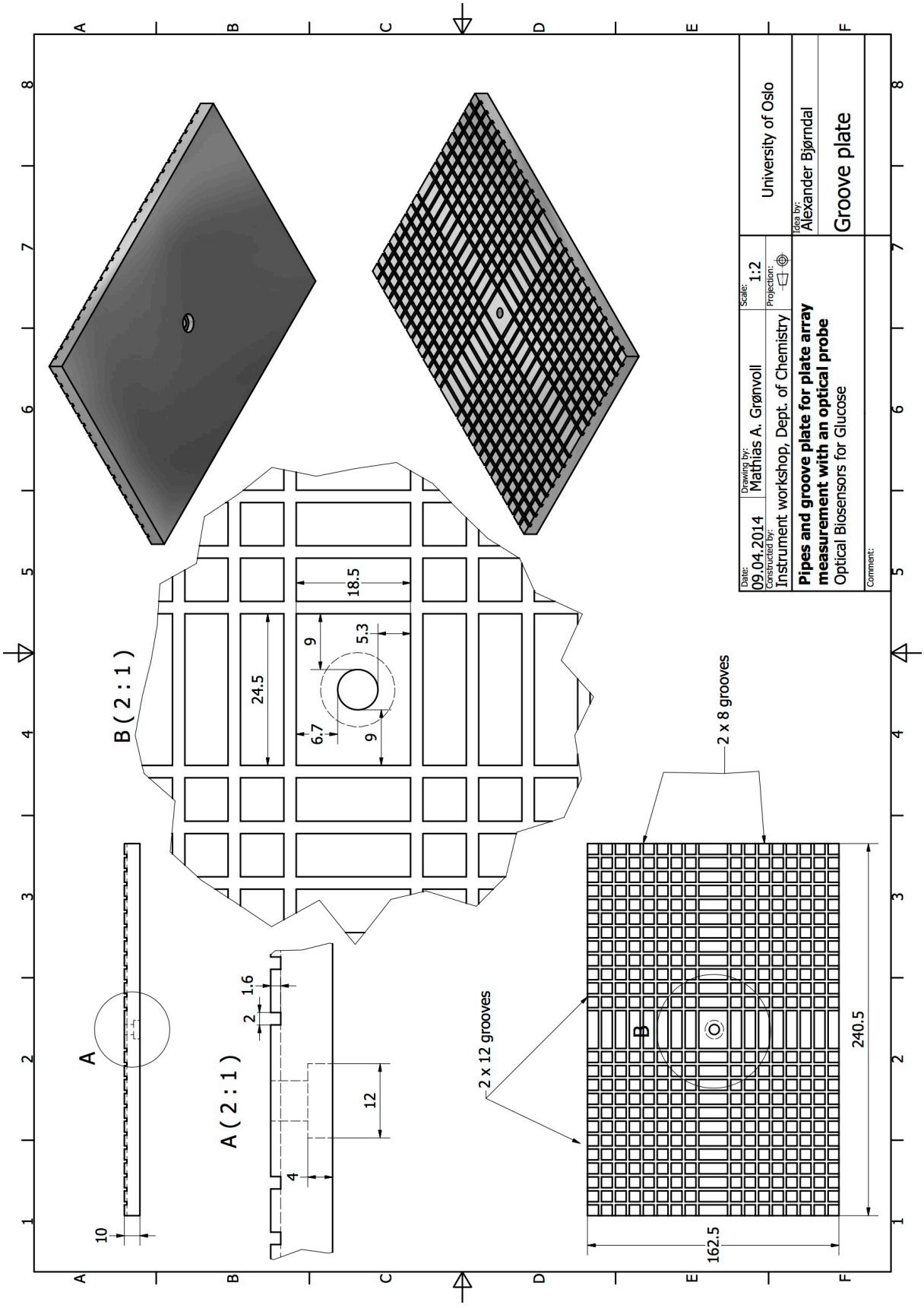

Figure 38: Groove plate used in the setup for plate array measurement with groove plate and pipes.

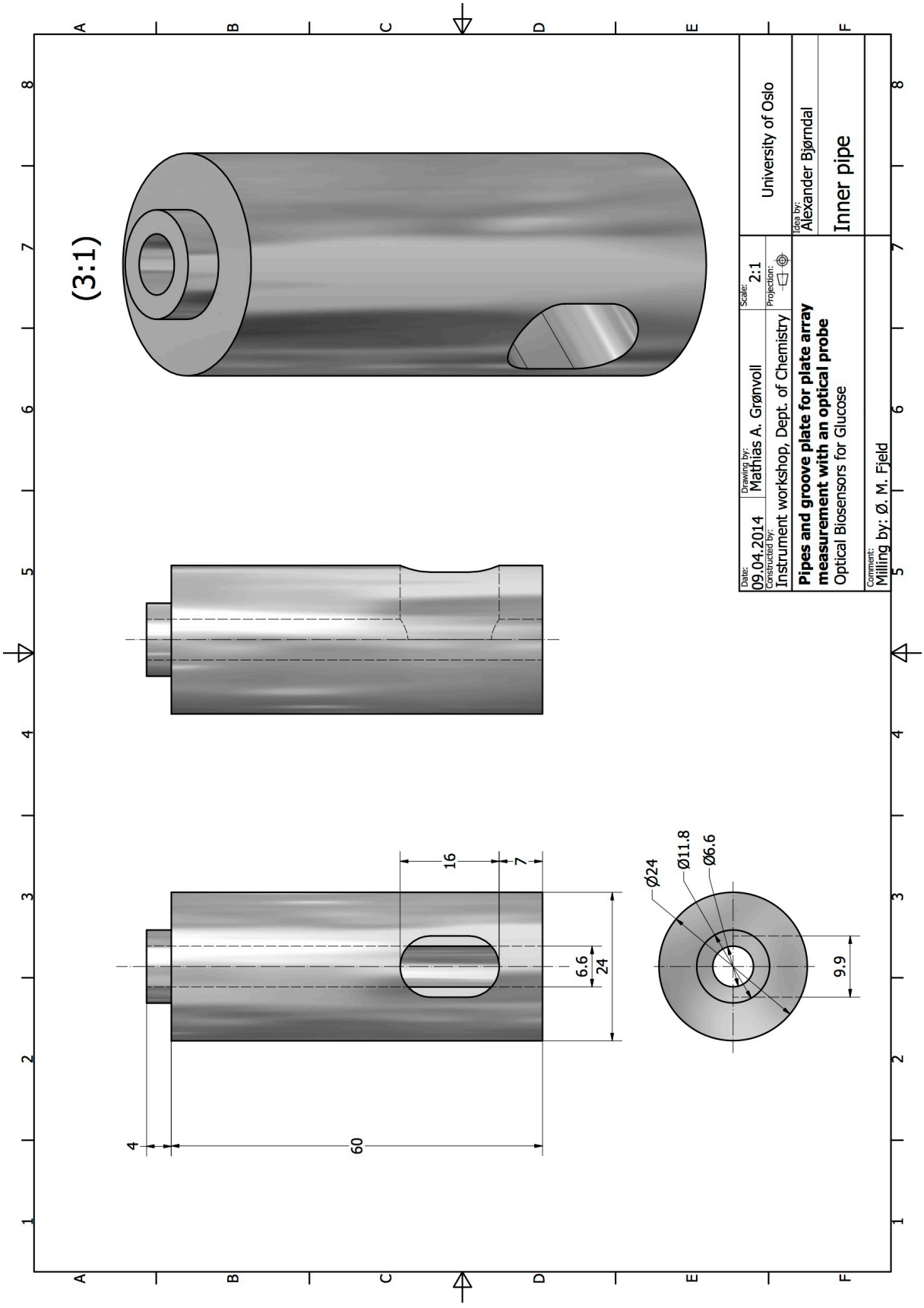

Figure 39: Inner pipe used in the setup for plate array measurement with groove plate and pipes.

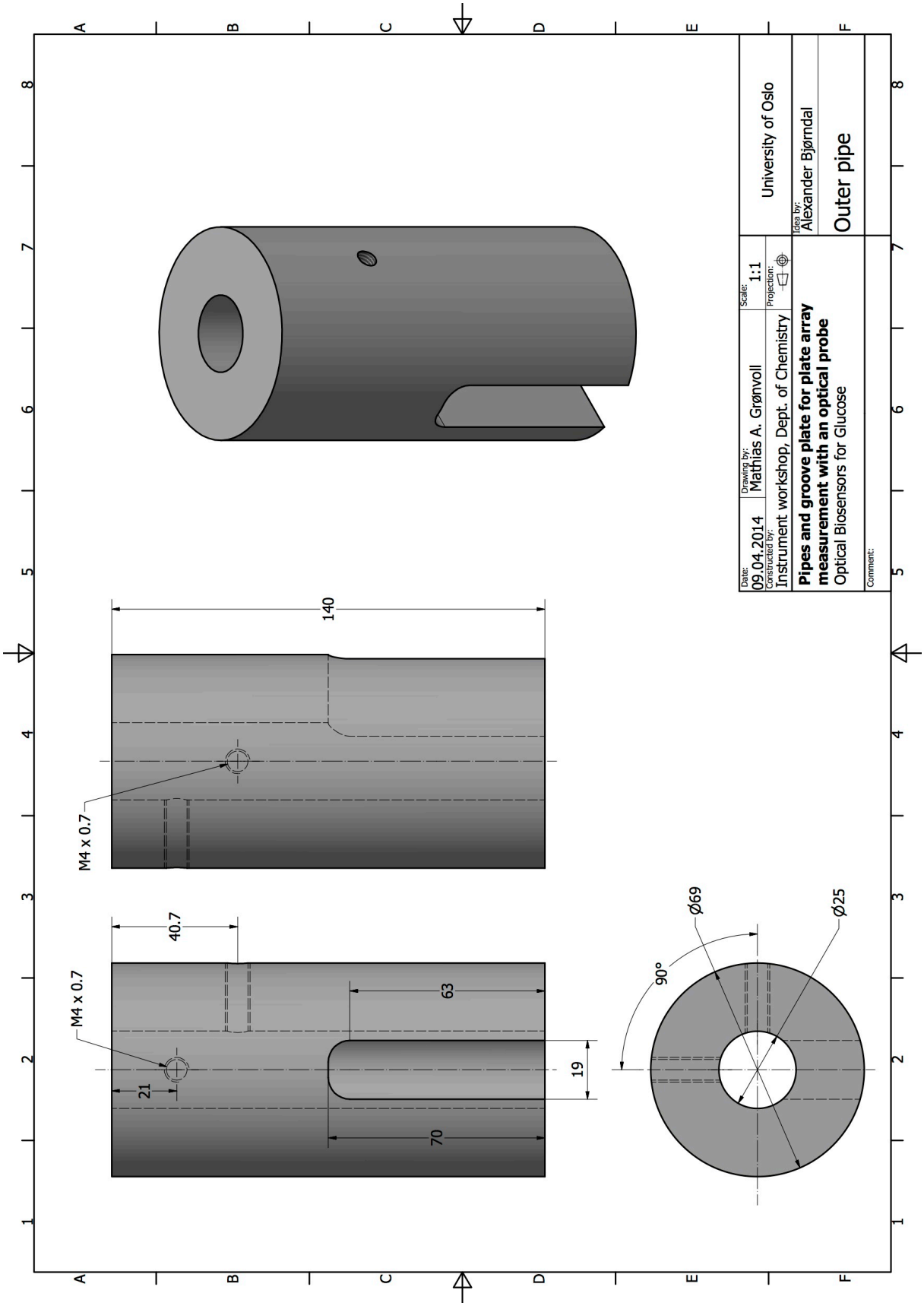

Figure 40: Outer pipe used in the setup for plate array measurement with groove plate and pipes.

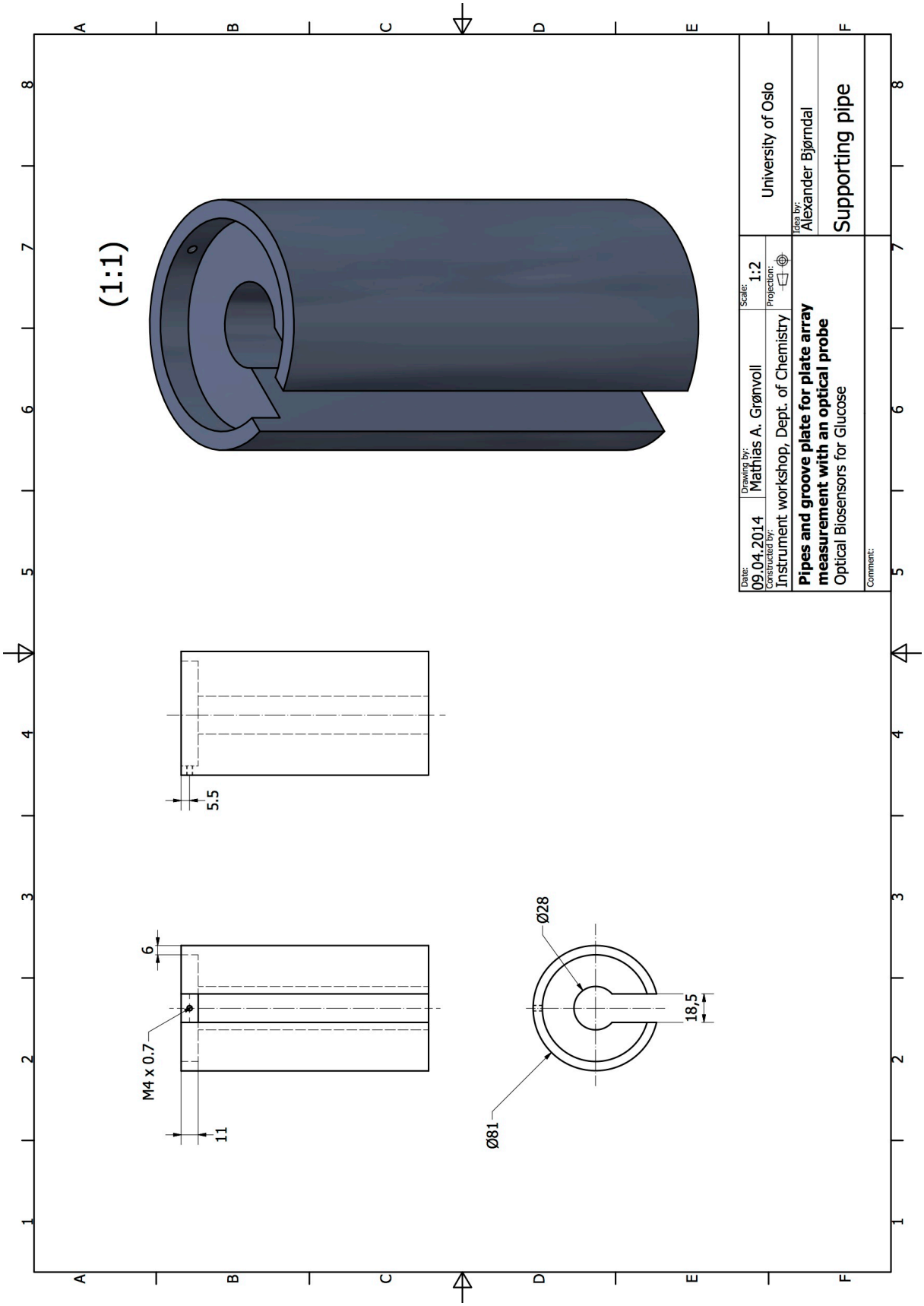

Figure 41: Supporting pipe used in the setup for plate array measurement with groove plate and pipes.

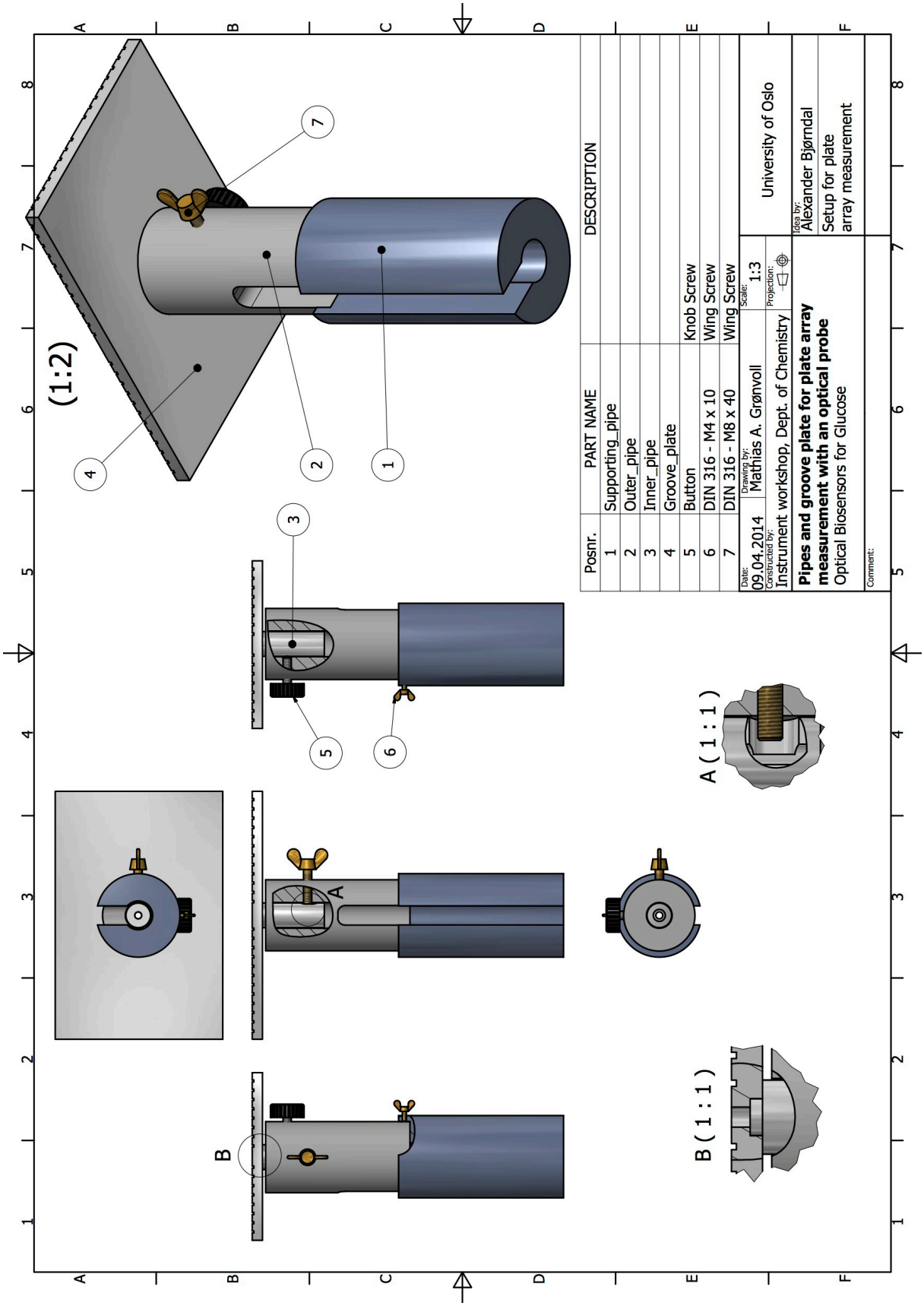

Figure 42: The whole setup for plate array measurement with groove plate and pipes.

Appendix I Predicted DGS ssNMR spectra

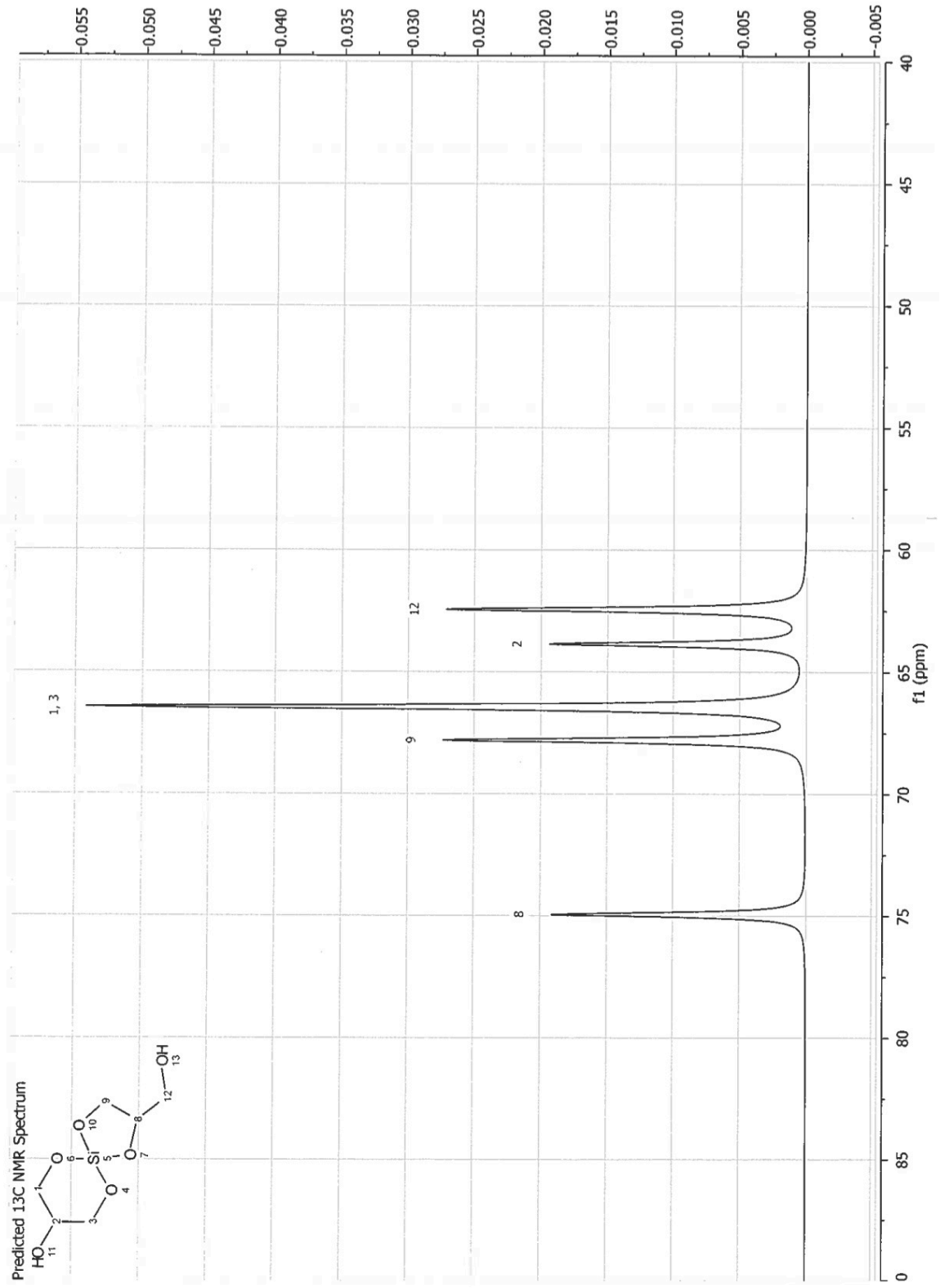

Figure 43: Predicted 13C NMR spectrum for the first of the proposed DGS structures seen in a paper by Brook* et al. *[36].

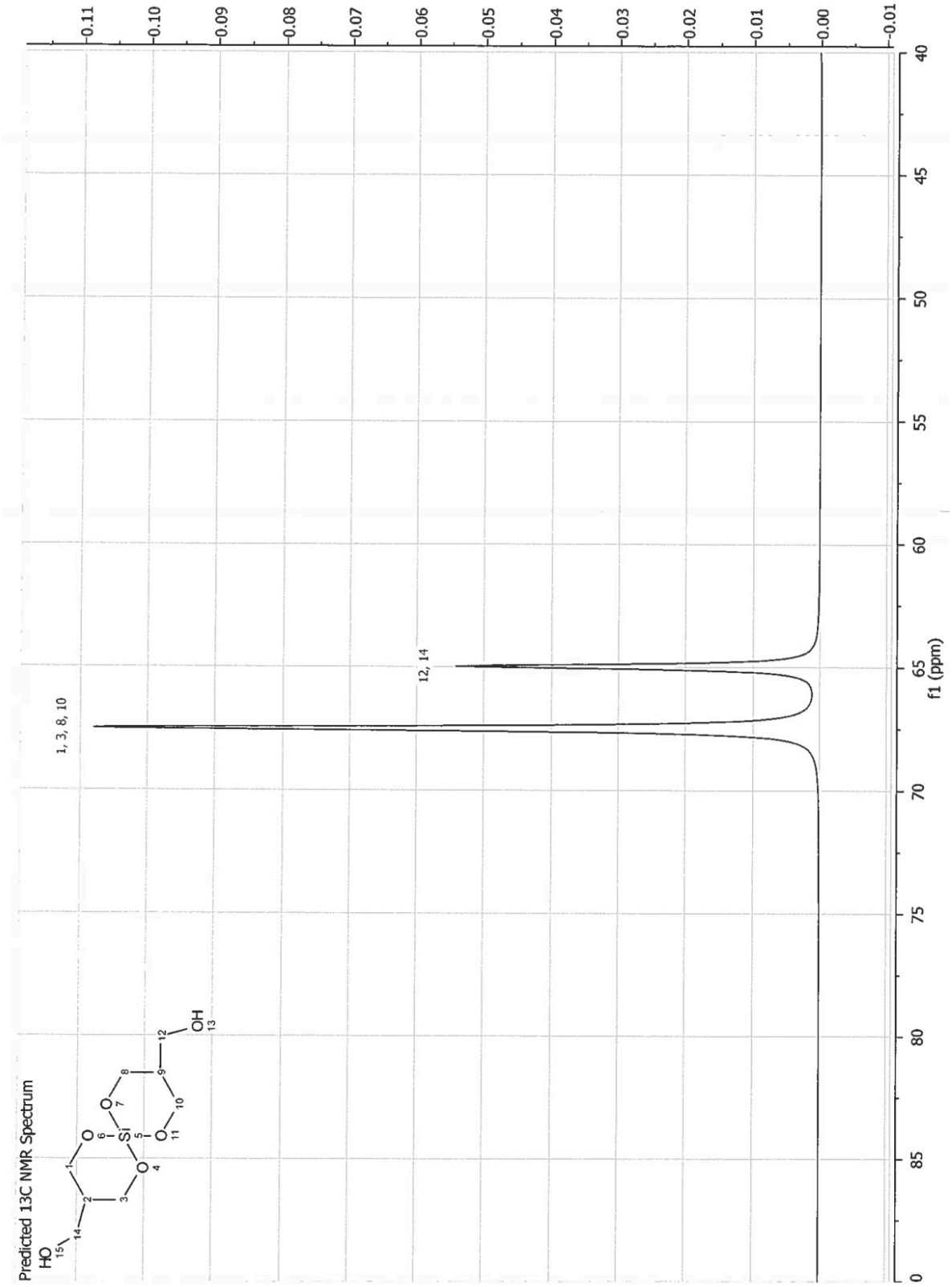

Figure 44: Predicted 13C NMR spectrum for the second of the proposed DGS structures seen in a paper by Brook* et al. *[36].

Appendix J Obtained DGS spectra

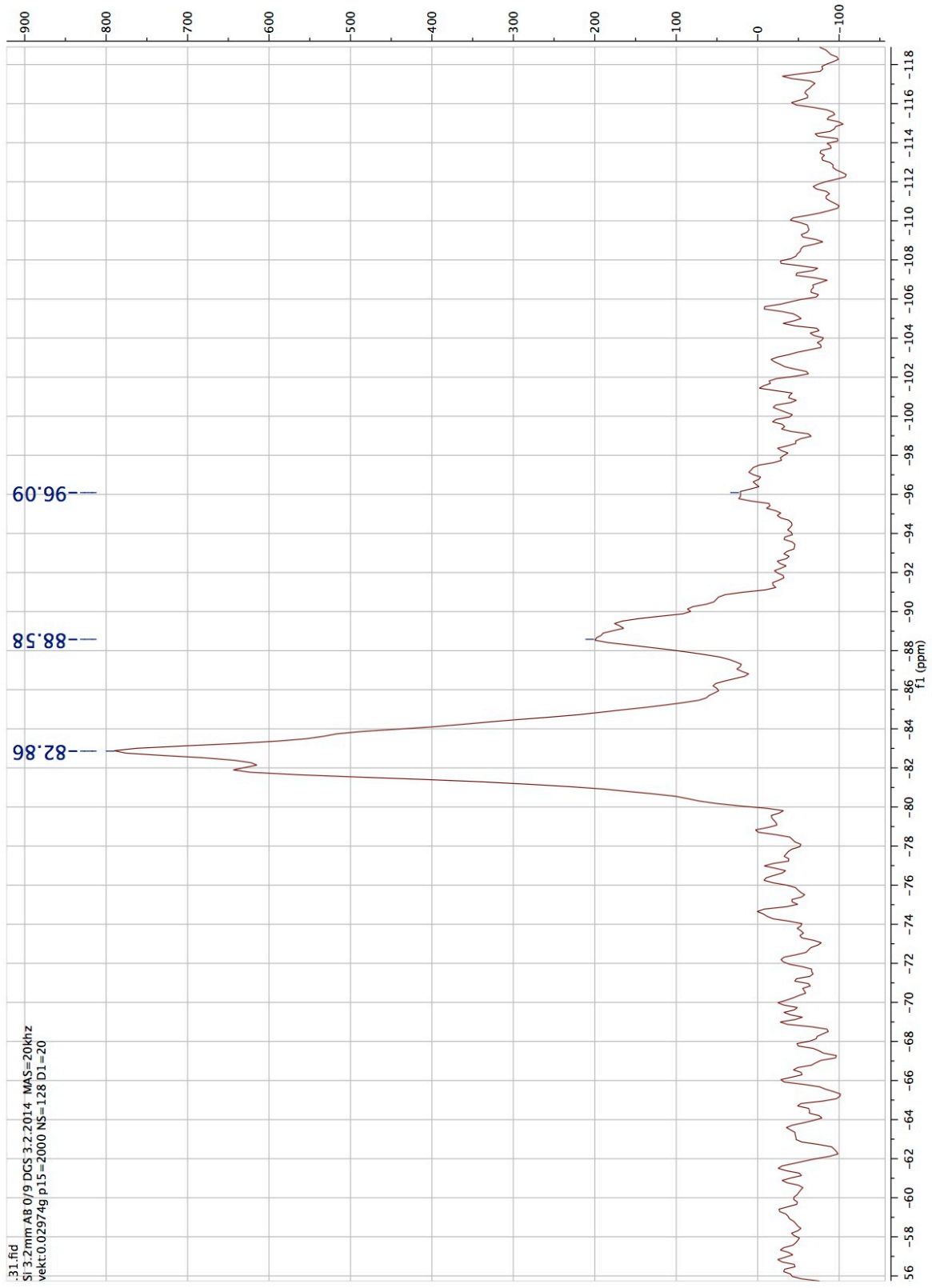

Figure 45: ^{29}Si ssNMR of DGS.

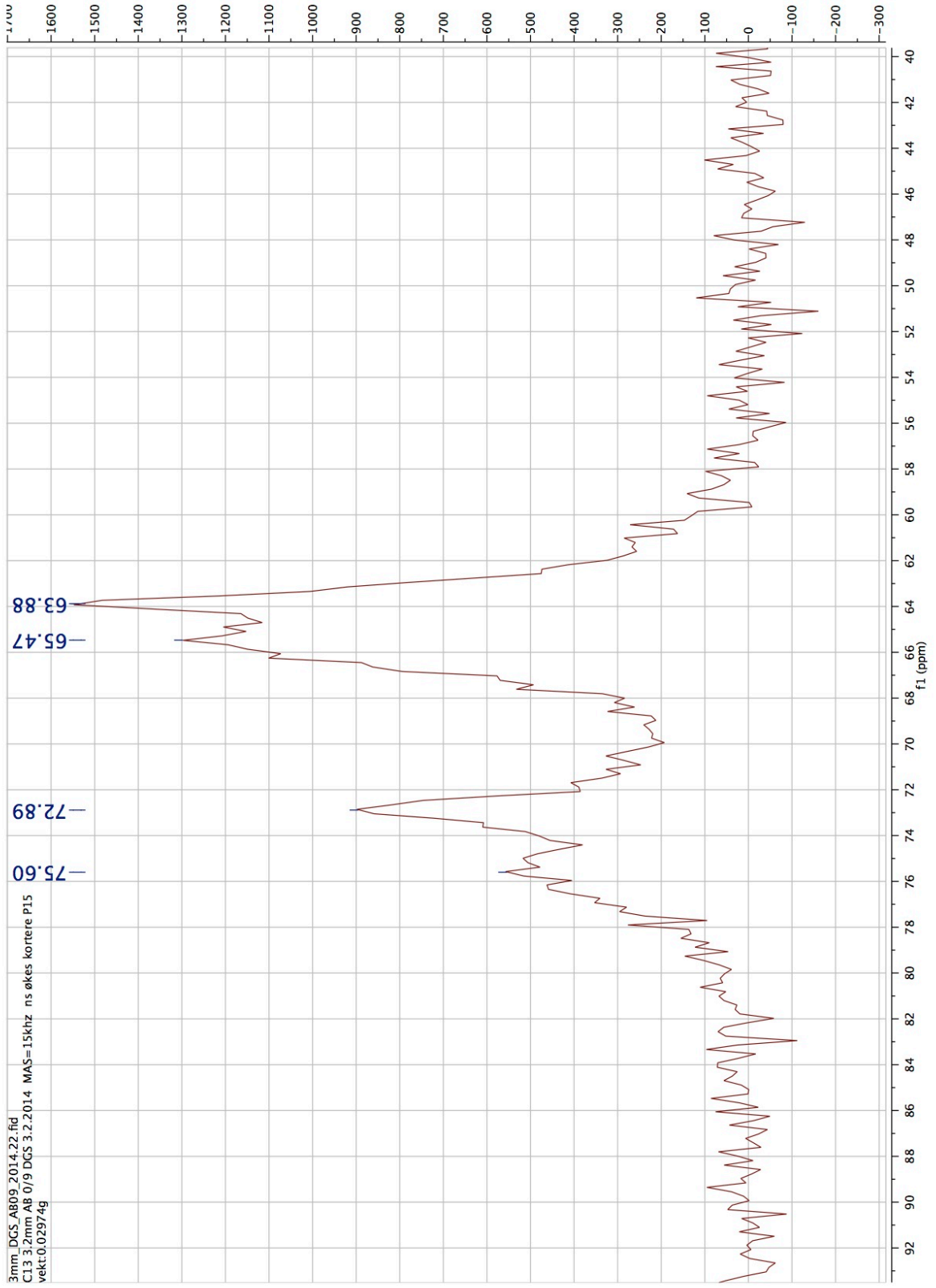

Figure 46: ^{13}C ssNMR of DGS.

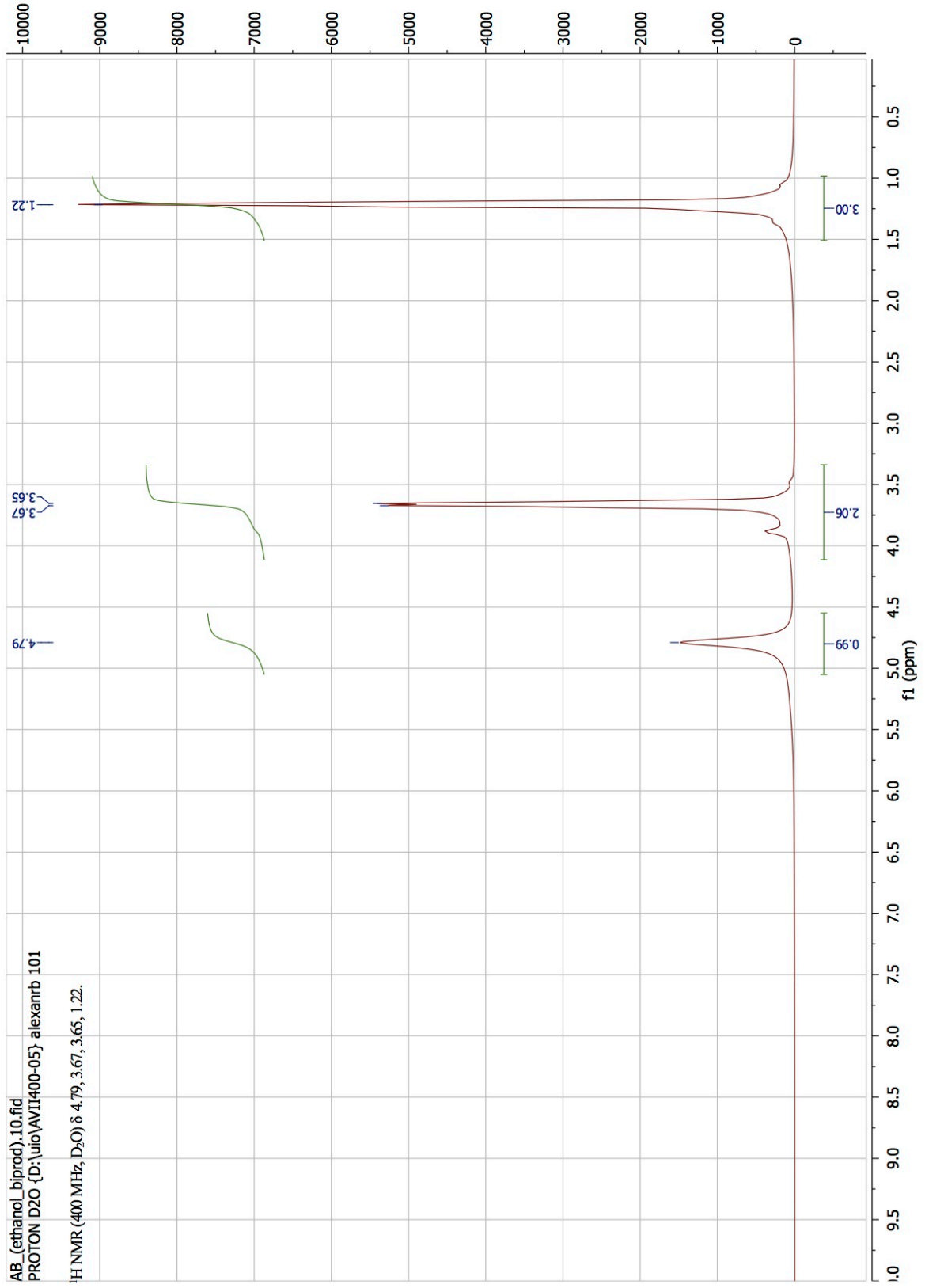

Figure 47: ^{1}H NMR of the by-product of the reaction of TEOS with glycerol.

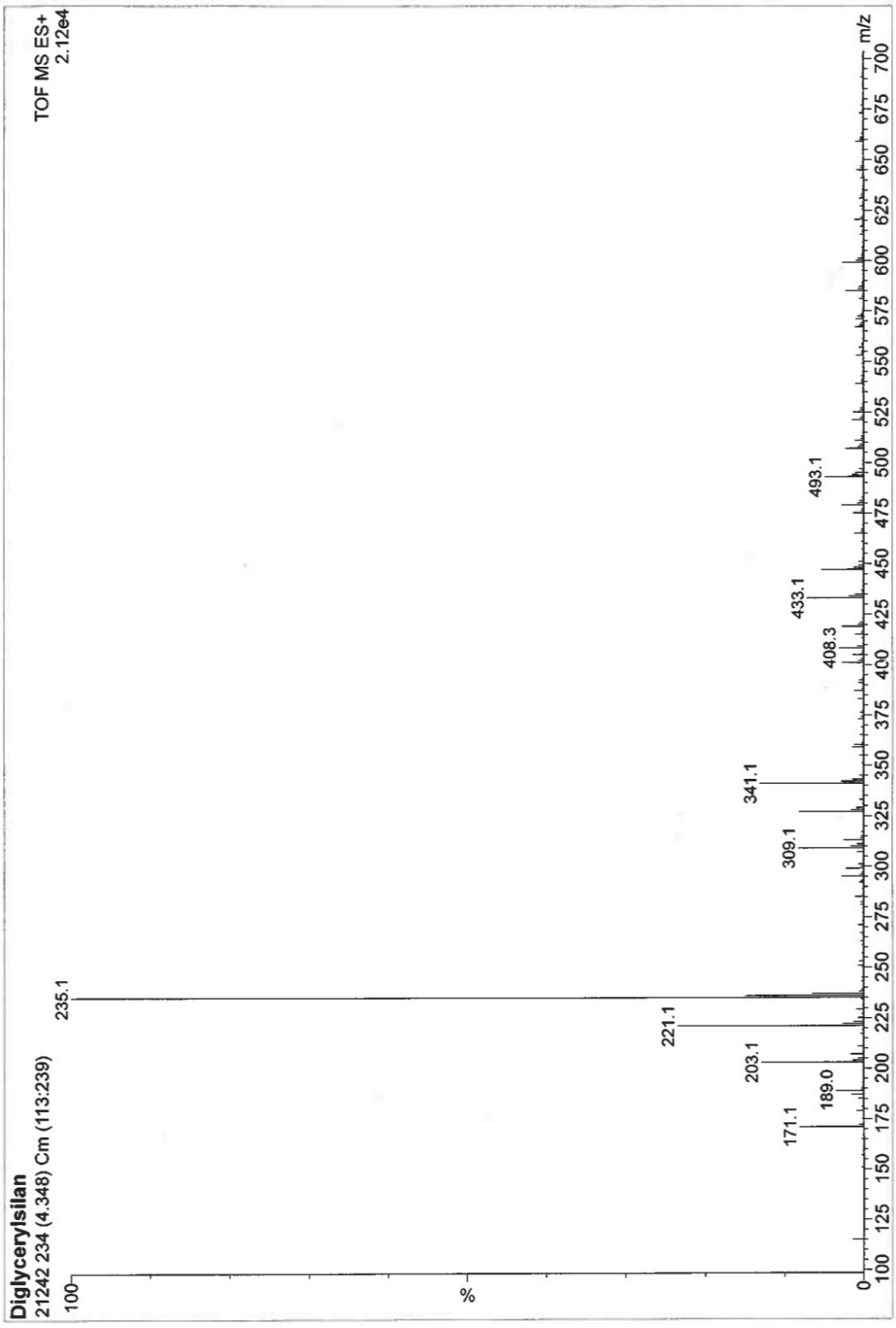

Figure 48: MS spectrum of DGS.

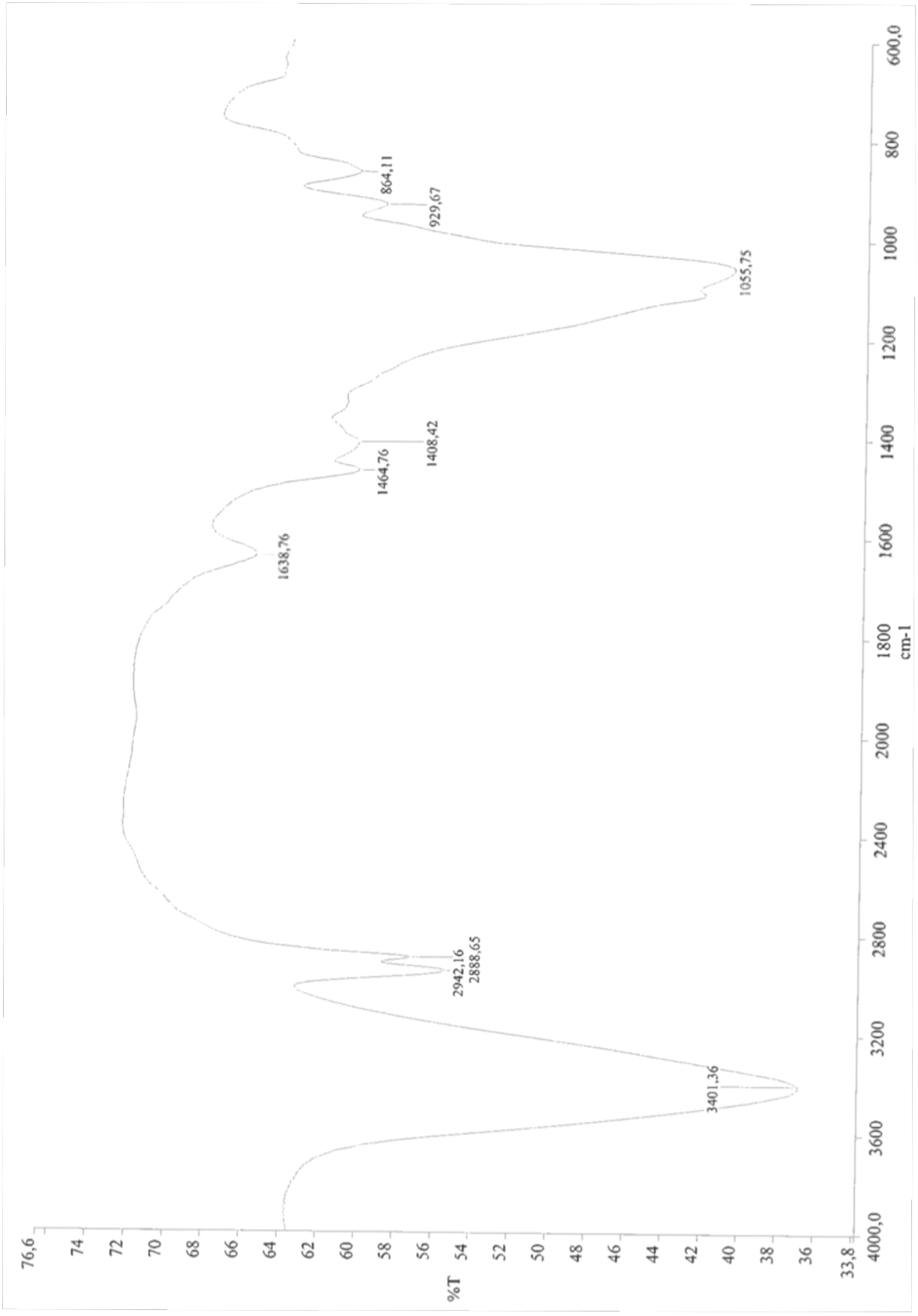

Figure 49: IR spectrum of DGS.